DEVELOPMENT OF A MULTIPHASE DETONATION TUBE

A Thesis

by

CALVIN JOSEPH YOUNG

Submitted to the Office of Graduate and Professional Studies of
Texas A&M University
in partial fulfillment of the requirements for the degree of

MASTER OF SCIENCE

Chair of Committee,	Jacob McFarland
Committee Members,	Scott Jackson
	Eric Petersen
Head of Department,	Guillermo Aguilar

May 2022

Major Subject: Mechanical Engineering

ABSTRACT

Engines operating on detonation-combustion cycles promise the high-performance, efficient propulsion necessary for sustained air breathing super- and hyper- sonic flight. Development of engines operating on such cycles requires a thorough understanding of the relevant physics involved. For many practical and performance purposes, liquid-fueled engines are a necessity for feasible flight platforms. It is therefore imperative to understand fully the mechanisms by which liquid fuel droplets injected into a detonation engine are processed by the detonation wave. This is a complex multi-phase process, consisting of simultaneous droplet breakup, evaporation, and reaction. While gaseous-fueled detonations are well studied and somewhat well understood, liquid fueled detonations have not received the same attention. Here it is proposed to design, engineer, construct, and test a facility that will be used to investigate the mechanisms of liquid fuel droplet breakup in a detonation environment. Such a facility will allow for full measurements both of bulk detonation properties and spatial and temporally resolved optical imagery of droplet processing by detonation.

DEDICATION

I dedicate this to my parents Dan and Rachel and everyone else who's been here along the way.

ACKNOWLEDGMENTS

This work would not have been possible without the support and guidance of a number of individuals. I would like to foremost thank my advisor Dr. Jacob McFarland for the opportunity to work on this project. I would also like to acknowledge Dr. James Chris Thomas and Dr. Eric Petersen for providing expertise in both fundamental detonation knowledge and practical design of experiments, as well as my friends and lab mates Vasco Omar Duke Walker and Benjamin Musick for contributing their individual technical expertise and support to this work.

CONTRIBUTORS AND FUNDING SOURCES

Contributors

This work was supported by Professor Jacob A. McFarland of the Department of Mechanical Engineering.

All other work conducted for the thesis was completed by the student independently.

Funding Sources

Graduate study was supported by grants from the National Sciences Foundation NSF: 2044767 and Office of Naval Research ONR: N00014-20-1-2796 .

NOMENCLATURE

CJ	Chapman - Jouget (and Michelson) Theory
ZND	Zeldovich-Neumann-Doring Theory
DDT	Deflagration-to-Detonation Transition
SBVR	Simultaneous Breakup,Evaporization, and Reaction
SDMI	Shock Driven Multiphase Instability
RDE	Rotating Detonation Engine
BR	DDT Obstacle Blockage Ratio
L_{crit}	DDT Obstacle Characteristic Length
λ	Detonation Cell Size
V_{CJ}	Chapman-Jouget Velocity
P_{CJ}	Chapman-Jouget Velocity
D10	Particle Mean Diameter
D20	Particle Diameter of Lowest 20th Percentile
D32	Particle Surface Area to Volume Ratio
D43	Particle Volume Weigthed Mean Diameter
SMD	Sauter Mean Diameter; D32
CAD	Computer Aided Design
FEA	Finite Element Analysis
Valving	
B	Manual Ball Valve
N	Manual Needle Valve

R	Gas Regulator
P	Pneumatic Actuated Ball Valve
S	Actuated Solenoid Valve

TABLE OF CONTENTS

Page

LIST OF FIGURES

FIGURE Page

LIST OF TABLES

TABLE Page

1. INTRODUCTION AND LITERATURE REVIEW

1.1 Introduction

Modern and next-generation flight platforms designed to operate at super- and hyper- sonic speeds require more efficient, compact propulsion systems than those currently available. Solutions to this problem has been proposed in a number of propulsion engine designs operating on detonation combustion cycles. In contrast to traditional constant pressure combustion cylces, namely the Brayton cycle, constant volume or near constant volume combustion cycles utilize detonations to combust fuel at relatively high temperatures pressures, yielding more complete combustion, higher thermal efficiency, and useful high-pressure exhaust products. This process may be simply modeled by the Humphrey cycle, illustrated in Fig.1.1 Examples of engines operating on constant volume cycles would be SCRAM-jets, supersonic ram-jet like engines, pulsed-detonation-engines, PDE's, and rotating detonation engines, RDE's.

The engineering of such engines is rather complex, requiring both a thorough understanding of the variety of involved physics as well as proper tools for design and development. For many practical and performance purposes, liquid-fueled engines are a necessity for feasible flight platforms. Liquid fuels are of practical interest over gaseous fuels for flight platforms as they are inherently denser and require relatively simpler and or safer fuel handling systems than those for compressed gases. Their composition may also be modified to suit particular purposes. In order to design an engine operating on a liquid-fueled detonation combustor, a proper understanding of the liquid fueled multiphase detonation is inherently necessary.

While gaseous fueled detonations have been investigated thoroughly throughout the twentieth century, multiphase detonations have not received the same treatment and remain relatively poorly understood. The multiphase detonation itself is a complex multi-phase process, consisting of simultaneous droplet breakup, evaporation, and reactions occurring at simultaneous length and time scales. Additional problems exist in understanding larger scale mixing and hydrodynamic

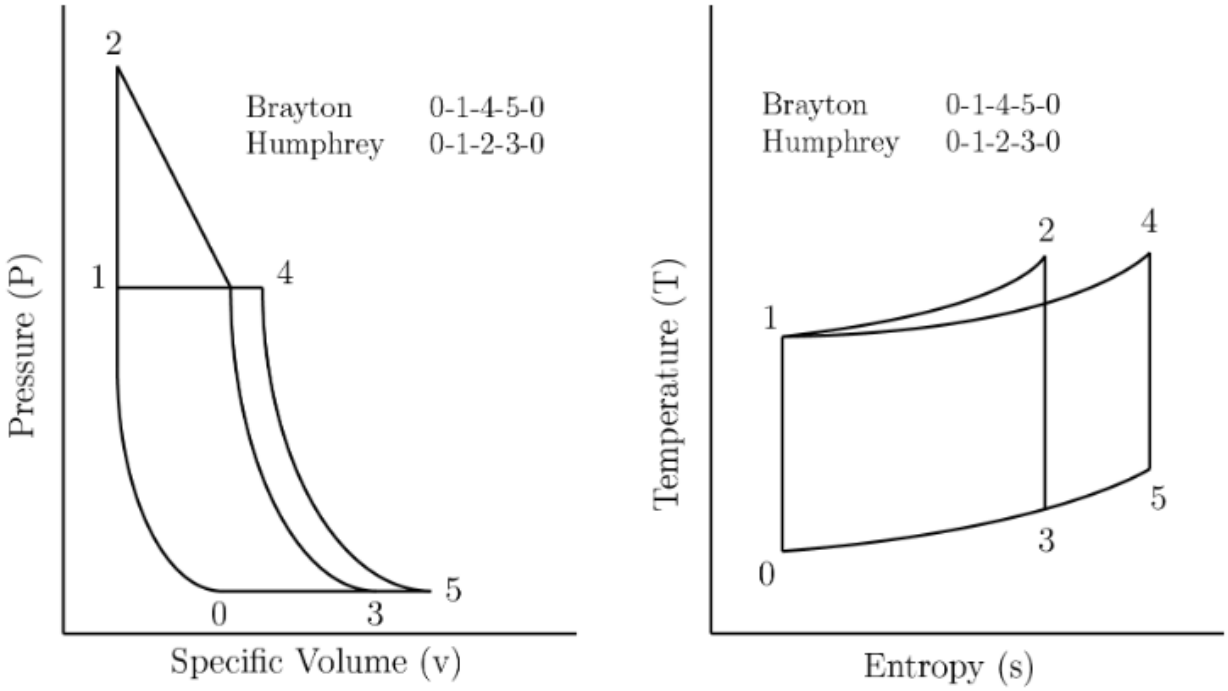

Figure 1.1: P-v and T-s diagrams comparing Humphrey (const. vol.) and Brayton (const. pressure) combustion cycles. Courtesy of AFIT [1].

phenomena due to injection patterns and combustion geometry, and the affects of those on the behaviors of the multiphase detonation.

Summarily, significant investigation is necessary to arrive at understanding of the mechanisms by which liquid fuel droplets injected into a detonation engine are processed by the detonation wave. Bulk properties of multiphase detonations of various fuel composition, such as velocity and pressure have been investigated, though sparsely and with often questionable reporting of equivalence ratios and droplet size distributions. The problems of droplet evaporization and combustion and high Weber number droplet breakup have been investigated thoroughly, though separately.

In this work, a facility to study multiphase detonations at all relevant scales to the problem is designed, engineered, constructed, and tested. The facility allows for measurement of the bulk properties of detonation pressures and velocity profiles well as access for optical imagery using modern digital optics and laser illumination techniques. These will allow through various methods

observation of the droplet field and individual droplets as they are processed by the detonation, as well as the detonation cells and induction and reactions zones. The facility will also allow for accurate measurement of equivalence ratio and droplet size, critical parameters to the problem. In doing so, the problem of multiphase detonations may be studied in greater detail and with measurements of greater accuracy than previously available. Data collected from these experiments will be used to inform models used in simulations, allowing for informed modification and verification. Broadly, the question this work and future work serves to answer is: How does heterogeneity influence detonations?

1.2 Literature Review

1.2.1 Theory

1.2.1.1 Detonation Theory, One Dimension

Combustion regimes may be divided into sub-sonic deflagrations and super-sonic detonations, the latter being of interest here.

The simplest one-dimensional approach to detonations is theory of Chapman, Jouget, and Michelson. This theory treats the a detonation as a shock with an energy release inside an infinitesimally small reaction zone, reactions ceasing at the local sonic plane. Here it is assumed that the flow is steady in a constant area channel, the gasses are ideal with constant specific heats, and the problem is adiabatic. Solving the conservation equations, two solutions exist at the intersections of the Rayleigh and Hugoniot curves, the lower point being the CJ deflagration velocity and the higher point being the CJ detonation velocity. Detonations may exist above the CJ-detonation point as strong detonations, or conversely below this point as weak detonations, in theory both of which will regress to the CJ velocity.

During the second world war, Zeldovich, Neumann, and Doring separately arrived at a modification of CJ theory to include finite induction and reaction zones, ZND theory. Here the detonation is divided into a preceding strong shock of infinitesimally small thickness, colloquially a Neumann pressure spike, and a reaction zone of finite thickness, with reactions ceasing at the sonic plate at

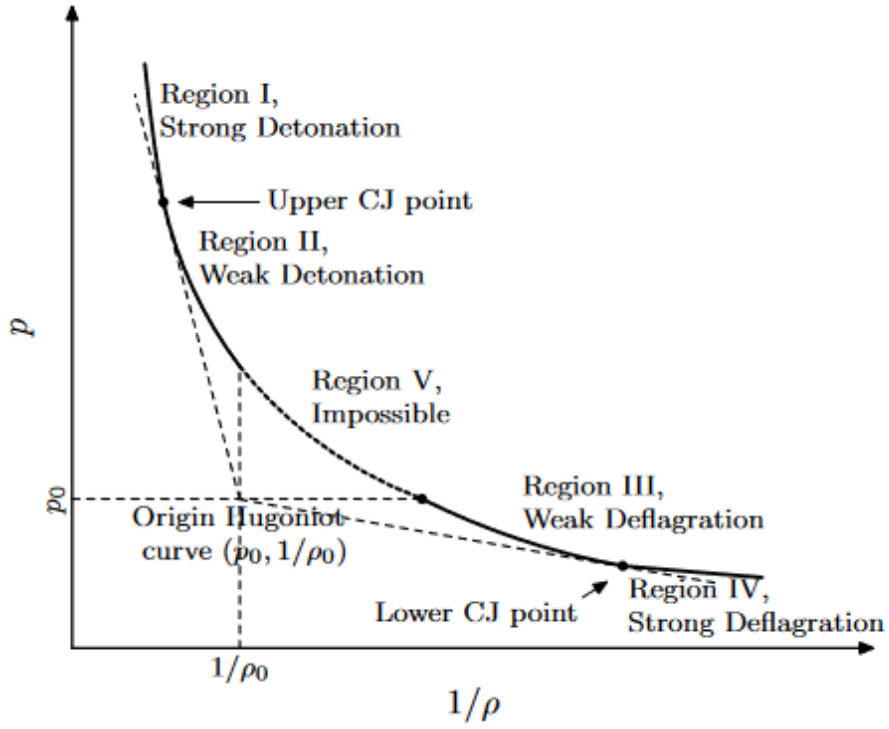

Figure 1.2: Hugoniot Curve with CJ Points annotated.[2]

the CJ-point. Between the shock and reaction zone there is an induction zone where the un-reacted species are excited.This theory importantly decouples the shock from the reaction zone, allowing for the energy from exothermic reactions to be transported forwards in the wave frame to support the shock, while the products expand backwards at subsonic velocities from the CJ point.

1.2.1.2 Detonation Theory, Multiple Dimensions

In the physical world detonations are a complex, inherently three-dimensional, dynamic phenomena consisting of incident and transverse shock waves and reaction and induction zones of varying length. Curvature in the incident shock front results in components with components in the axial and transverse direction. As the shock propagates, the transverse components interact at a triple point of extreme high temperature and pressure. This phenomena is commonly observed as a regular cellular pattern tracing the trajectories of the triple points, Fig. 1.4, yielding a characteristic length scale detonations, cell size, λ [7].

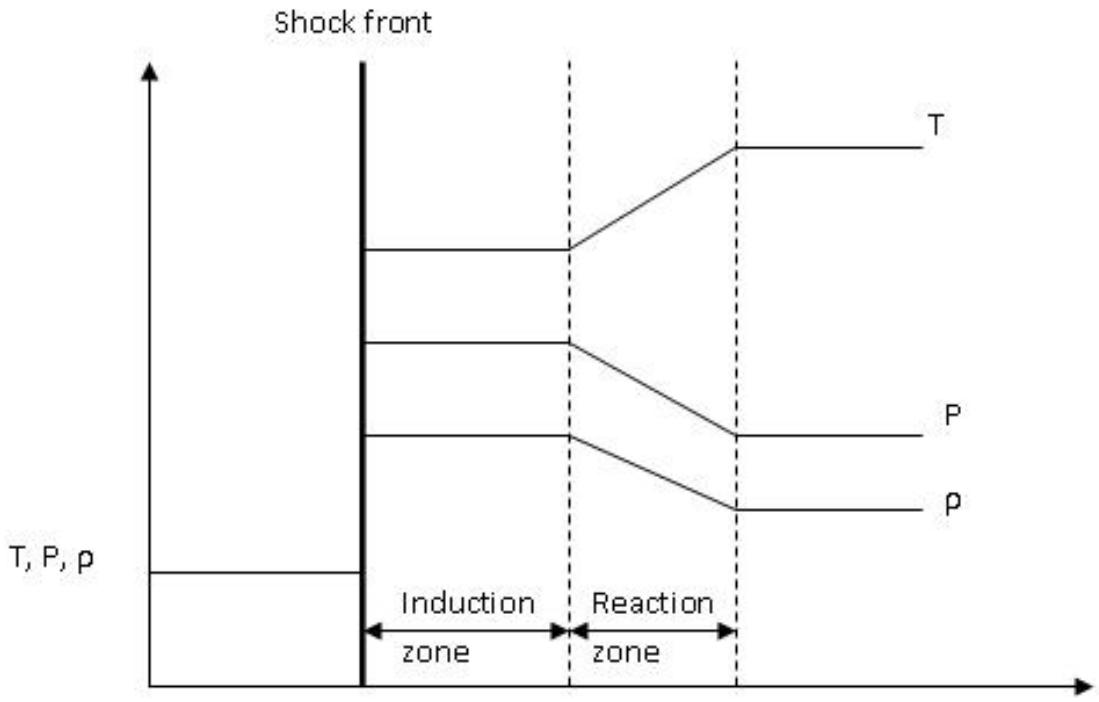

Figure 1.3: Structure of Detonation wave according to ZND Theory, shock, induction, and reaction zones annotated.[2]

The detonation cell size has been observed to vary in relation to equivalence ratio, initial pressures and temperatures of the fuel-oxidizer mixture. This quantity allows for empirical correlation to dynamic parameters such as induction zone length, reaction rate, and initiation energy for certain gaseous mixtures [8]. Cell size has in gaseous detonations has also been observed as a limiting parameter for detonation propagation and stability in tubes. Detonations may propagate in an unstable manner with at least one cell, with a diameter 7λ 13λ necessary for stable propagation [9].

1.3 Multi-Phase Effects

The bulk properties of homogeneous, gaseous detonations may generally be treated with one-dimensional theory to a satisfactory extent. The complex multi-dimensional behaviors have have been addressed in a limited fashion by theory and extensively through experimentation. Satisfactory three-dimensional numerical and theoretical treatment remains elusive. The addition of liquid

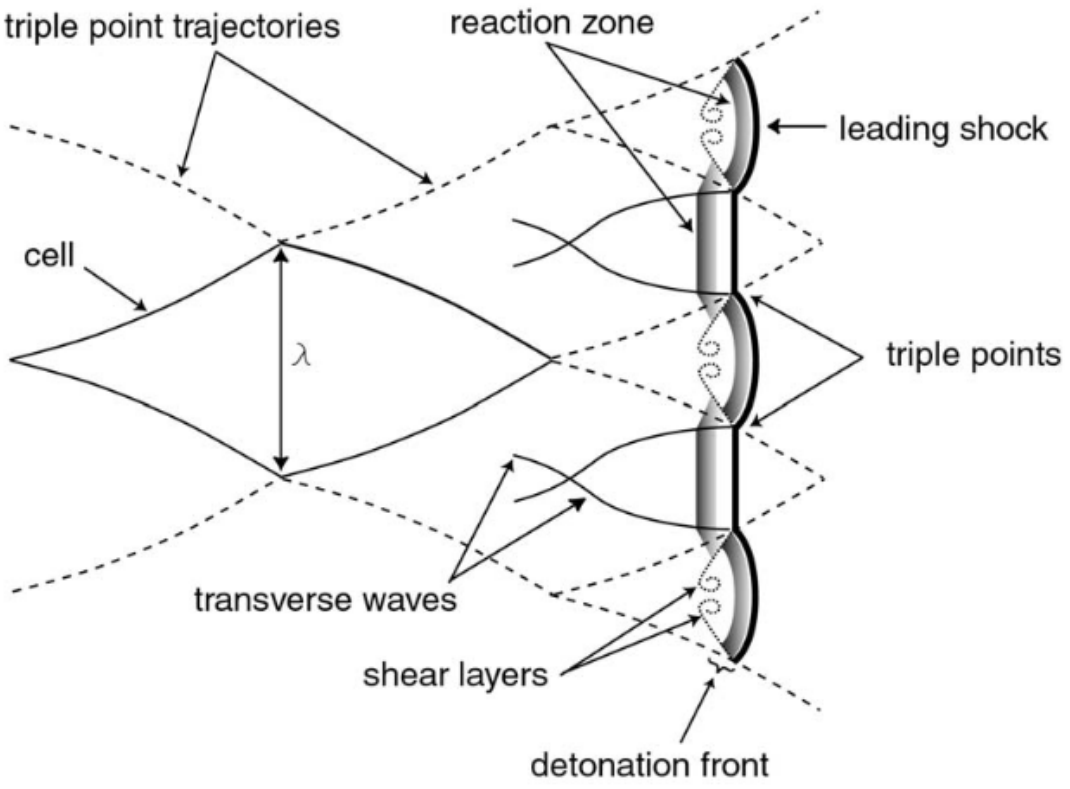

Figure 1.4: Cartoon of 2-Dimensional structure of detonation wave. Detonation cell width λ annotated. [2]

fuels to the problem adds additional thermodynamic and hydrodynamic components, further complicating matters in all dimensions.

In order for a liquid fuel droplet in gaseous fuel to be reacted, the liquid must undergo a phase change into a vapor. Classically, the rate at which the droplet evaporation and vapor diffusion into the surrounding environment occurs has been modeled under constant conditions by the d^2 law, a thorough treatment of which can be found in Crowe [10]. The process of vaporization in a combustion environment becomes complex, as a range of conditions must be considered, from the surface of the droplet at the boiling point (if not at a super-critical temperature) through the vapor cloud and a mixture of broken hydrocarbons, to reactions at the flame front. Early experimental investigatons by by Godsave [11] in the 1950s fit a linear rate of droplet size decrease under constant conditions. Later modeling by Ranz and Marshall [12] and Abramzon [13] extended

theory to include variable physical properties, mechanisms of heat,mass, and species transfer both inside the droplet and in the vaporization region.

A droplet experiencing sudden acceleration due to an incident shock wave will undergo a process of deformation and breakup due to hydrodynamic forces acting on the droplet. At high Weber numbers, on the order of 10^6, such as those seen with small (25 um) droplets and shocks at detonation wave velocities, this breakup effect is catastrophic. The droplet breakup process is treated by hydrodynamic stability theory in a semi-empirical relations as chain of successive instabilities; initially a primary deformation due to aerodynamic forces, resulting in secondary Rayleigh-Taylor and Kelvin-Helmholtz instabilities, resulting in child droplets being shed from the parent droplet [14]. Recent experimental work by Herbert et.al [3] provides a thorough experimental investigation of water droplet breakup at Mach 4.4 and We O10^5. Figure 1.5 of their results is provided to illustrate the process.

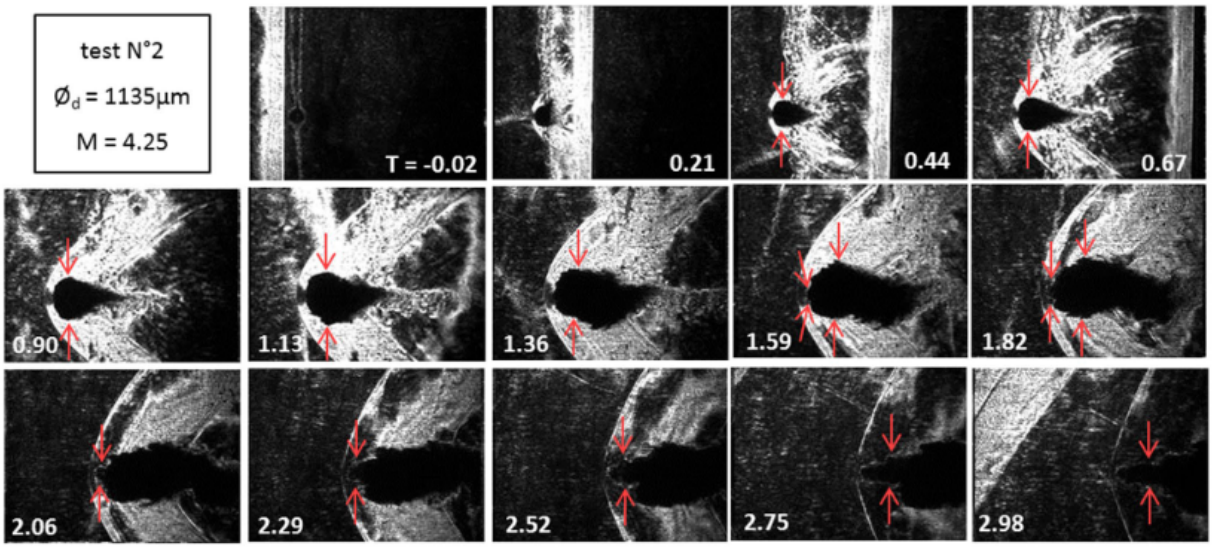

Figure 1.5: Schlieren imagery of shocked water droplet breakup at Mach 4.4 and Weber numbers 10^5 [3]. Note morphology of droplet over breakup process and generation of child droplets.

One might surmise at this point that the events of droplet vaporization and deformation are cou-

pled, and they would be correct. As the parent droplet is shattered it is simultaneously evaporating, while aerodynamic forces carry the vapor through the wake of the particle. Simultaneously, child droplets caught in the wake will be evaporating in the vapor field. As the droplets undergo vaporization and morphological changes, reactions are occurring within the flow-field, altering temperature dependent fluid parameters such as surface tension viscosity and vapor pressure. These events are occurring simultaneously during overlapping time and length scales, with co-dependencies such as evaporation and droplet heating due to the shock heating and heat from the exothermic reaction, and vapor production limiting available reaction rates.

For the practical purpose of simulating a multiphase detonation in a device such a propulsion engine, models for droplet vaporization and breakup must be implemented. As models must be verified to be trusted, it is required that somebody provide the means to verify them. Data for verification here would likely be the rate of vapor production from the droplets, the droplet survival times, and the length of the induction and reaction zones.

1.4 Detonation Tubes

1.5 Multiphase Detonation Tubes

The mechanisms of multiphase detonations have been previously investigated experimentally, to varying degrees of success. While many adjacent problems have received attention, such as the detonation of hydrocarbon vapors or more application driven research in liquid fueled pulsed-detonation engines, work on the fundamentals of liquid droplet processing by detonation has been found to be sparse. Kailasanath [15] provides a review of attempts to study liquid fueled detonations, also known as spray or multiphase detonations in tubes [1].

Dabora [4] investigated the problem in the late 1960s with a vertical tube, studying diethylcyclohexane (DECH) in oxygen. His tube was square, 4.16 cm in diameter, and approximately 3.7m in length with a hydrogen-oxygen initiator tube at the upstream end. Optical access was provided by rectangular windows flush with the tube walls, approximately 2 meters from the top. Droplets

[1] Generally the experimental apparatus consists of a long slender 'detonation tube' of sufficient strength to contain a detonation, a method of filling the tube with particles and oxidizing gas (air or oxygen), and an ignition source, as well as various diagnostics.

were generated with vibrated capillary needles, with the resultant droplet sizes and equivalence ratio estimated with shadowgraph imagery. Sizes were estimated to be 290, 940, and 2600 μ. Pressure data was collected via transducers in the tube walls, while imagery was performed with flash Schlieren in an optically accessible section.

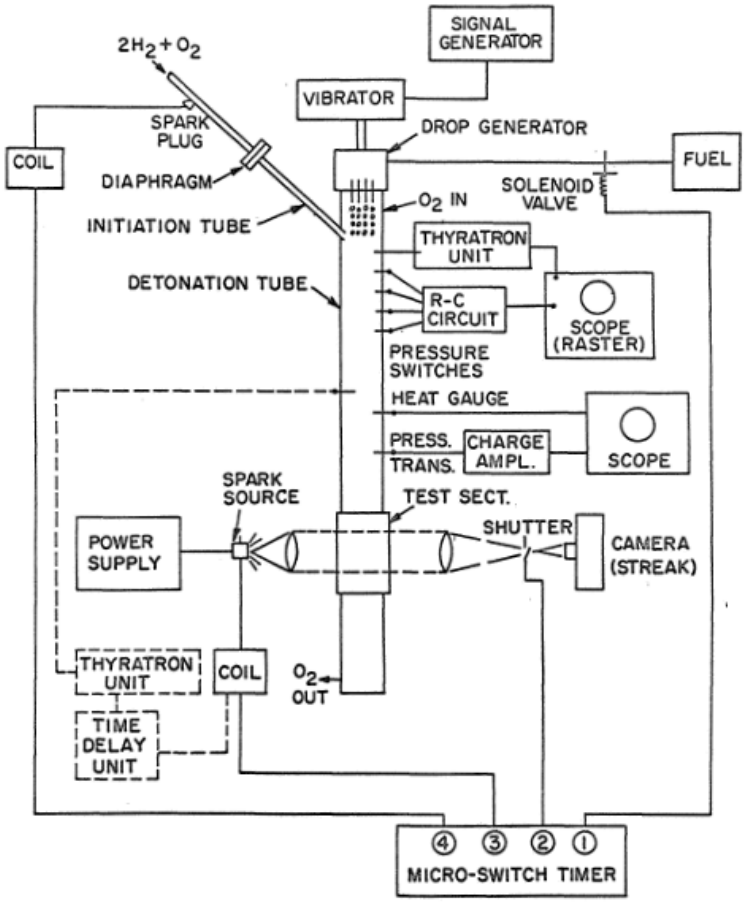

Figure 1.6: Multiphase detonation tube of Dabora [4] used in 1960s.

Investigations in the 1980s by Lu [5] involved a similar vertical tube, this time with droplets of hectane (substitute for gasoline)and various additives in air. His tube was square, with a diameter of 4.7 cm and a length of approximately 1.8 meters, again with a H2+O2 initiator, and optical thru- access at some point downstream in the tube. In his configuration there are additionally two large blowdown tanks mounted to each side of the downstream end of the tube for expansion and

containment of detonations. Droplets of size 0.5-10 μ were generated via ultrasonic nebulizer, estimated given manufacturer specifications of the device.

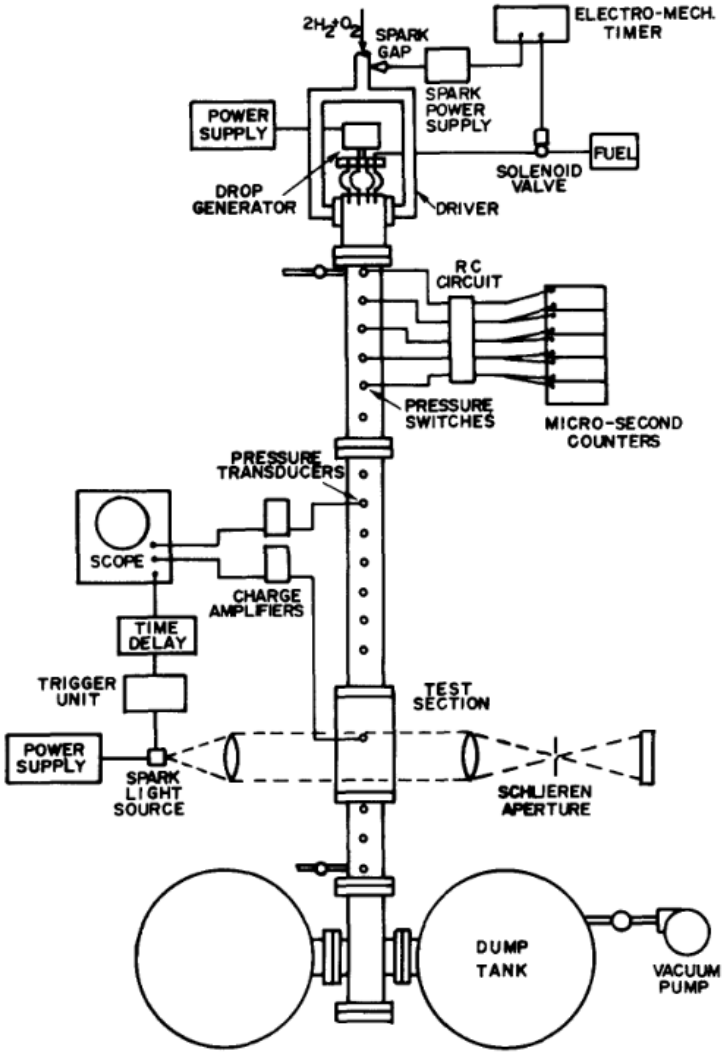

Figure 1.7: Multiphase detonation tube of Lu [5] used in 1980s.

A study by Papavassiliou [16] in the early 1990s investigated detonations in a decane spray. This tube was also vertical, 6.4cm in diameter and about 3 meters long, ignited by either spark or explosive charge in conjunction with a turbulent element (Shchelkin spiral). Droplets were generated by means of an ultrasonic nebulizer and carried into the tube by a flow of oxygen and nitrogen,

with droplet sizes of 5 μ estimated. Equivalence ratio was extrapolated from mass remaining in the nebulizer post-experiment. These experiments involved no optical imagery, instead relying on smoke foils placed at either the middle or downstream end of the tube to determine cell sizes. Wave velocities were measured with ionization probes and pressures with a singular ressure transducer near the downstream end.

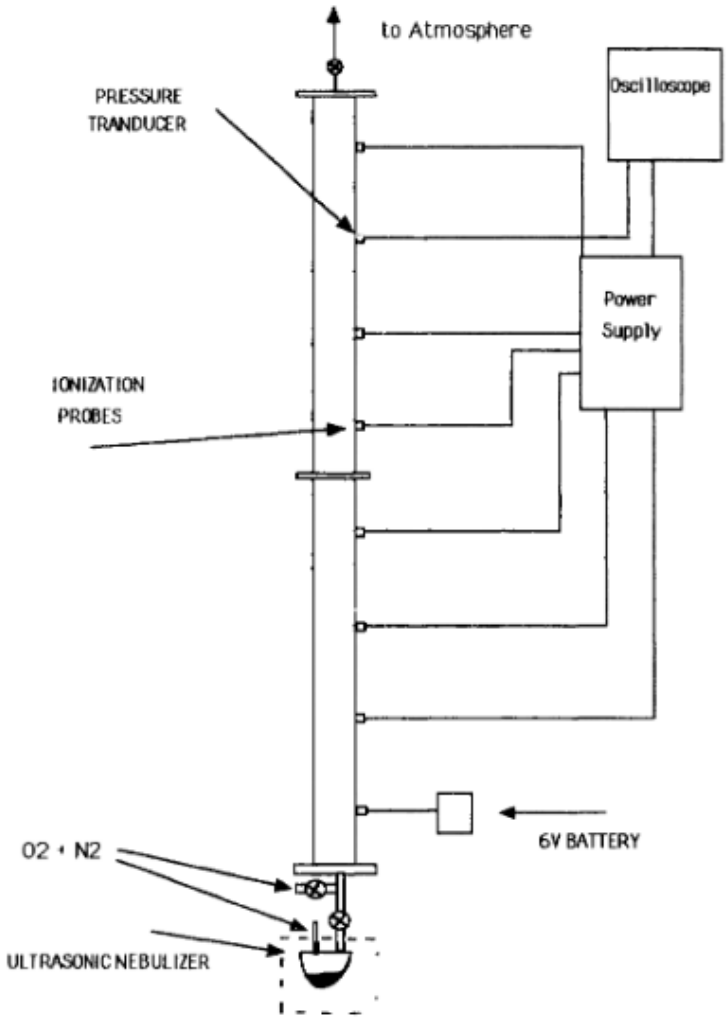

Figure 1.8: Multiphase detonation tubes of Papavassiliou [6] used in 1990s.

Previous investigations of multiphase detonation leave much to be desired. In the aforemen-

tioned experiments, droplet size is either assumed or estimated using relatively crude methods. As droplet size is of great importance to the problem, this is a clear issue when considering the validity of reported results. The bulk pressure and velocity data reported is limited to whatever the resolution and accuracy of the available devices used were; while the resolutions and capabilities of the sensors and data systems are not explicitly reported, it is clear that metrological technology has advanced in the past 30-50 years. Further, the optical diagnostics implemented in many of these studies is archaic compared to the modern tools available. A new facility, with modern diagnostics, would provide great benefit to the field through accurate data on detonations in liquid droplets, with verifiable droplet sizes and equivalence ratios, and high-resolution, high-speed imagery of the process at multiple scales, from the bulk detonation cells to individual droplets.

2. FACILITY DESIGN

2.1 Design Requirements and Methodologies

This section will serve to detail the design methodologies, engineering considerations, and individual elements of the facility. The design process was iterative, with many choices undergoing modification due to engineering concerns, evaluation and re-evaulation of desired functionalities, consideration of available components and cost of certain choices, and alterations due to available manufacturing processes. Above all else, the facility was to be safe to operate, posing no inherent danger to the experimental staff, equipment, or laboratory complex.

2.1.1 Design Requirements

To determine the necessary shape of the facility, a review of relevant literature was conducted. Here it was established the requisite dimensions of the detonation tube. The literature on detonation tubes investigating heavy hydrocarbons is rather sparse, so many of the decisions were based on the aforementioned work of Papavassiliou (McGill University) [16] investigating detonations in decane fog and air/oxygen mixture, as well as that of Dabora [4] and Lu [5]. Here the reported cell sizes for 10 um decane sprays in oxygen were reported as approximately 4 mm at a stoichiometric fuel air ratio.

For a desired cell ratio of cell size to tube diameter for detonation propagation $D/lambda$ $7 - 13$ in smooth tubes this would put the necessary tube diameter somewhere between 28 and 52 mm. The tube in this investigations of Papavassliou was approximately 6.4 cm internal diameter, while Lu [5] and Dabora [4] used tubes of 4.7 and 4.16 cm diameter respectively, with mid to heavy hydrocarbons. From previous literature, necessary length of the tube was estimated to be between 2-3 meters, with Papavassiliou reporting successful smoke-foil measurements from foils placed at the midpoint of their tube, approx 1.5 meters from the ignition source. The dimensions and details of the tubes surveyed are outline in Tables 2.1-2.2.

The design pressures and detonation wave speeds were estimated from both literature and the

Group	Length [m]	Dia. [cm]
Dabora	3.7	4.2 x 4.2 SQ
Lu	4.57	4.1 x 4.1 SQ
Papavassiliou	3	6.4 RND
FMECL Tube	2.95	5.7 x 5.7 SQ

Table 2.1: Dimensions of surveyed multiphase detonation tubes and designed facility.

Group	Fuel	Droplet Size [um]	Initiator	Accelerator
Papavassiliou	Decane	5-10	Bridgewire/Blasting Cap	500mm Spiral Coil
Dabora	DECH (JP10?)	290,940,2600	H2-O2 Det. Tube	N/A
Lu	Heptane	700,1400	H2-O2 Det. Tube	N/A
FMECL Tube	Dodecane/JP10	0-100	Spark	500mm Spiral Coil

Table 2.2: Fuels and ignition methods of surveyed tubes and designed facility.

use of the Shock and Detonation toolbox provided by Joseph Shepherd's laboratory at CalTech [17]. Papavassiliou, being the closest experimental work to that of the proposed facility, provided a starting point for estimating these values. Here the highest pressures and velocities were reported at a stoichiometric fuel air ratio, being approximately 4 MPa and 2300 $\frac{m}{s}$, respectively. These values were supported by similar results from 1D calculations in SD-Toolbox.

2.1.2 Engineering Considerations

With the requirements established from a physical standpoint, necessary features and functionalities were identified. Features such as ignition systems, detonation-development/enhancing devices, gas handling and porting, optical and pressure diagnostic access, and a method of safely disposing of the detonation wave were identified here.It was also decided that the tube be vertical, in order to gain the assistance of gravity when injecting droplets. The facility was also to be scalable and modular to allow for various experiments beyond the scope of the initial projects the tube was designed for, as well as to provide life-cycle improvements as necessary.

The static design pressure was decided to be double the estimated 4 MPa CJ pressure, 8 MPa

or 1200 psi, with a minimum allowable factor of safety of 2 (effective factor of safety > 4 against the estimated CJ pressure. This design point was chosen for two reasons. ASME guidelines allow for transient events 1.3 times the maximum allowable working pressure; in the case of an errant DDT event somewhere in the tube a design pressure of 8 MPa would allow for a transient event 2.6 times the CJ pressure, within reasonable expectaiton for DDT pressure [18]. The increased static pressure requirement also serves as a a safeguard for any complex mechanical shock loading issues that would otherwise require involved analysis.

Engineering analysis was performed on all components in order to determine both feasibility and safety of design choices. For pressure-bearing components guidance was taken from relevant industry design standards, where possible, namely the ASME Boiler and Pressure Vessel Code Section VIII [19] and the NFPA [18]. Finite Element Analysis (FEA) simulations were performed on all components and joints to verify calculations. In certain cases where code did not directly provide guidance, parts were designed to a higher factor of safety as reflected by the simulations in order to give greater assurance. Appendix A contains details on all FEA simulations. In order to easily visually and modify the design and provide continuing support to the facility, extensive use of computer aided design (CAD) modeling was implemented; a full computer model of the tube and all bolts, fittings, etc. exists for internal use and has proven exceptionally useful for reference and design additions/modifications.

Early on it was decided that the tube should be of a square cross section. A square cross section provides flat tube walls, allowing for normal flat windows to be placed flush against the inside surface. A round tube feeding into a test section with a square cross section was also considered, however it was not known how this change in geometry would affect the stability of the detonation, so a square cross section throughout was chosen. Given the necessary shape of the tube, several designs were iterated through in order to arrive at the final solutions. Given the requirement of a square cross sectional tube, few nominal sizes of readily available tubes with sufficient wall thickness and diameter were available. The chosen nominal size was 3 inch OD square tube with 3/8 inch thick walls (approx 57mm internal diameter). This was the smallest size available, thus

the requiring the smallest volume of fuel and oxidizer, that would provide a sufficient internal diameter for detonation propagation.

Many final design choices were influenced by the availability of raw materials and components. For any non-critical dimensions, Imperial units were used in the design to simplify acquisition of material and components. Similarly all bolts and fittings were chosen to be SAE/Imperial specification, as these are generally much cheaper and more widely than fittings in metric units. Nominal sizes of available material were chosen where possible, such as the raw steel tube shape, flange diameters and thicknesses, etc. Significant use of commercial off-the-shelf components was made in the construction of the facility. Pressure bearing components such as valves, tubing, and fittings were chosen to have equivalent or greater pressure ratings than the design pressure.

2.2 Tube Sections

In the below sections the individual components of the detonation tube are described in detail. This serves to outline the purpose, features, and functionality of the section as well as their relation to the operation of the tube as a whole. An annotated image of the facility as constructed is provided in Fig. 2.1.

2.2.1 Ignition Section

At the upstream end of the tube lays the ignition section. This section serves two purposes; **(i)** provide a location for an ignition source and **(ii)** provide porting for injection of gases and liquid fuel into the tube volume. The section is 150 mm long, with two side ports the standardized 1-1/8 x 12 plugs, with an additional top port on a blank flange. One of these side ports is the location of the spark ignitor, while the opposite port is the connection port for the fill gas manifold. The port on the end flange serves as the location for mounting the fuel injector.

Side port ignition was chosen for both practical and performance purposes. As the end port was to be used for the droplet injection site, the side wall was the next natural choice. This location also serves to keep the ignition source away from the stream of droplets produced by the injector. Side injection is also theorized to enhance deflagration; as the expanding flame from the ignition

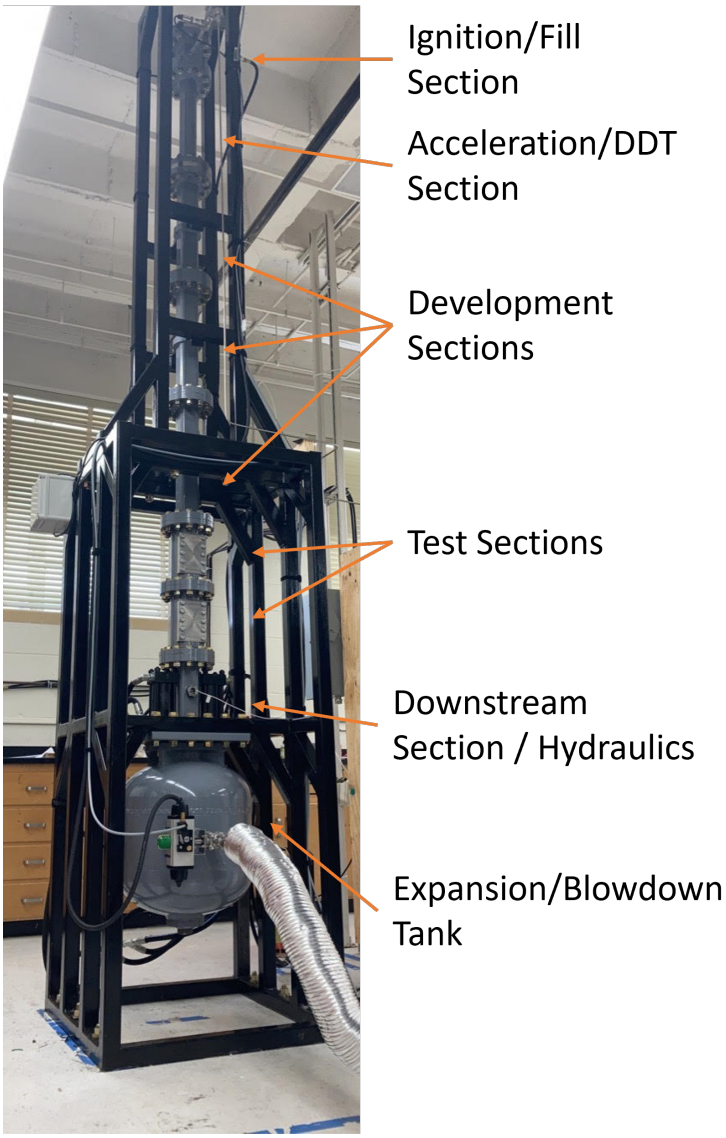

Figure 2.1: Image of facility as constructed. Individual section annotated.

source reaches the end of the tube, the wave is reflected onto itself, yielding an increased pressure.

2.2.2 Acceleration Section

The next section of the tube is the acceleration section, which is designed to accelerate the flame from the ignition source to a detonation wave in a short distance. The deflagration-to-detonation transition(DDT) mechanism is a well studied phenomena and somewhat well understood from an empirical standpoint. Fundamentally, the idea is to create turbulence in the deflagration and

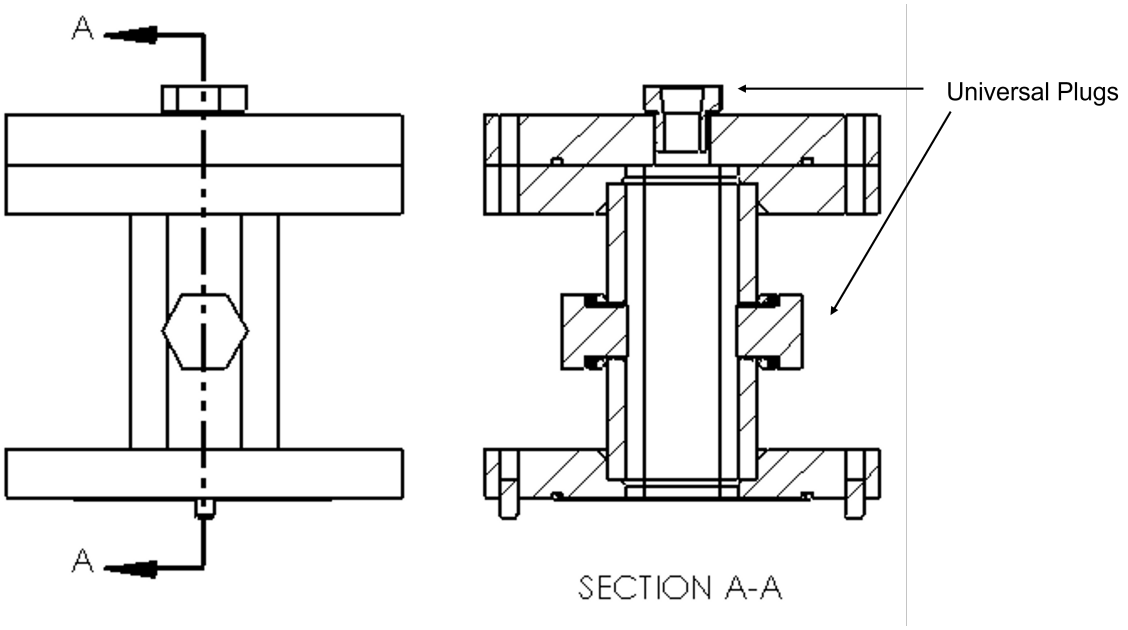

Figure 2.2: Schematic of Ignition Section. Note universal 1-1/8 x 12 plugs on sides and end of section.

accelerate it to close to the sonic plane, at which point a spontaneous transition from deflagration to detonation will occur. This effect was notably reported with rough wall tubes and turbulence-introducing elements in the 1950's and 60's by Russian scientists, namely R.I Shcelkin [20].

Parameters for turbulent element dimension are given by the blockage ratio, the ratio of the cross section of the tube to the unobstructed area of the turbulent element, and the characteristic element spacing (2.1)-(2.2). Desired blockage ratio was estimated from Peraldi [9] to be approximately 0.43. Desired ratio of critical length L to cell size λ was estimated from Dorofeev [21] as $\frac{L}{\lambda} > 10$. Methods of calculating the length of the turbulent element necessary for DDT were difficult pin down. It was eventually decided to use an element approximately 500mm in length similar to that used in [16].

$$BR = 1 - (\frac{d}{D})^2 \tag{2.1}$$

$$L = \frac{D}{1 - \frac{d}{D}} \tag{2.2}$$

The turbulent element chosen for this facility was a set of carbon steel springs. These were commercially available and calculated to have a blockage ratio of 0.41 and $\frac{L}{\lambda}$ ratio of approximately 16.8, close to empirically reported desired values. Two springs were welded together to achieve the desired length. In order to hold the turbulent element in place a flange with a reduced cross section is bolted between the acceleration section and further downstream sections. This flange also contains an expansion geometry at an angle of 30 degrees to diffract the detonation into the proceeding square tube. This angle is within the critical bounds of diffraction angles reported by [22].

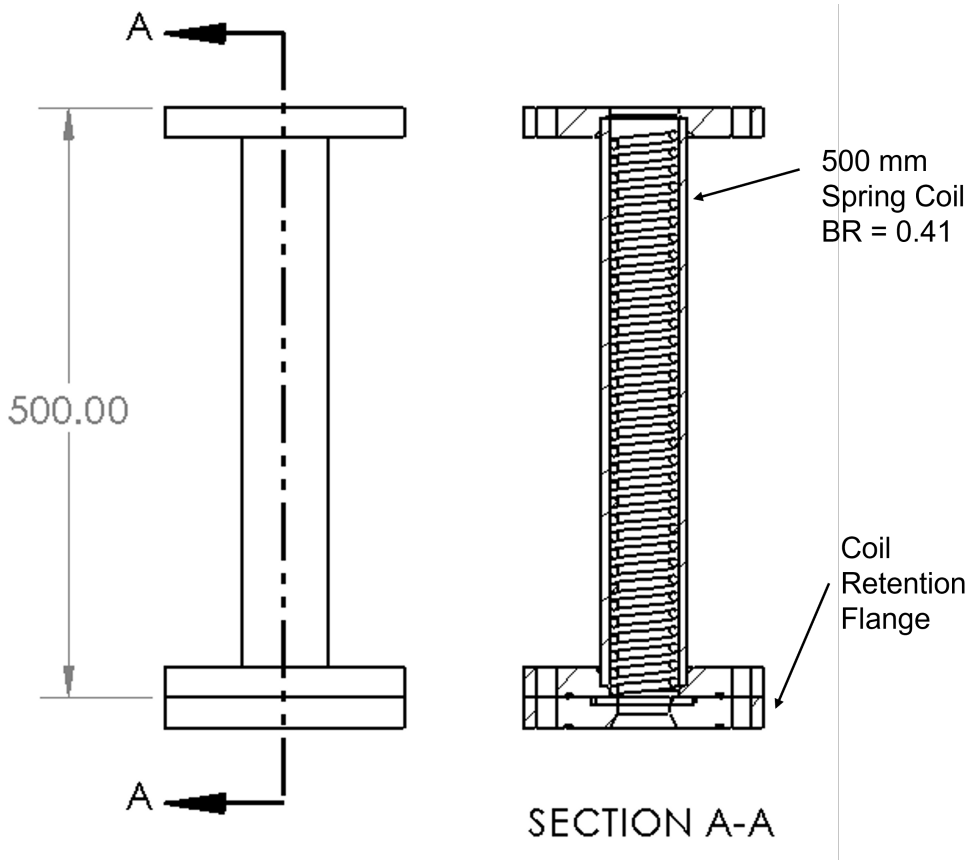

Figure 2.3: Schematic of Acceleration Section. Note Shcelkin coil and flange with expansion geometry to aid transition to development sections.

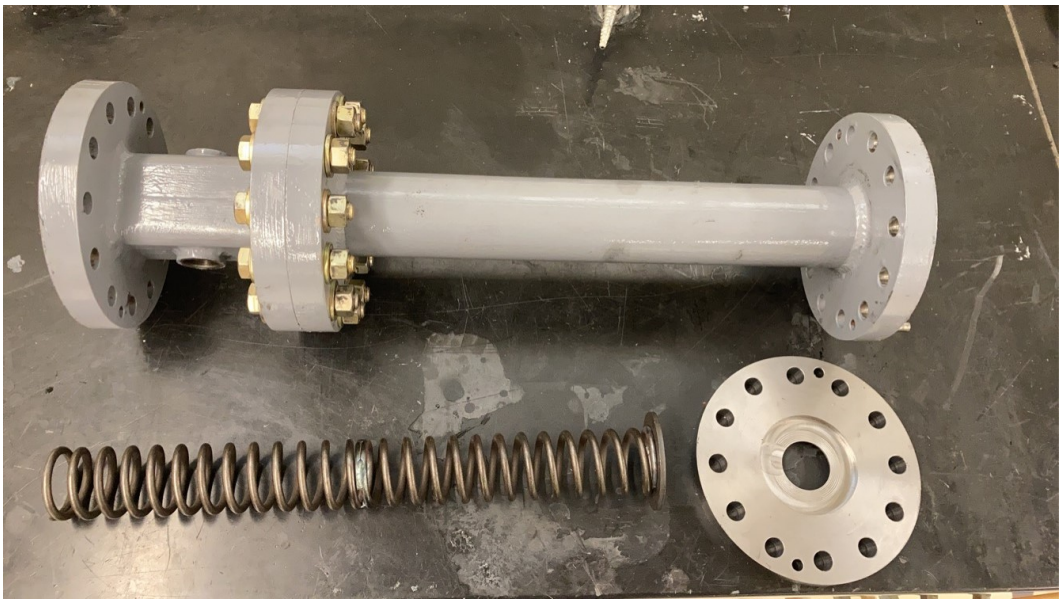

Figure 2.4: Ignition and acceleration sections dissembled. Note fabricated Shcelkin spiral assembly and retention flange.

2.2.3 Development Section

Proceeding from the acceleration section are three 500 mm unobstructed sections of tube of square cross section. These sections serve to allow the detonation to stabilize as it travels down the length of the tube before reaching the optically-accessible test sections. The overall length of 1.5 m for development was chosen estimating development distances of other aforementioned detonation tubes in the literature. With the modular design of the tube, additional sections may be added if more development length is deemed necessary.

Two ports for pressure transducers, ionization gauges, or photo-diodes are placed along the length of the development sections, 250mm apart and 125mm from each end. These allow for measurement of the detonation wave velocity and pressure profiles as it travels down the tube. Due to the size of the tube and wall thickness being relatively small, analysis was taken to determine how to reinforce the region around the pressure transducer mounting holes.

According to the ASME standards, reinforcement is necessary for pressure vessels of rectangular or square shape. Each section is thus reinforced at the middle with a steel band welded to

the tube. This band also serves as a tie-in point where the development sections are bolted into the tube frame. Bolting the tube to the frame at this point serves to reduce any sort of harmonic vibration encountered in operation.

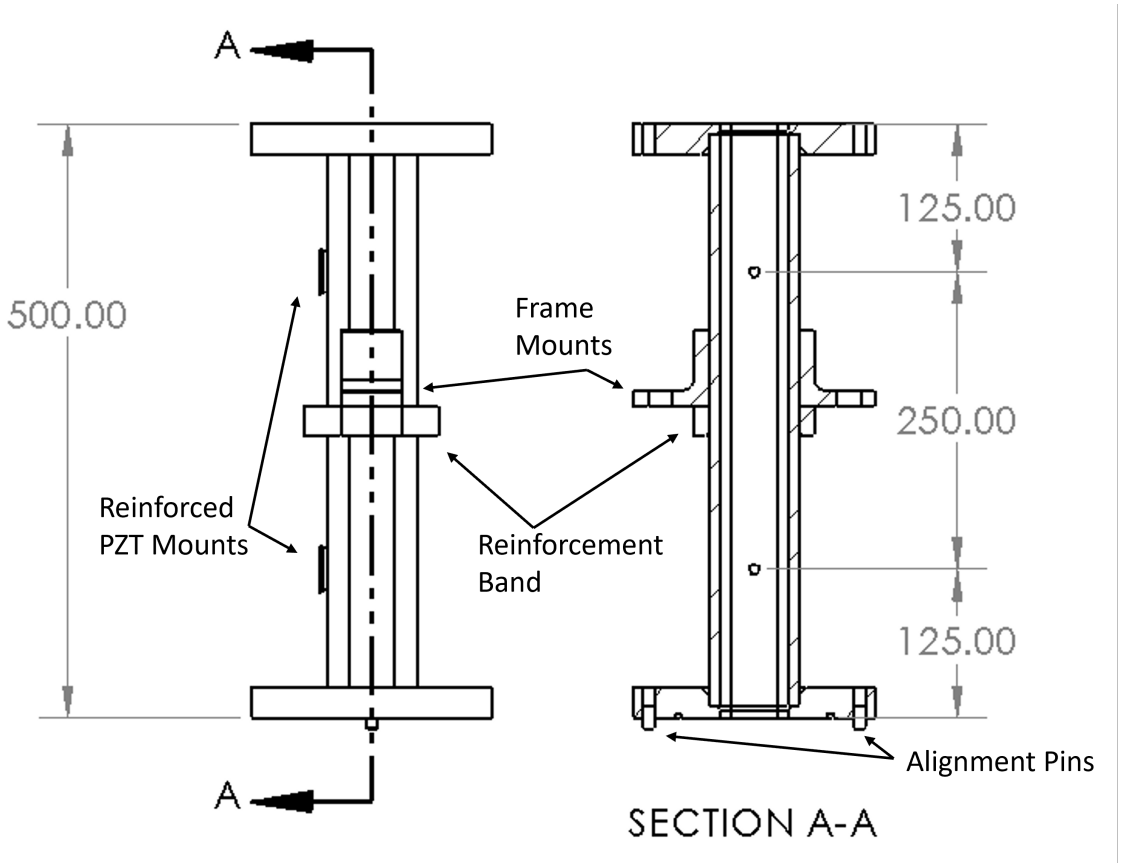

Figure 2.5: Schematic of development Section.

2.2.4 Test Section

It was required that the tube have optical access for high-speed imagery, laser-optical PDPA particle size measurement systems, and laser illumination, with the possibility of multiple imagery techniques to be used in concert during an experiment. To this end, it was decided that two test sections would be required. In order to provide optical through access necessary for PDPA systems and optical techniques such as Schlieren or Shadowgraph imagery, it was decided that the test

sections were to have opposing windows on each side of the tube.

The design of the test sections posed a unique challenge in the development of the facility. Ideally the windows would need to be as wide as feasible, while sitting flush with the inside of the tube, as well as being of sufficient length to capture multiple frames with high speed video cameras, or to use multiple high-resolution cameras in a single window (i.e. imagery at multiple light wavelengths). This posed a significant design issue as a rectangular hole cut into the wall of a square tube degrades the structural integrity of the tube to unacceptable levels.

Ultimately it was decided to machine the two test sections out of solid rounds of 4140 alloy steel, as this would provide the structural integrity for the window cutouts. All geometry, to include the flanges and mounting surfaces for the window coverplates was machined from the solid stock. The square cross section through the center of the test sections was wire-EDM machined to the desired shape. The maximum size of cutout in the wall of this section for the tubes was determined through FEA simulations to be 4.25 x 1.5 inches with 1/4 inch radii.

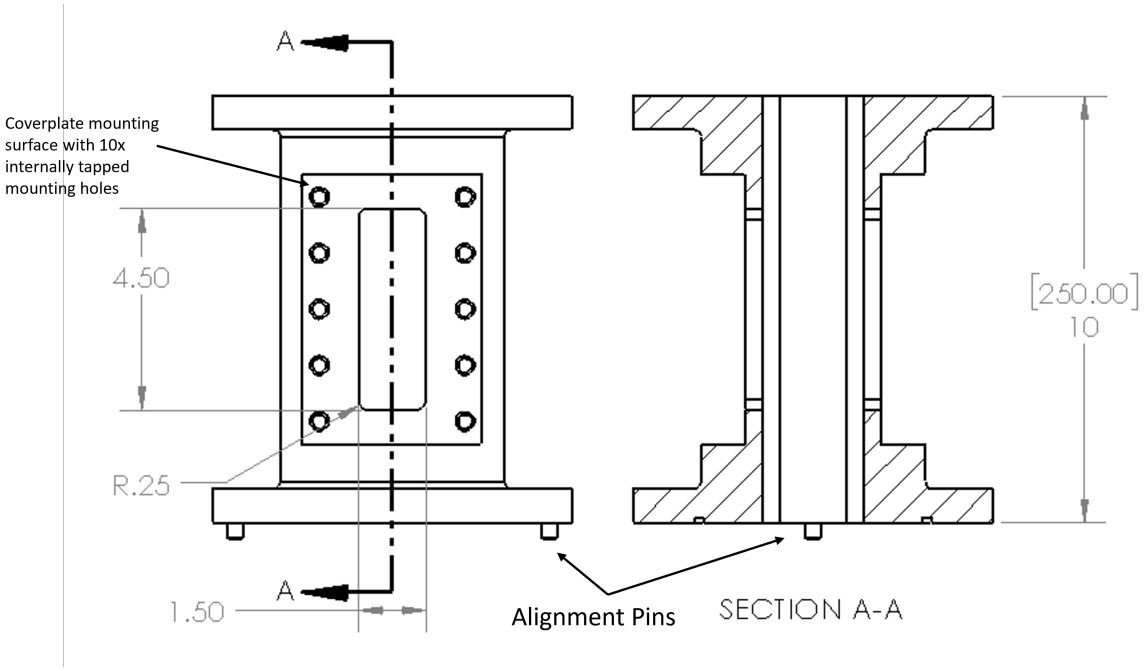

Figure 2.6: Schematic of Test Section. Dimensions of window cutout annotated. Section is symmetric for optical thru-access.

Material for the windows was selected as waterjet-cut tempered borosilicate glass. These were selected as they met both the estimated factor of safety criteria from both design guidelines [23] and FEA simulations. The windows are held into pockets machined in 304 stainless steel cover plates by 3M LocTite Hysol 1C 2-part epoxy, recommended by craft workers in the TAMU Chemistry Department. The windows are replaceable by kiln-heating assembly to remove epoxy.

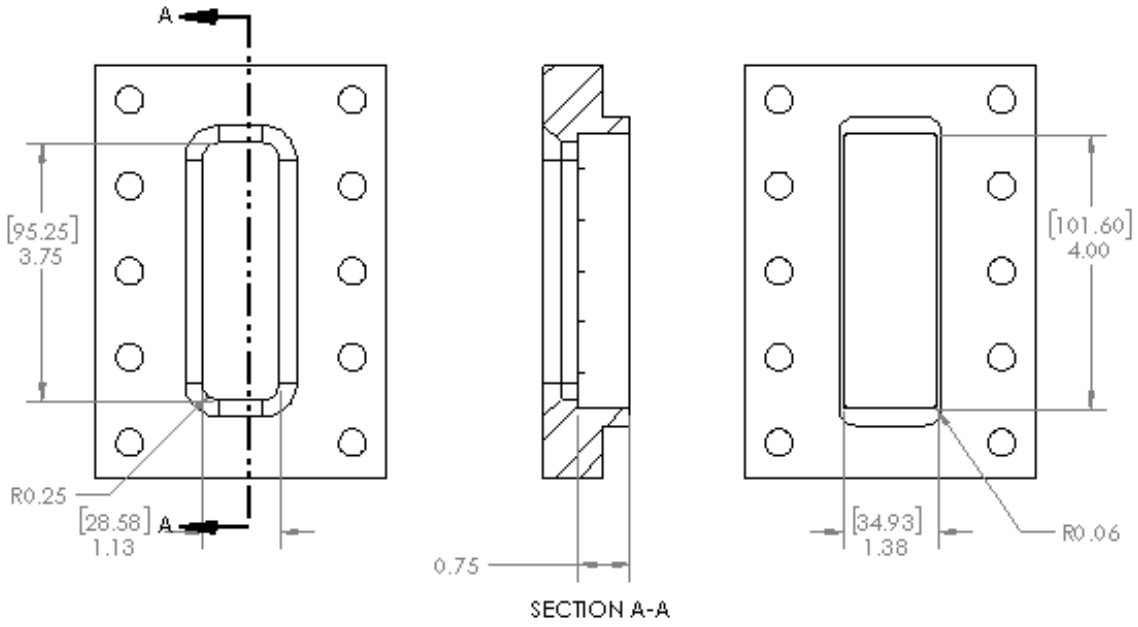

Figure 2.7: Schematic of Test Section window coverplate. Dimensions of visible area annotated. Note chamfer for expanded access to sides of viewing area.

A mounting system for optical diagnostics was designed to allow for both test sections to be used simultaneously. As it was desired that the frame be both modular and rigid, it was constructed from 45 mm extruded railing. The optical frame itself is mounted to the detonation tube frame by means of two crossmembers, with four vibration-damping rubber isolators in order to protect sensitive diagnostics from vibrations due to either the hydraulic systems or experiment itself.

Figure 2.8: Image of mounting frame for optical diagnostics.

2.2.5 Blowdown Section

In order to safely dispel the detonation wave, it was decided to implement an expansion chamber of a relatively large volume compared to the volume of the tube. This expansion chamber, or tank, filled with a heavy inert gas, quenches the detonation and allows for cooling and expansion the combustion products to temperatures and pressures low enough for the system to be safely vented to the exhaust system in the room. The chamber also serves to provide axial optical access for laser insertion.

A blank end flange at the end of the tube would not have been an acceptable option as this

would have resulted in the possibility of extreme high pressures. A reflected shock traveling at the estimated CJ velocity and pressure was estimated to push the static pressure to approximately 2.5 times the CJ pressure. With the additional considerations of possible DDT event at the end of the tube which could further multiply static pressures by a factor of 2-2.5, pressures would far exceed design pressures. A detailed discussion of such events is provided by Shepherd [24].

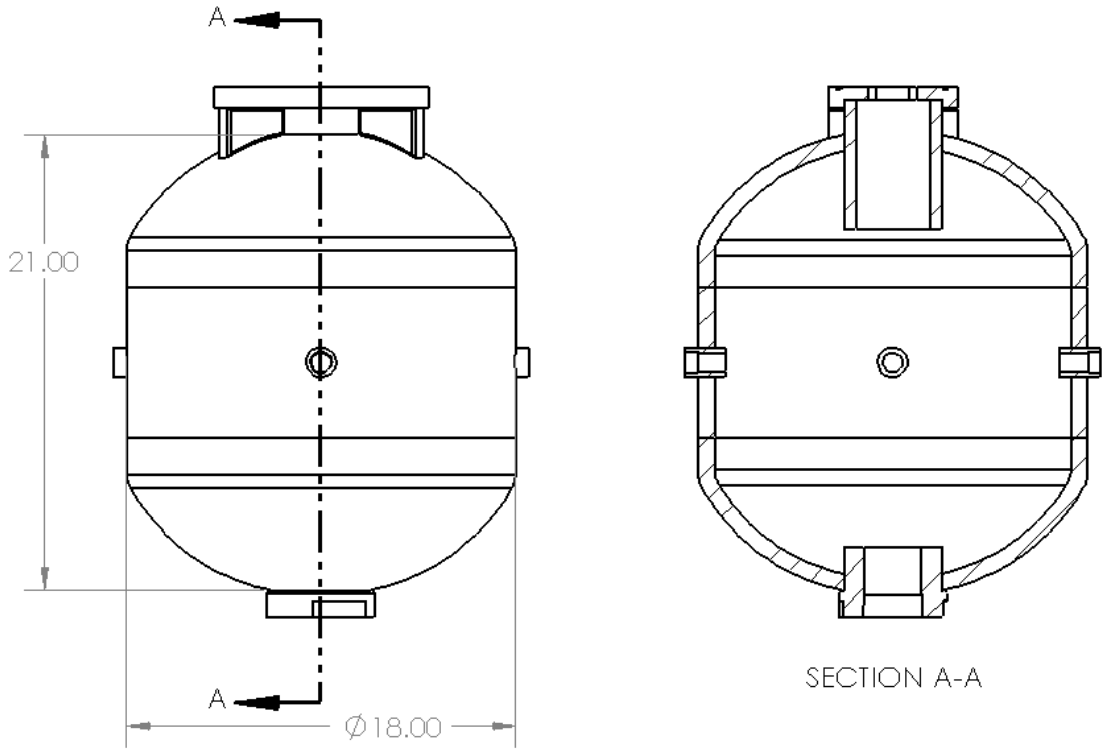

Figure 2.9: Schematic of blowdown section.

In order to separate the tank volume from the detonation tube during an experiment and keep the inert gas from mixing with the fuel-oxidizer mixture, or inversely keep fuel and oxidizer from the tank volume, it was necessary to devise a way of inserting a replaceable diaphragm between the two. The tank is held in place with two hydraulic rams, each capable of 12,500 lbs of clamping force. These rams raise and lower the tank, mating a reinforced flat section on the top of the tank to a special tube section on which the rams are mounted. The clamping force of the rams secures

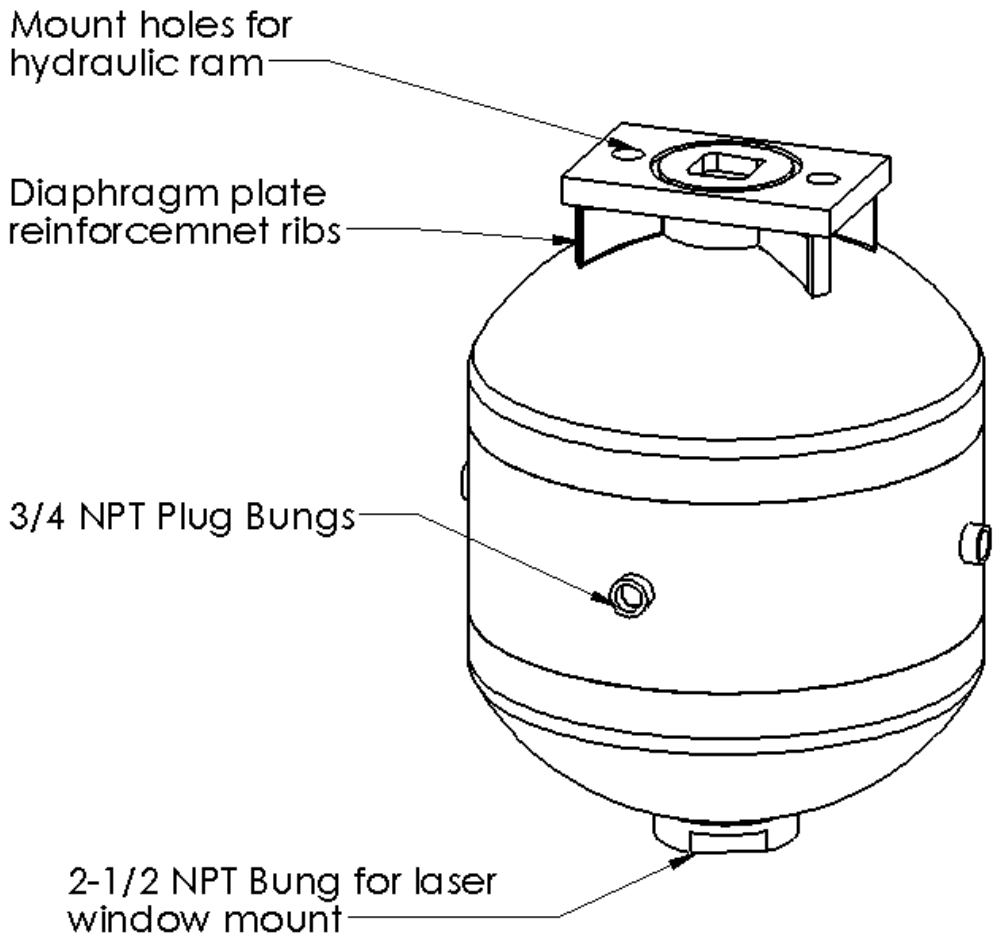

Figure 2.10: Blowdown section, features annotated.

a plastic diaphragm between the faces of the two sections, each face sealed with an O-ring.

The downstream tube section serves multiple purposes. On one end is welded a flange of the standard pattern to all of the other sections of the tube. The other end is welded to a 1 inch thick carbon steel plate that bolts into the frame to support the weight of the tube assembly. This plate is also where the hydraulic rams that secure the tank are mounted. In addition, there are two ports of the standard 1-1/8 x 12 plug size used in other places in the tube that allow for mounting of pressure transducers and valves.

The volume of the tank was limited by availability of materials. It was decided to proceed with

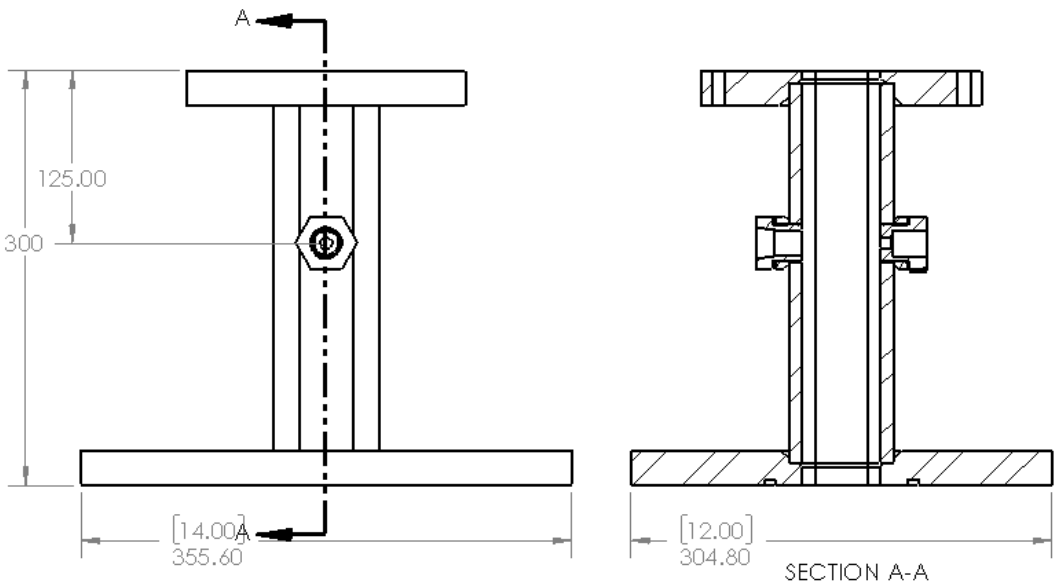

Figure 2.11: Schematic of downstream section.

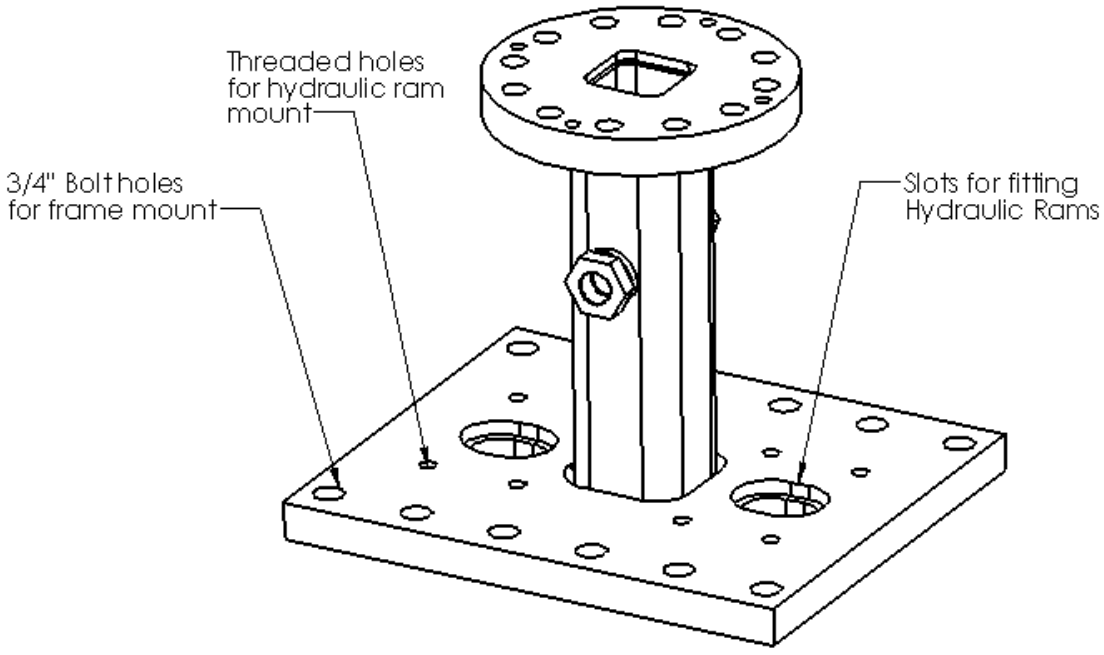

Figure 2.12: Downstream section, features annotated.

a design consisting of a section of 18 inch diameter Schedule 80 pipe and two ASME standard elliptical tank heads welded to each end. Welded to the circumference of the pipe section are four 3/4 NPT ports, to provide locations for valves in order to fill and vent the tank. There is also a 2-1/2 NPT reinforced port at the bottom of the tank to allow for mounting of optical windows through which a laser sheet may be inserted; this allows for laser illuminated imaging of events in the test section when using clear diaphragms. As the system was highly unorthodox to the relevant standards, extensive use of finite element simulations was made on the tank assembly, both for internal pressures and stresses on the flat plate the hydraulics are affixed to.

The final temperatures and pressures of the combined system of the tube and tank post-experiment were estimated from simple thermodynamic calculations. Here the detonation itself was neglected and the tube was considered to be a volume of hot post-detonation stoichiometric combustion products. The pressures and temperatures of these products were estimated as those expected from an adiabatic expansion from the CJ point to a pressure 0.4 times the CJ pressure [18] and zero velocity. The tank is considered to be a volume of quiescent CO_2 at STP, this being a readily available inert gas. The equilibrium state was estimated by adiabatically mixing combined system and then the equilibrium between the mixture and the mass of the tube, approximately 400 kg of carbon steel. Equilibrium calculations in both gaseous propane and liquid dodecane and oxygen yielded similar pressures and temperatures on the order of only tens of kPa and several Kelvin above STP. In practice a thermouple placed in the side wall of the expansion tank registered approximately 40 C internal gas temperature immediately post experiment, dropping to ambient 20-25 C within a period of several minutes.

2.2.6 Misc. Tube Design Features

To provide a degree of modularity to the detonation tube, a universal plug design was selected and implemented in the ignition and diaphragm loader sections. These plugs were machined in bulk from 1.5 inch carbon steel hex bar and threaded to 1-1/8 x 12 UNF. In doing so, the blank plugs could be machined to fit pressure transducers or any size of NPT or UNC/UNF thread necessary for plumbing. FEA analysis and ASME code were referenced for the length of the plug threads

State	Pressure [MPa (PSI)]	Temp [K (F)]
Initial	0.1 (14.7)	298 (68)
CJ Point	4.13 (600)	3883 (6530)
Adiabatically expanded products	1.6 (232)	3120 (5156)
Adiabatic Mixing of tube and tank volumes	0.48 (50.34)	910 (1179)
Equilibrium between mixed gas and tube mass	0.11 (15.5)	295 (72)

Table 2.3: Dimensions of surveyed multiphase detonation tubes

and reinforcement of the opening in the tube walls to ensure that the design would be sufficient.

In order to ensure a smooth transition between tube sections and avoid any discontinuities in the internal surface that would disturb the wave, several measures were taken. The raw carbon steel square tube had an internal weld seam that was ground down flush with the walls. Each flange was socket welded to the tube both internally and externally, with the internal weld seam ground flush to the proper dimensions. Additionally, the flanges on each section were designed so that one flange would have a press-fit set of dowel pins and the other a set of slip fit holes; each tube section is mechanically located to each other to ensure continuity.

2.3 Systems

2.3.1 Control System

A control system was built in LabView to handle the operation of the tube and data collection and diagnostic synchronization. This system allows for full control of tube systems from a safe, remote location. The system operates in two phases. In the first phase any of actuated valves in the system are able to be operated as necessary for readying an experiment. Here pressures in the gas manifold system are displayed. From this stage, the user has the option to either proceed with or abort the experiment, either of which closes and disables control of the actuated valves in the system. In the case proceeding, the ignition system is actuated and the data collection system begins recording for a predetermined time and collection rate. In the case of an aborted experiment, the system purges the tube with dry Nitrogen to safe partial pressure outside the flammability limits.

After a set time-out period, control of actuated valves is re-enabled, allowing for venting of the tube to the laboratory exhaust system.

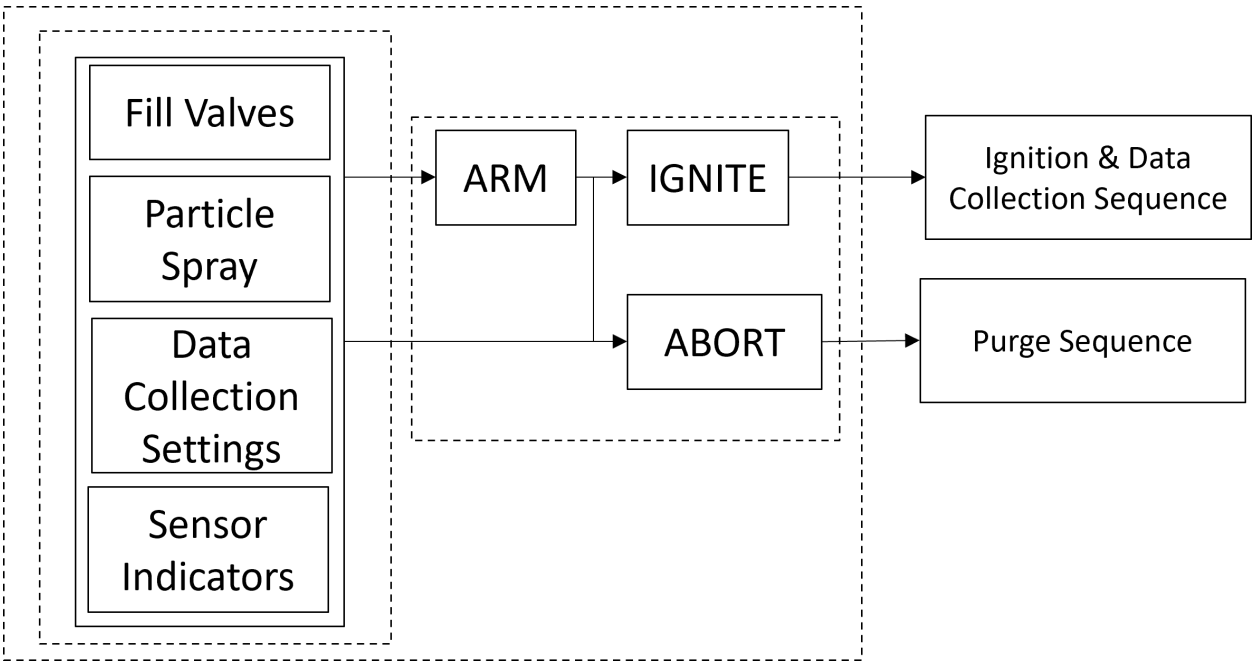

Figure 2.13: Block diagram of labview control system.

2.3.2 Ignition system

A reliable, repeatable source of ignition is required for experiments. In order to provide this, an ignition coil driver circuit was created from readily available components, consisting of a triac, capacitor, step-down transformer, and automotive injection transformer. A commonly available household dimmer switch contains a triac, a switch which is signaled to open and close by the frequency of the supply voltage, standard 120 VAC 50 Hz, at a rate determined by the position of the dimmer switch dial. As the triac opens and closes the circuit, the capacitor is allowed to charge and discharge. As the device charges and discharges, the polarities are switched, doubling the discharge voltage.The switched AC power acts similar to the pulsed DC power the ignition coil is designed to operate from.

The capacitor used initially was a 440 VAC 10 MFD AC Motor capacitor. The operating voltage was set to nominally 240 VAC by adjusting the dimmer switch while measuring voltage across the terminals. Discgarge energy was estimated by Eq 2.3 with an efficiency of about 90 percent to be approximately 260 J. This energy was found to be sufficient to initiate detonation in propane-oxygen mixtures. Spark voltage was estimated through Paschen's law. The spark plug was gapped to various distances until a spark could no longer be attained at a gap distance of about 5 mm. In atmospheric air this corresponds to a breakdown voltage of approximately 2 kV. It is considered that a larger capacitor may be necessary to ignite a multiphase mixture, or some other method such as an exploding bridgewire or an explosive charge may be necessary.

$$E = \frac{1}{2}CV^2 \tag{2.3}$$

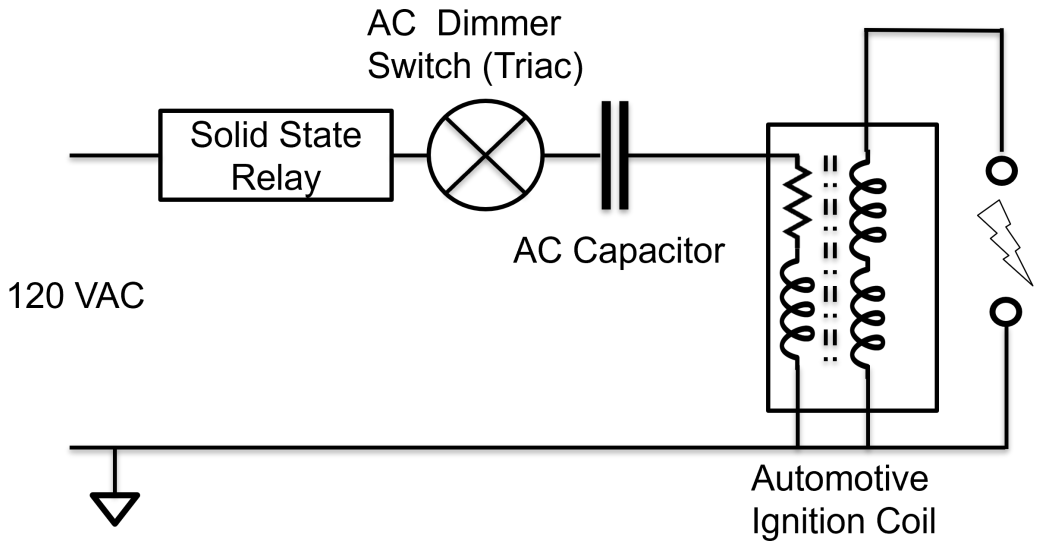

Figure 2.14: Diagram of Ignition System

2.3.3 Pressure Diagnostics

The tube is ported for pressure transducers in six evenly spaced locations, 125 mm apart, along the length of the development sections with an additional port downstream of the test sections, 1000 mm from the previous transducer. The transducers in the development section allow for measurement of both the pressure profile of the detonation event and a method to estimate detonation wave velocity. The single transducer downstream allows further determination of changes in detonation behavior through the test sections, as well as an observation of any reflected waves from the diaphragm separating the tube and tank sections.

The transducers chosen for this facility were the PCB Piezotronics CA102B04 dynamic pressure transducers. These transducers are capable of reading pressures up to 1000 psi with an overrange of 2000 psi, pressures greater than expected or observed, at a rate of up to 1 MHz frequency with a rise time better than 1 us. This model is also electrically isolated and capable of sustaining the flash temperatures of the detonation, environmental concerns addressed through conversations with PCB field engineers.

2.3.4 Manifolds

2.3.4.1 Gas Manifold

A system to handle gas filling, vacuum, and exhaust venting is necessary for all experiments, both for liquid and gaseous fuels. The system as design consists of both manual and actuated valves, with several important safety measures.

Valves on any port of the tube open to either the gas manifold or exhaust system were required to be both flame/fire resistant as well as being rated to sufficient pressure for the detonation. Pneumatic actuated fail-close valves with graphite seals were sourced from Assured Automation for the gas fill port at the top end of the tube and the exhaust port in the tank. These allowed for safe operation of the manifold with the operator separated from the facility by a protective barrier. Pneumatic operated ball valves were selected as they do not provide no hazard of an electrical ignition source and operate on relatively slow open/close times as to not send an errant shock through

a combustible mixture, a possibility with fast-acting solenoid valves. Manual ball valves of similar construction sourced from Discover Valve were selected for applications where a combustible mixture would not be present in operation.

The fill system was designed to allow for partial-pressure filling of the tube with gasous mixtures from vacuum to atmospheric or near atmospheric pressures. The regulators on each tank are rated to accept vacuum, with similarly rated gauges. High pressure needle valves are used to individually separate the combustible mixtures, purge N2, vacuum, and line to the tube, as well as to isolated the combustible mixture gauge and vacuum gauge from high pressures of the N2 purge line. In addition to serving as isolation valves, the needle valves serve as blocker valves/orifices through which a detonation could be isolated, should such an event arise. A detonation arrestor is further placed in between the pneumatic fill valve and gas manifold system, should the fill valve fail.

2.3.4.2 Particle Generation System

To fill the tube with particles, a pressurized spray-injection system was implemented. The fuel supply system consists of a 300 mL Swage-Lok sample cylinder rated to 1800 psi with valves for filling and draining liquid fuel as well as an isolation valve to the nitrogen supply. A hard line leads from the bottom of the pressurized fuel vessel to the injector system. The injector system consists of a replaceable spray nozzle, backflow check valve, high-pressure solenoid, and compression fitting mount. The spray nozzles selected are easily replaceable and may be switched out for different orifice diameters. The check valve protects the high pressure solenoid from any back pressures through the nozzle inside the tube. The entire assembly is affixed to the tube using a 5/8 inch compression fitting secured to a cylindrical coupling. This allows for the assembly to be easily removed in seconds, allowing nozzle replacement between experiments. In practice, fuel mass flow rates may be modified with through either modifying supply pressure or the addition of a orifices between the supply and injector assemblies.

2.3.4.3 Hydraulic System

A simple hydraulic system was assembled in order to operate the rams that raised and lowered the blowdown section and sealed the tube/diaphragm during experiments. This system consisted of 10 kpsi pump with an integrated three way Up/Neutral/Down switch, an adjustable crossover relief valve, and an isolation valve on the 'pull' side. The pump would be kept on during experiments to provide a constant 3000 PSI pressure to the rams clamping the diaphragm in place. The crossover relief valve kept pressure from building up in the system and also allowed for relief of any transient pressures due to loading from internal gas pressures on the blowdown tank during an experiment. The isolation valve further allowed the system to be sealed with pressure on the rams for extended amounts of time (i.e. sealing the tube for 24 hours to allow for diffusion mixing of gas fuels). Electrical or vibrational noise from the pump was not evidently observed in the data collection systems.

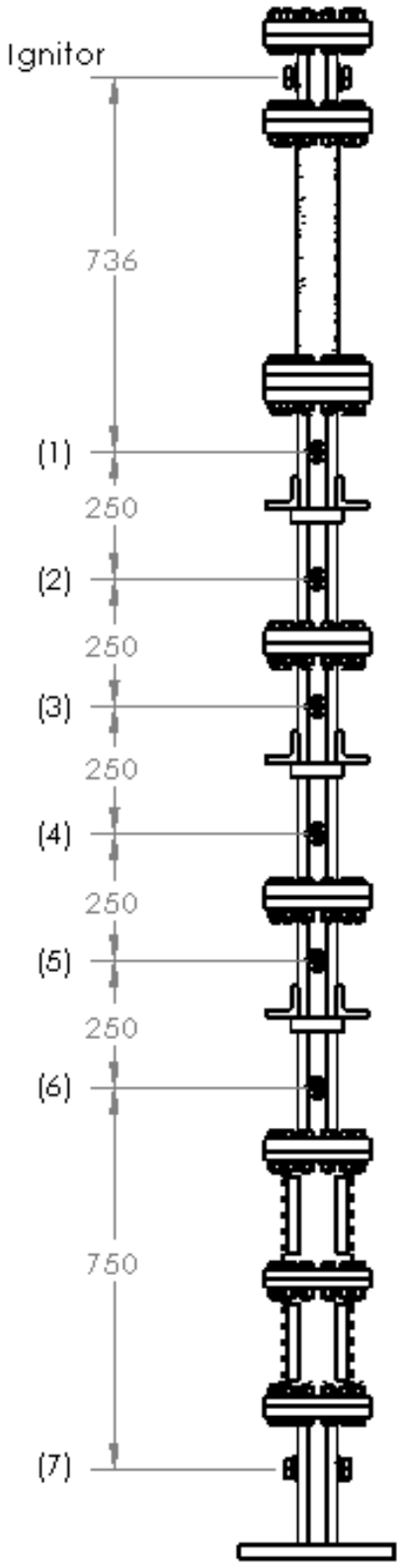

Figure 2.15: Diagram depicting pressure transducer locations and spacing, including distance to ignition source.Dimensions in [mm]

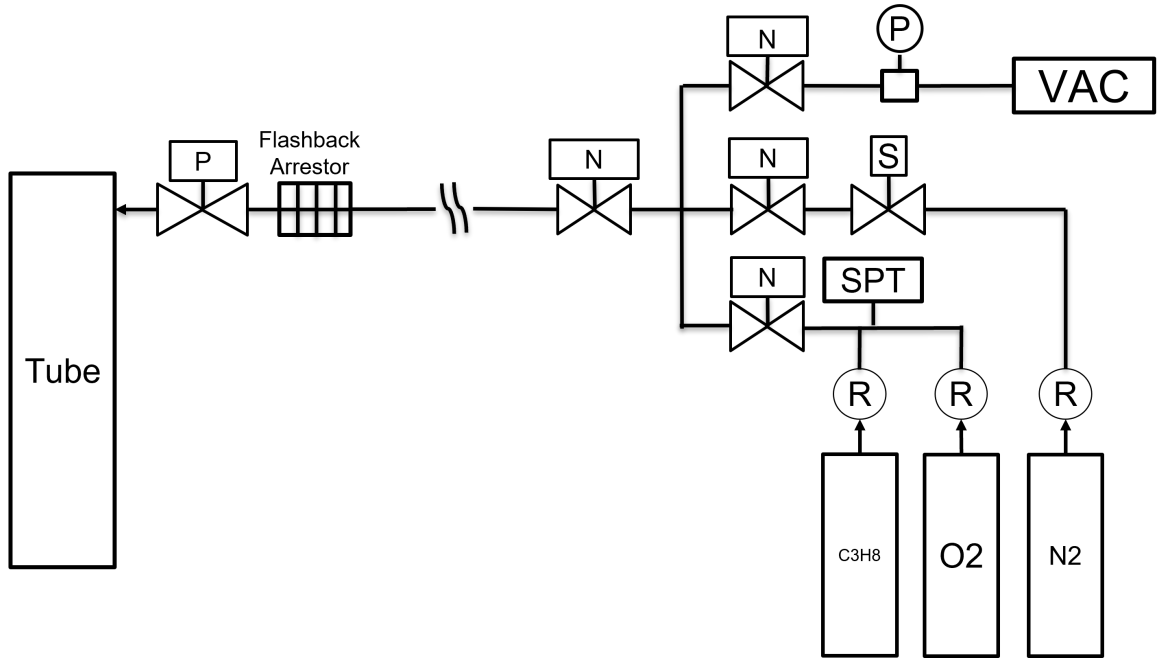

Figure 2.16: Gas manifold for filling tube at ignition section.

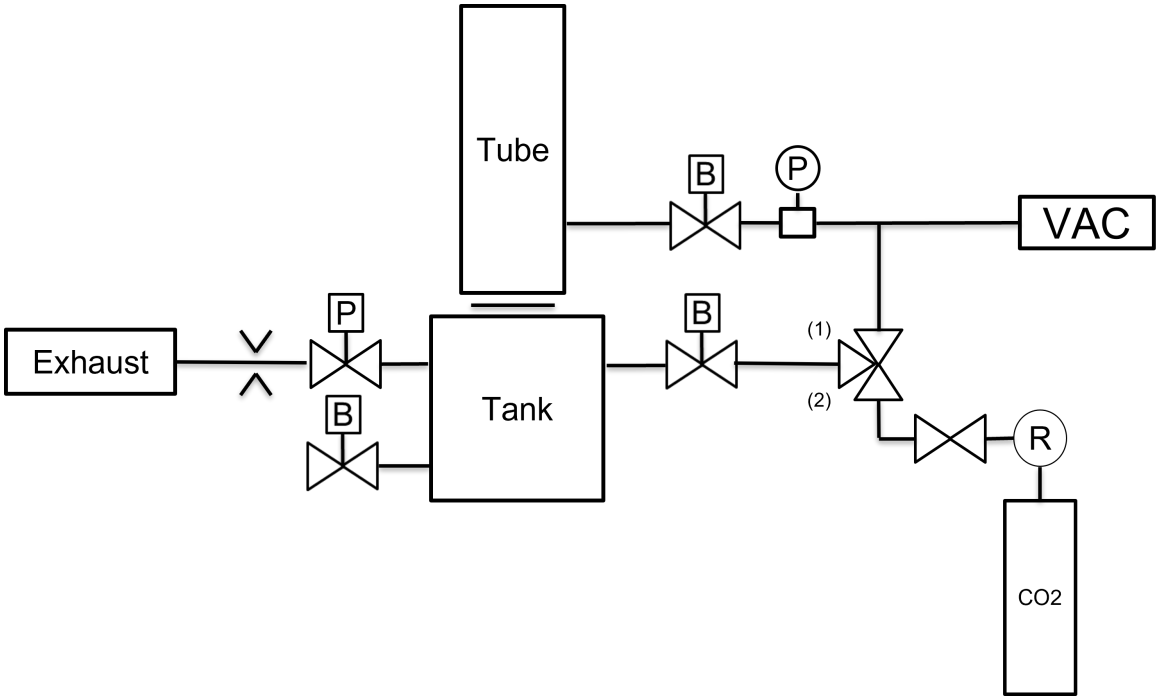

Figure 2.17: Gas manifold for vaccuming tube/tank, filling tank w/ inert gas, and exhausting.

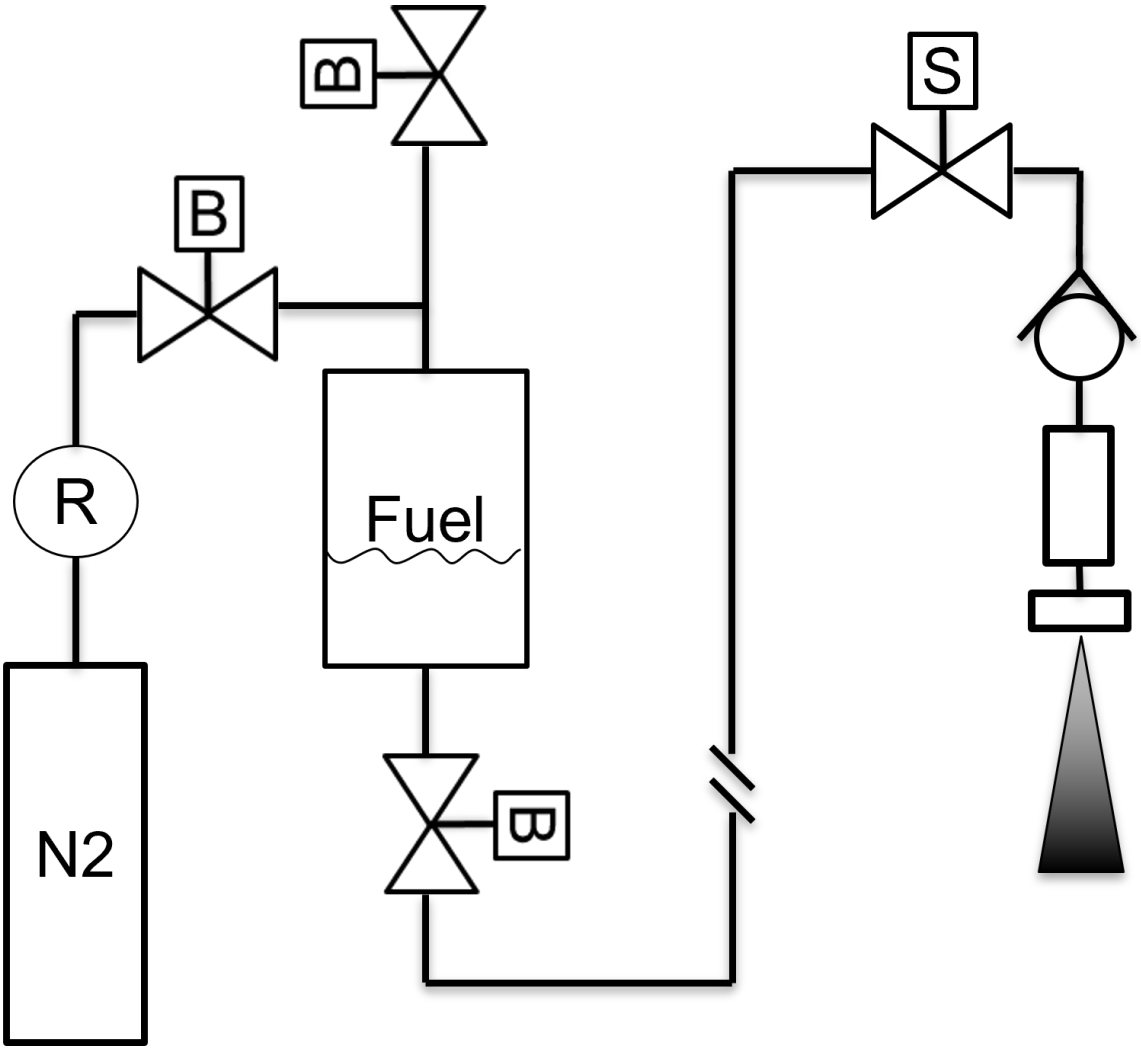

Figure 2.18: Diagram depicting pressurized fuel supply and injection system.

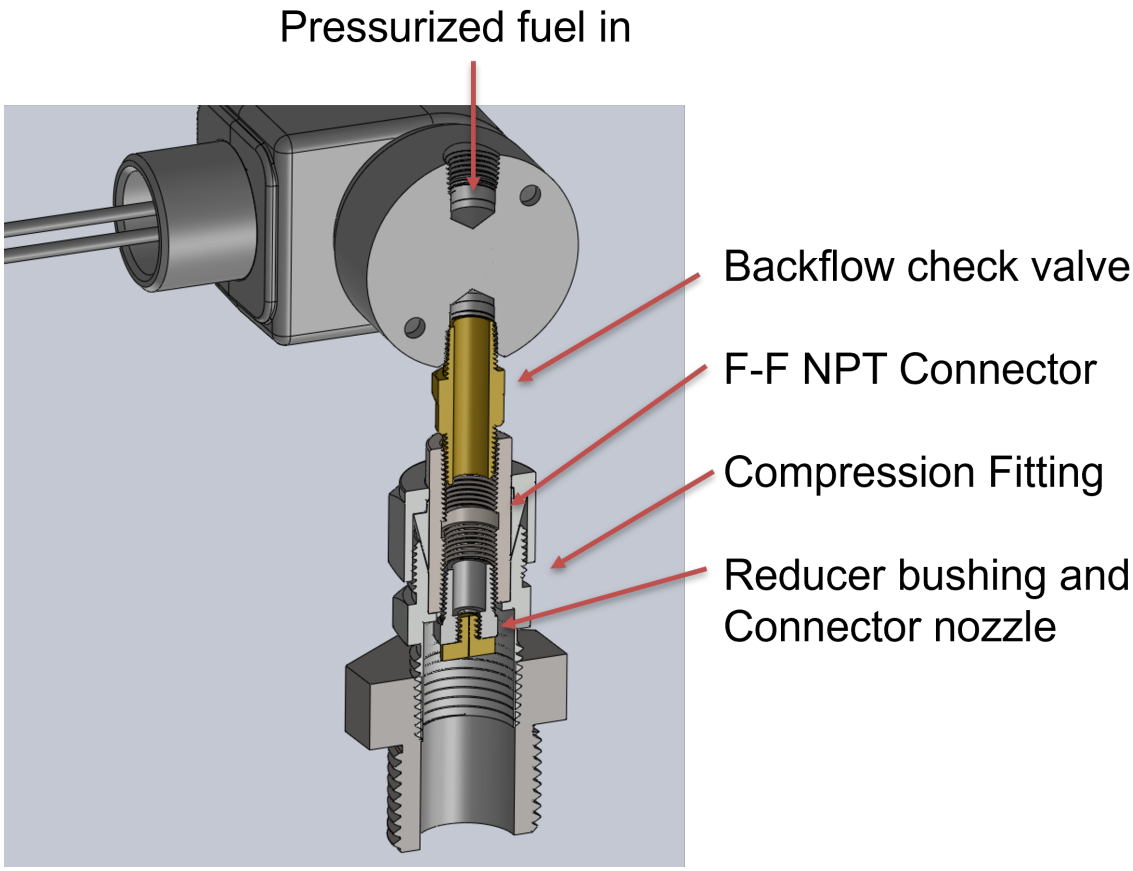

Figure 2.19: Annotated diagram of spray control assembly.

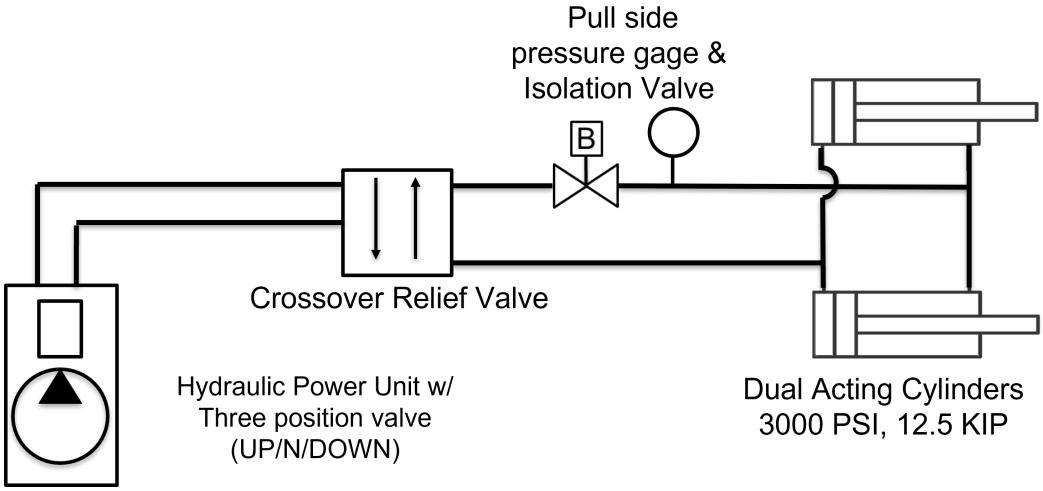

Figure 2.20: Annotated diagram of hydraulic system.

3. VALIDATION EXPERIMENTS

3.1 Gaseous Fuel Experiments

In order to test the tube systems, operating procedures, and data collection systems, a run of experiments of detonations with in a stoichiometric propan-oxygen mixture was conducted. This particular mixture was selected as it should detonate at CJ velocities and pressures similar to those predicted or reported for the liquid hydrocarbons of interest. [25]. Propane is also cheap, commonly available, and requires few additional safety considerations.

3.1.1 Filling Procedure

The procedure for readying experiments was conducted as follows: **(i)** Both the tube and tank volume were vacuumed using room vacuum. **(ii)** The blowdown tank was filled to 1 atm with CO2. **iii** The tube was filled with oxygen to atmospheric and vacuumed to flush out remaining nitrogen. **iv** The tube was then filled with oxygen to the desired partial pressure. **(v)** The tube was filled with propane to the remaining pressure up to 1 atm. **(vi)** The mixture was then allowed to diffuse for the estimated amount of time until the mixture reached homogeneity. Partial pressures were calculated as 84.43 kPa absolute for oxygen and 16.89 kPa for propane.

An estimation for the 1D diffusion times of propane into oxygen was calculated with Fick's diffusion law, Eq. 3.1 , using empirical coefficients from [26], D being 0.115 cm^2/s. The resultant values are plotted in Fig. 3.1. The problem is set up as two quiescent mixtures separated at time t=0. The calculations showed that a diffusion time of approximately 96 hours would be required for the mixture to attain homogeneity. It was expected that the mixing time would be lower than calculated due to hydrodynamic mixing, the tube being filled at the partial pressure with oxygen before the propane was inserted at a higher pressure. Experimentally it was observed that diffusion times between 24 and 96 hours showed little appreciable difference in measured pressures and velocities.

$$J = -D\frac{d[n]}{dx} \tag{3.1}$$

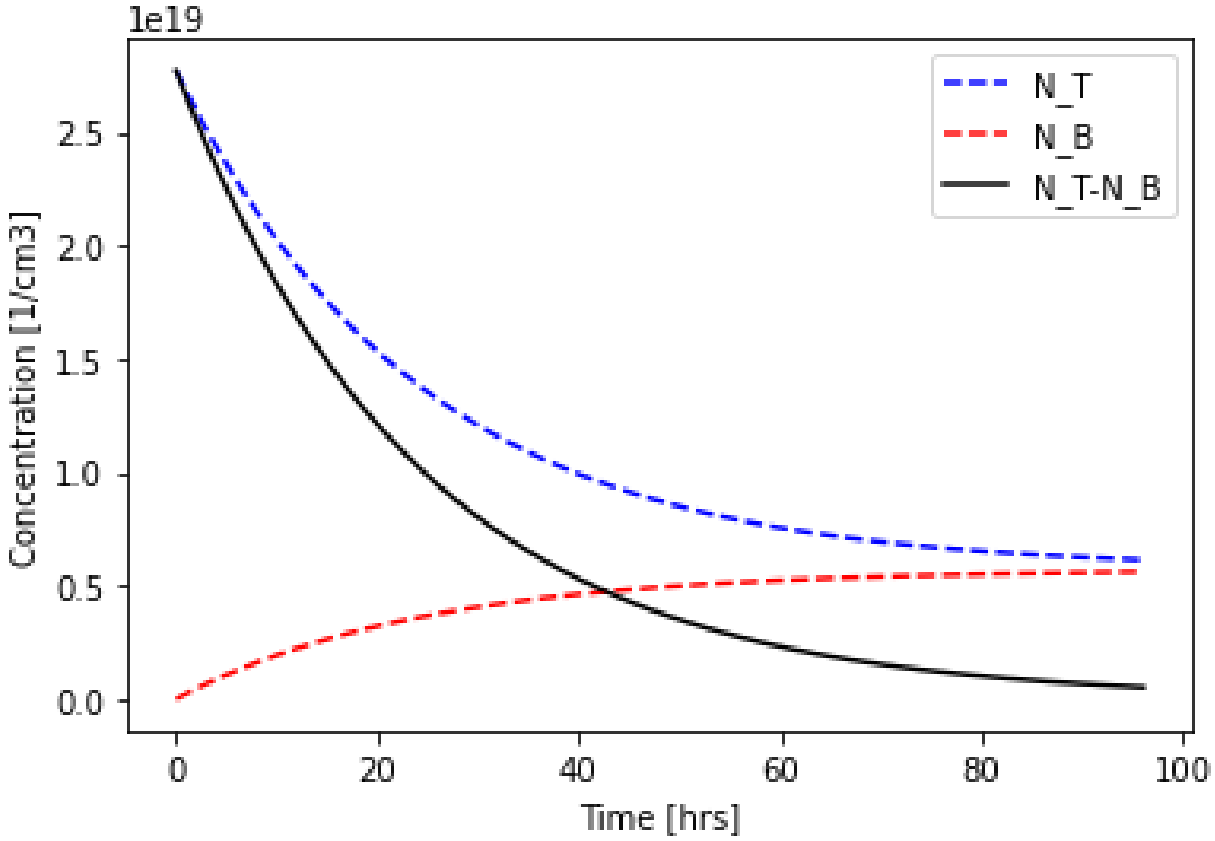

Figure 3.1: Calculated 1D diffusion times according to Fick's law with empirical coefficient. NT, NB molar concentrations of fuel in initial volumes propane,oxygen regions.

Initially only three pressure transducers were inserted into the tube, PZT's 1,3, and 5, at locations 1, 5, and 7. These locations were chosen as they were 1000mm apart. Eventually two more pressure transducers were added, 2 and 4, at locations 3 and 4 downstream of PZT 1 in order to observe the detonation wave as it developed; PZT 1 indicated the profile of the detonation wave immediately as it exited the acceleration section.

PZT	PZT Loc	Dist. From Ignitor [mm]	δx
1	1	720	0
2	3	1220	500
3	5	1720	250
4	4	1470	250
5	7	2720	1000

Table 3.1: PZT numbering, locations, and absolute and relative positions within the tube.

3.1.2 Gaseous Fuel Experiment Results

Initial experiments were run with lean ratios less than stoichiometric in order to limit the loading of the tube in case of failure. These runs also served to test and modify the developed procedures, as well as establish operating parameters such as time and rate of data collection, ignition spark on time, and post-experiment equilibrium time to exhaust.

For each experiment the readings from the dynamic pressure transducers was recorded and post-processed into plots to determine the detonation pressures and velocity. The detonation velocity was calculated by taking an intermediate point on the leading edge of the pressure spike, midway between static and the peak pressures. The CJ pressure was estimated from the peak values. A representative sample of pressure traces from experiments is provided in appendix 2.

Figure 3.2 depicts experimental results with a full complement of pressure transducers at a nominal equivalence ratio of 1.1. This experimental run is representative of a successful experiment is presented here for discussion. Measurements of spike pressures and velocities based on spacing and rise time align well with theory (P_CJ within $+2.5 - 8.5$ percent and V_CJ within $+1$ percent.

For each pressure profile the structure of a detonation is qualitatively present; there is a strong preceding spike followed by an expansion to approximately 0.4 P_{CJ}. In all experiments the first pressure transducer, 125mm from the exit of the acceleration section, yielded lower spike and post-detonation pressures than the transducers at other locations. The reasons for this behavior were unclear; the most likely explanation was a transient event as the detonation emerged from the

acceleration section and expanded into the development sections. For each subsequent transducer the pressure profiles were more uniform and showed similar behavior. For each experiment the last pressure transducer in the tube (location (7), downstream of the test sections) registered what appears to be a reflected wave from the diaphragm separating the tube and blowdown section, as well as a relatively high post-detonation pressure, similar to re-shock in a shock tube. This re-shock like event was not taken to be of great concern as pressures subsided relatively quickly.

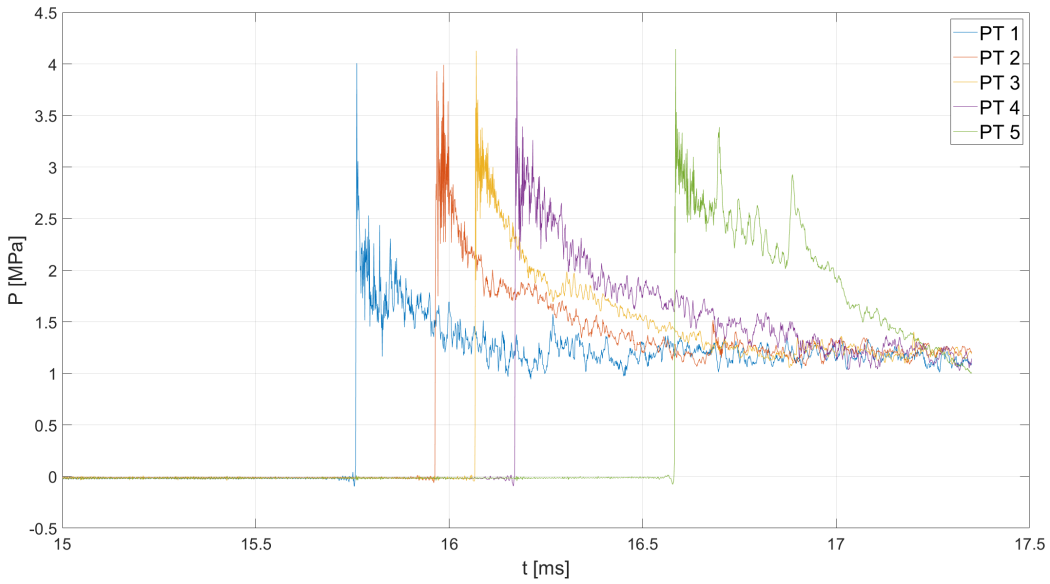

Figure 3.2: Pressure traces from propane-oxygen experiment RUN 13, nominal ER 1.1

ER=01.112	P [MPa]	P_{CJ} [m/s]	V_{ign} [m/s]
Experiment	3.93-4.148	2427-2433	517
SD Toolbox (CJ Cond.)	3.83	2409	

Table 3.2: Measured and Calculated CJ velocities and pressures, Propane Oxygen Experiment RUN 13. Time of arrival from ignition to first pressure transducer included.

The signals from the static pressure transducers appeared to be much noisier than signals recorded from similar transducers used in the laboratory's Mach 2.5 shock tube facility. The apparent noise caused some concern, as it could indicate an issue with the tube systems and obscure the events occurring inside the experiment. After several conversations and a site visit with a PCB Piezotronics engineer, it was ascertained that the likelihood of the such noise in the transducer data was low and they were likely recording real events, as all systems were properly installed, shielded, and grounded. A plausible explanation would be the inherent three dimensional structure of the detonation, with reflected transverse waves traveling at or behind the detonation front.

The question of what the spike pressures of the signals indicated was also of particular interest. As per conversations with the PCB engineer, these signals were also likely real. The SD Toolbox calculations for the ZND structure of a propane-oxygen detonation indicate a combined exothermic and induction length $O(10[um])$ and time $O(100[ns])$. The stated rise time of the pressure transducers is at least or better than 1 us. Given this information and the signals registered, it is likely that spike the pressure transducers recorded was not the Neumann spike but instead a component of the induction and reaction zones near the CJ pressure.

3.1.3 Validation of Tube Systems

The run of propane-oxygen detonation experiments proved that the detonation tube could operate safely at similar loadings to those predicted in the multiphase experiments. After about 15 experiments the tube components were analyzed for signs of degradation; no outward structural issues or leakage were observed. Valves, fittings, and other ancillary components showed signs of sooting but no degradation. It was noted that the spark ignition system did experience fouling and needed regular cleaning.

4. LIQUID FUEL EXPERIMENTS

An initial run of experiments were conducted to investigate the behavior of the spray systems and to observe any idiosyncrasies of a multiphase environment inside the tube. These experiments served to provide insight into operation of the multiphase experiment and demonstrated that a thorough understanding of initial conditions was necessary in order to arrive at a repeatable experiment.

4.1 Spray Nozzle Characterization

The spray nozzles used in multiphase experiments where characterized ex-situ in order to determine operating parameters. This type of nozzle had previously been investigated for use in the lab's shock tube facility and showed repeatable size distributions with water and acetone. They are also relatively economical and readily available, making them an attractive option for a detonation environment as damage to the nozzle was a concern. Nozzles of various available orifice diameter were investigated for mass flow rates and generated particle size distribution at various fuel supply pressures.

Mass flow measurements were conducted for a set of 0.3 mm and 0.1 mm orifice diameter nozzles. The measurements consisted of operating the nozzle for one minute while collecting the output in a graduated cylinder, which was then weighed and the volume collected observed. An important observation in these studies was that the 0.1 mm nozzles were subject to failure after several runs, the likely candidate for such being particulate matter in the fuel clogging the nozzle. In-line fuel filters of 10-25um rating were implemented in the system which appeared to rectify the issue. Mass flow rate studies were performed for each filter size in order to characterize their effect on operation.

Droplet size measurements were conducted ex-situ with a TSI PowerSight PDPA (phase doppler particle analyzer) system. This system operates by analyzing collected scattered laser light from two lasers intersecting on a measurement region, returning the size distribution $(D10/D20/D32/D43)$

of particles as well as a component of axial velocity in the spray direction. Nozzles of 0.1 and 0.3 mm orifice diameter were tested at supply pressures of 40 and 80 psi. The resultant size distributions were similar and showed little variation with supply pressure. Several of these distributions are provided in Appendix C.

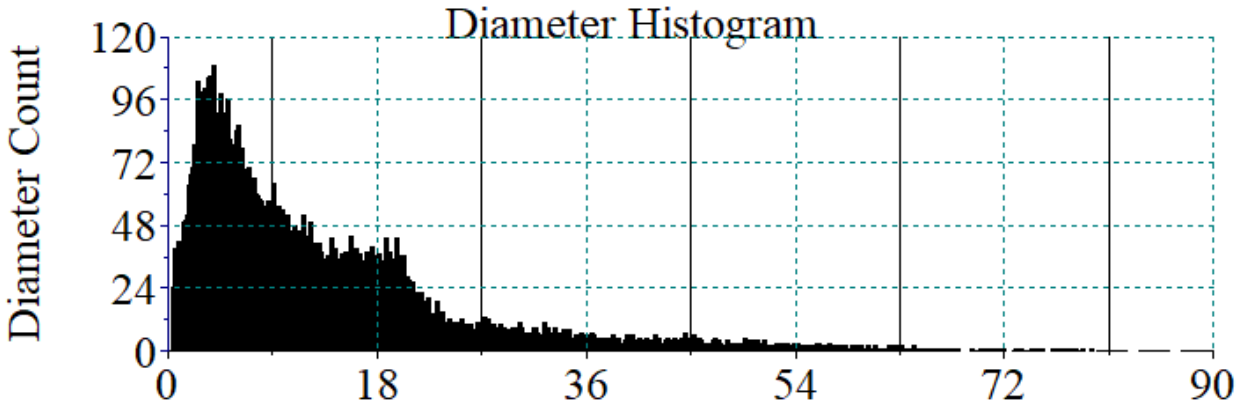

Figure 4.1: Histogram of Diameter [um] vs. Count for 0.1 mm nozzle operating at 80psi. Ex-situ data. Measured 100 mm from exit on nozzle centerline.

Ultimately an 0.1 mm orifice diameter nozzle operating at 80 psi was selected for initial experiments. This nozzle size provided similar droplet size measurements to the 0.3mm nozzle at a narrower spray angle, which was desirable as mass loss to the walls of the tube is a concern. These nozzles also provide a lower mass throughput than the 0.3mm nozzles, which was deemed desirable as it allowed for greater control over mass of fuel injected into the tube.

4.2 Initial Experiments

For the initial experiments the tube was filled with Oxygen to a pressure of 1 atm in a similar manner to the propane-oxygen experiments (one fill and vacuum flush cycle) and droplets were inserted through an 0.1 mm spray nozzle at a supply pressure of 80 psi for a period of 15 seconds, correlating to approximately 5 grams of fuel inserted to the tube, slightly fuel rich at 1.3 times the stoichiometric ratio. The additional mass added to account for possible wall losses. After 15

seconds droplets were visible through the test section windows.

Several attempts were made in this configuration before an ignition was made. The sparking time of the ignitor was increased from the 50 ms to 100 ms and the data recording time was increased to 5 seconds in order to observe any phenomena that occurred. Between attempts the tube was vacuumed for a period of five minutes to remove any residual fuel. Eventually a successful ignition was made, resulting in a deflagration event. After this attempt the spark ignitor was pulled and replaced as severe fouling was observed.

A second run of initial experiments was performed simultaneously injecting both oxygen and fuel. Previous investigations with multiphase detonations [16] mention the assistance of a co-flowing gas stream to disperse particles inside the tube. This run of experiments was performed in a similar manner to the first and with the same particle injection times. The results were again deflagrations, however ignition was observed to be much more reliable. Eventually a detonation-to-deflagration like event was observed in the tube. The travel time between transducers was estimated to be somewhere in the range of 1000 m/s and the measured spike pressures were above the 4 MPa expected for this type of detonation, possibly indicating a DDT event.

Several areas of concern for investigation were identified after the initial run of experiments, with some guidance from the literature.Primary concerns were a gradient in droplet size distribution in the tube, a related problem of a gradient in equivalence ratio, and wall losses. Successful characterization of these initial conditions were determined to be a key to a repeatable experiments. It was also posited that initiation energy was less than sufficient for ignition of the system; proposed solutions such as increased capacitance of the sprark circuit or use of bridgewires were explored for future experiments. Pressure traces for these runs are provided at the end of Appendix C.

4.3 Initial Conditions

4.3.1 In-Situ Droplet Size Measurements at Test Section

After the initial run of experiments the PDPA system was set up for in-situ measurements of particle sizes within the tube. Operating at atmospheric pressure with the nozzle setup as the experiments, too few particles were observed for the system to register meaningful data sets. Qualitatively, it was observed that 'large' droplets were falling quickly through the test section and no small droplets or 'fog' were observed. The spray system was eventually ran for a period of up to ten minutes and empirically no small droplets were observed in the test section.

This led to a theory that the small droplet were either extincted to the walls of the tube or were not traveling a meaningful distance down the tube in that time. Simple estimates from Stoke's drag for free falling droplet, Eq. 4.1 indicate that a 25 um droplet would fall to the test section in about 4 minutes; for a 10 um droplet that time would be 27 minutes, and for a 50 um droplet 1 minute.

$$V_T = \frac{g(\rho_p - \rho_l)D^2}{18\nu} \tag{4.1}$$

To test these theories, an empirical exploratory study was undertaken. A qualitatively light co-flow of nitrogen gas was applied by cracking a needle valve as a variable orifice. Particles were then injected and the flow observed. Within 15-30 seconds of fuel injection a discernible combination of a fine mist and quickly falling large droplets was observed. Measuring the size distribution of droplets in this flow, the PDPA was able to obtain full datasets and returned droplet size distributions similar to those observed with the nozzles ex-situ. An example in situ data set is provided in Fig. 4.2 with additional distributions distributions are provided in Appendix C.

4.3.2 Numerical Modeling of Falling Droplets

In order to better understand the problem of droplet size distribution within the tube and the effects of a co-flowing gas, and to create a tool to analyze initial conditions and help design experiments, the problem was investigated numerically. The range of particle diameters was taken from the PDPA data, with the discrete diameter and diameter count data being binned to reduce

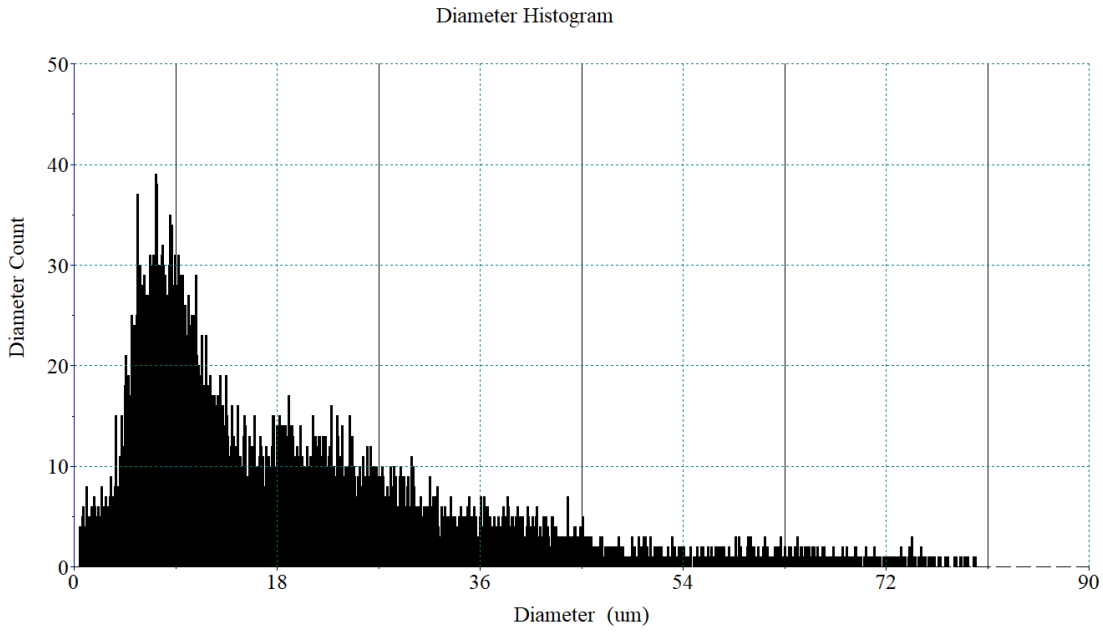

Figure 4.2: Particle size histogram from 0.1 mm nozzle at 80 PSI supply pressure, measured in-situ in test section approx. 2.5 meters from injection w/ co-flow of nitrogen. Measurement time 45-120s. Diameters in [um].

computational load. These particles were treated as packets; the equations of motion solved for a single particle at the binned size and extrapolated for the particle count in the bin. Initial velocity for the model was taken as a mean of values from the PDPA data; there was no evident correlation from the measurements between droplet size and initial velocity.

The equations of motion for a single spherical particle(Eqs. 4.2, 4.3,4.4) were solved for a set period of time, with and without a carrier gas. Drag was considered in both directions, either acting to decelerate the particle from intial velocity or acting in the direction of motion of the carrier gas. As the flow field is relatively sparse with volume fraction of liquid droplets < 0.001, particle-particle coupling was assumed negligible and the equations were solved for each binned particle size separately.

$$F_p = F_D + F_g \tag{4.2}$$

$$F_D = C_D A \rho \frac{1}{2} V^2 \tag{4.3}$$

$$C_D = f(Re) \tag{4.4}$$

The numerical model was run for a set duration of time in a one dimensional domain 3 meters in length. At each timestep a new echelon of particles following the binned diameters and diameter counts was introduced at $x = 0$ at the initial velocity. At each time step the position of each particle size was queried in order to create a histogram at every x-location inside the tube. Particles that reached the end of the tube, $x = 3m$, were considered extinct from the flow field and not counted. With known droplet size counts at discrete x-locations, the model further allows for estimation of spatial gradients in equivalence ratio and their time-dependent evolution.

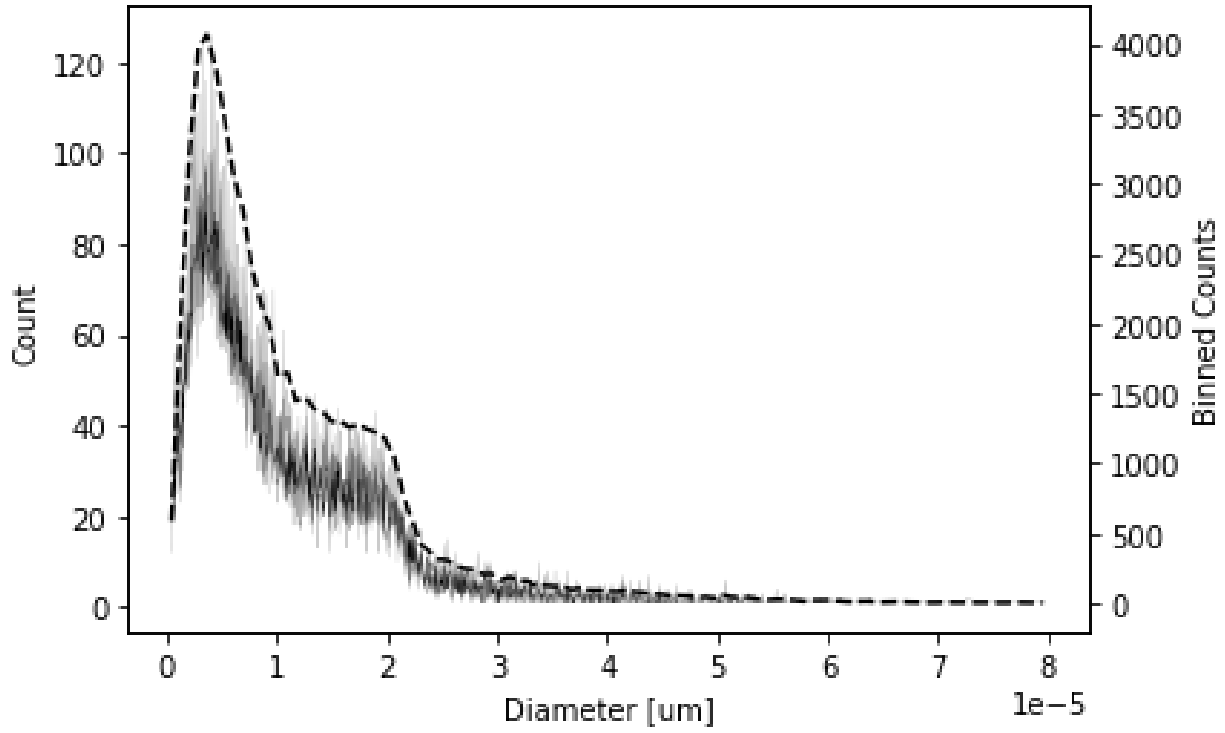

Figure 4.3: Comparison of raw particle size and count from exsitu data to fitted values (dashed line).

The results of the numerical modeling indicate agreement with empirical observations; with no carrier gas flow, large particles travel the length of the tube relatively quickly under their own gravitational acceleration, while small particles remain nearly stationary. With a carrier gas flow of 10 liters/min, small particles are pushed down the tube and arrive within a minute. Additionally, in the presence of a carrier gas flow, the particle size distribution at every point in the tube is predicted to close to uniform at steady state (spatial gradient in droplet sizes disappears).

4.3.3 Wall Loss Estimations - Mass Retention Methods

The literature suggests that wall losses may be significant in some scenarios. These losses may be defined as droplets exiting the flow field and forming a film on the walls of the tube, possibly resulting in a film detonation and complicating the experiment. Papavassiliou [6] notes in his decane-fog experiments wall wetting occurring as a time-delayed effect (co-flowing oxidizer with fog, wetting observed only after some 30 seconds). Joseph Shepherds group at CalTech [27] noted in hexane and dodecane vapor experiments requiring 1.3 to 1.6 times the calculated mass of fuel to be injected at partial pressure, with prior literature on similar experiments indicating up to 2 times the calculated amount of fuel being necessary. The reasons for the discrepancy in required fuel mass were posited as being due to soot in the walls absorbing condensed fuel.

Wall wetting was empirically observed in our own facility and necessarily needed to be quantified. In order to do this, the following measurement was devised; The plastic diaphragm separating the tube and blowdown tank would be replaced with a filter paper of sufficient density to capture particles above 2 um. Set flow rates of carrier gas would be flowed through the tube, and particles injected for a set amount of time. Given the known mass of particles injected and the change in mass of the filter paper at the bottom of the tube, an estimate of particle extinction to the walls could be made. An estimate of extinction can then be fed back into the numerical model to improve predictive capabilities.

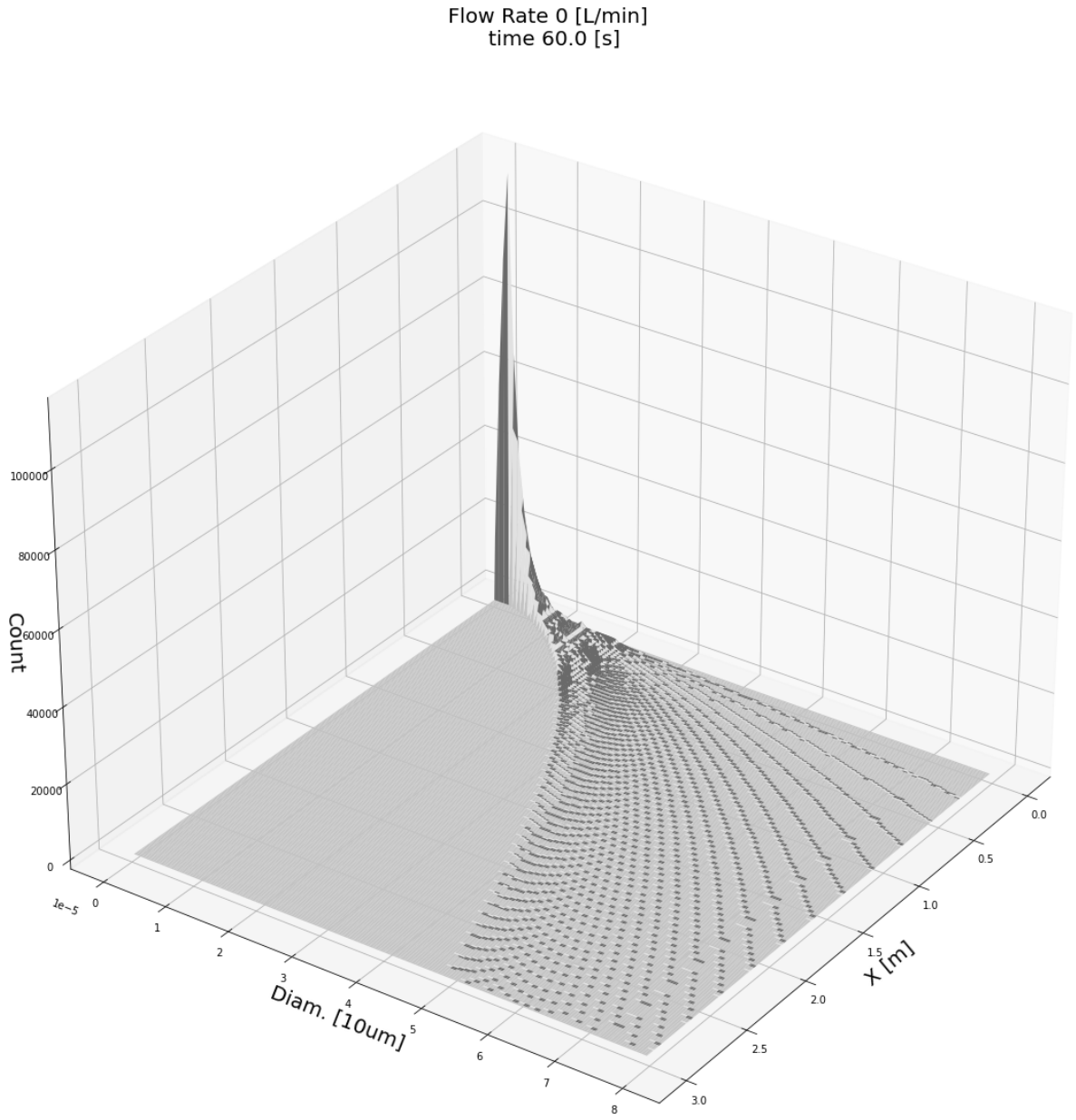

Figure 4.4: Histograms of numerically calculated diameter [10um] and particle count along axis of tube with gas no gas coflow. Time 1 min., injection 15 g/min fuel.

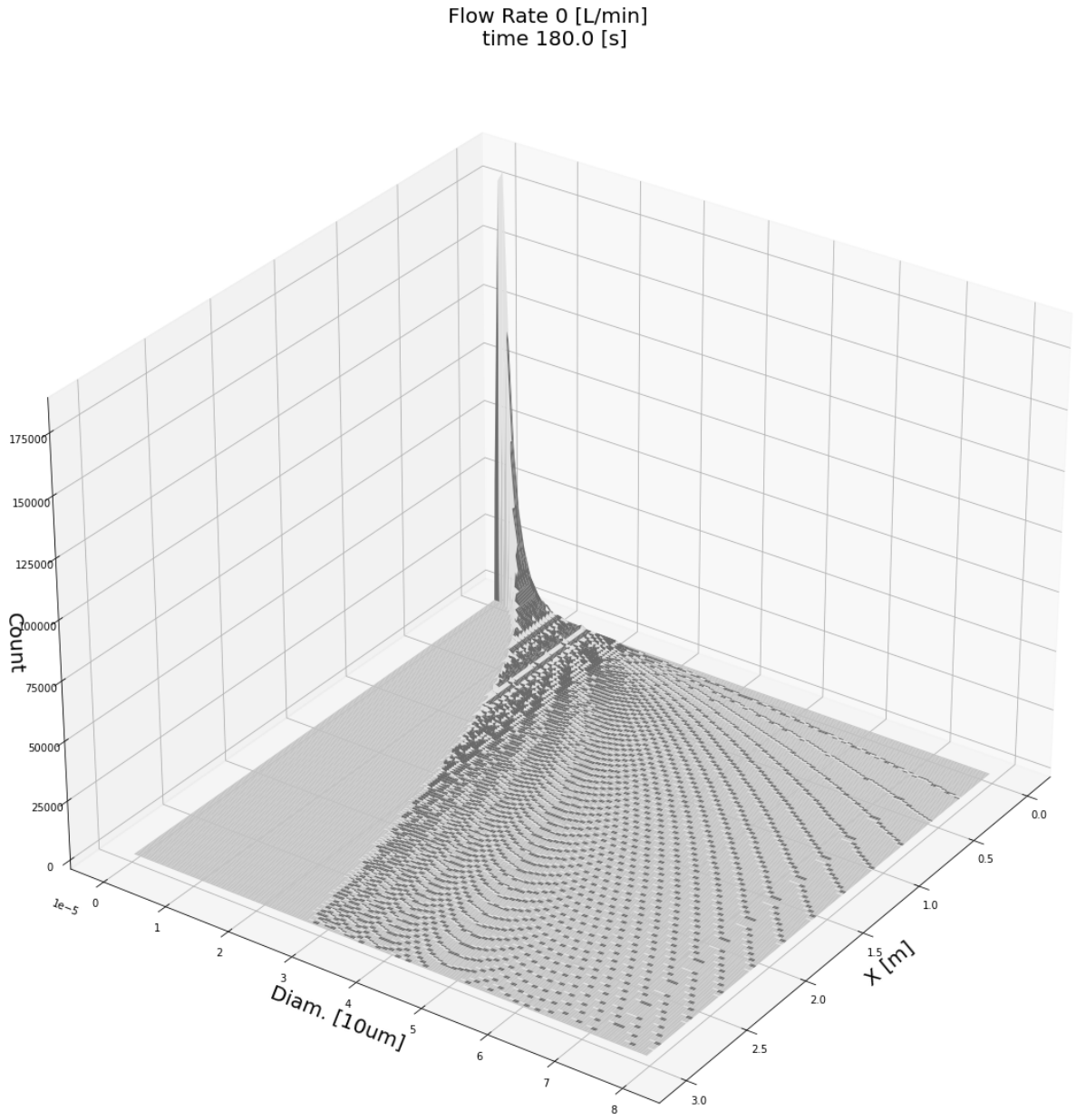

Figure 4.5: Histograms of numerically calculated diameter [10um] and particle count along axis of tube with gas no gas coflow. Time 3 min., injection 15 g/min fuel.

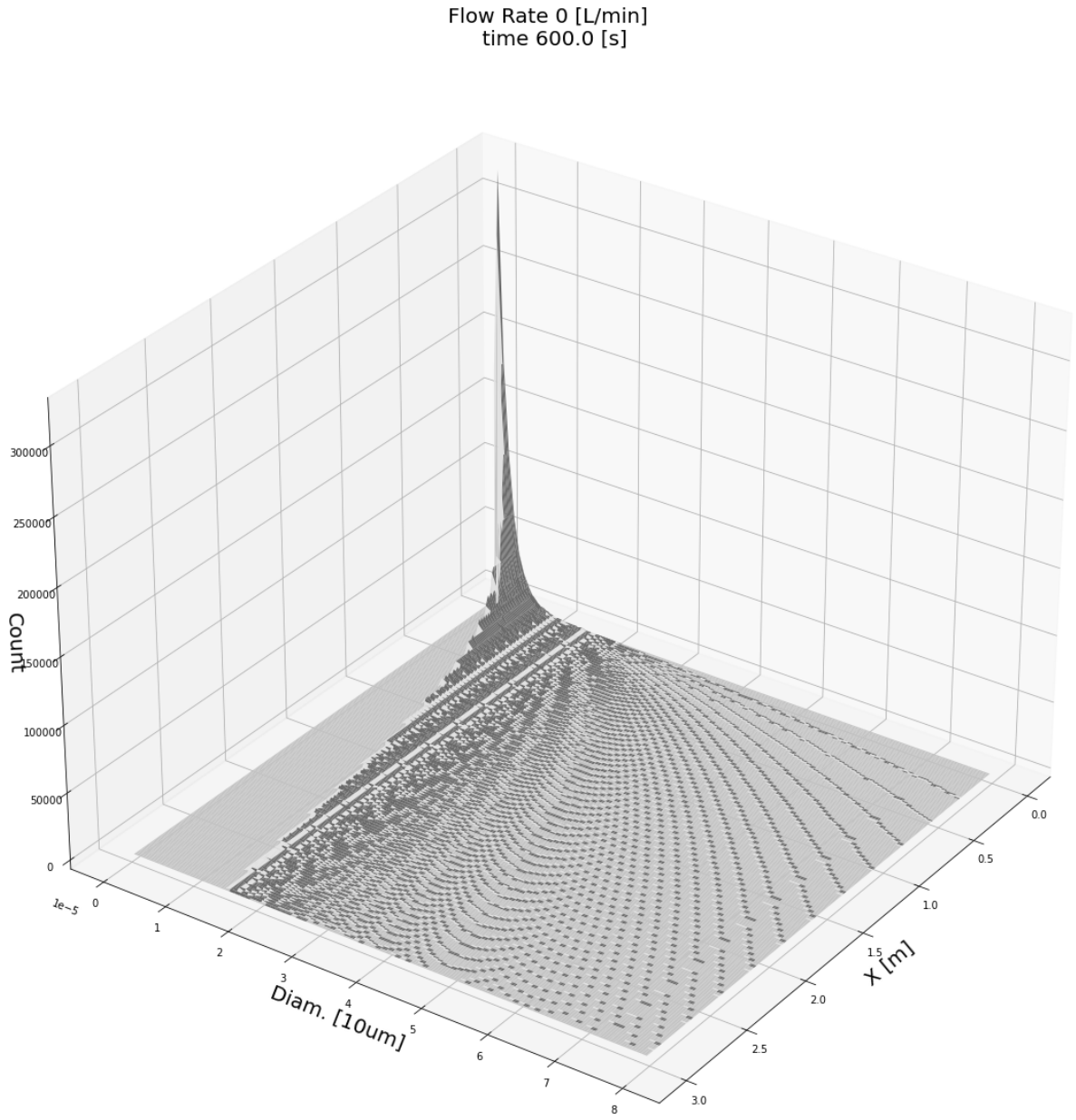

Figure 4.6: Histograms of numerically calculated diameter [10um] and particle count along axis of tube with gas no gas coflow. Time 5 min., injection 15 g/min fuel.

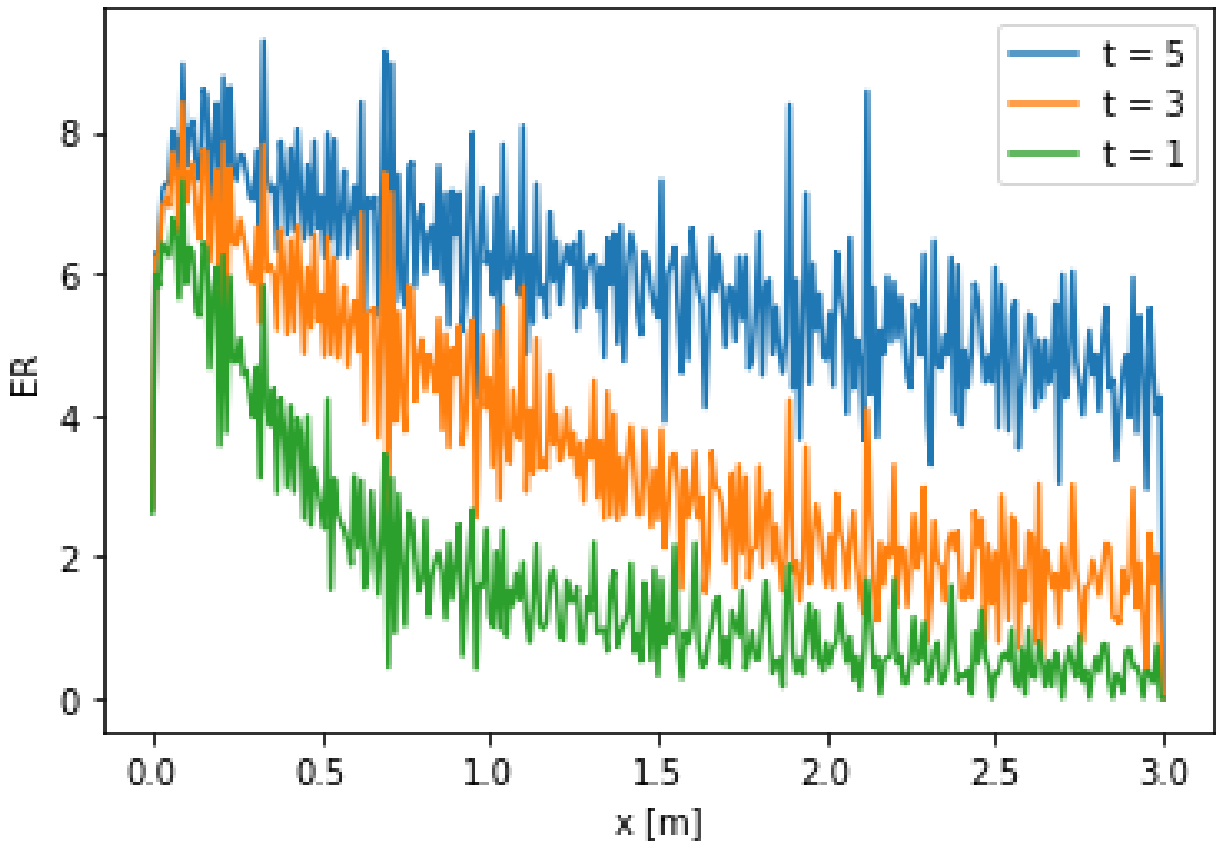

Figure 4.7: Equivalence ratio for calculated particle distributions along axis of tube without coflow. Times 1,3,5 minutes., injection 15 g/min fuel.

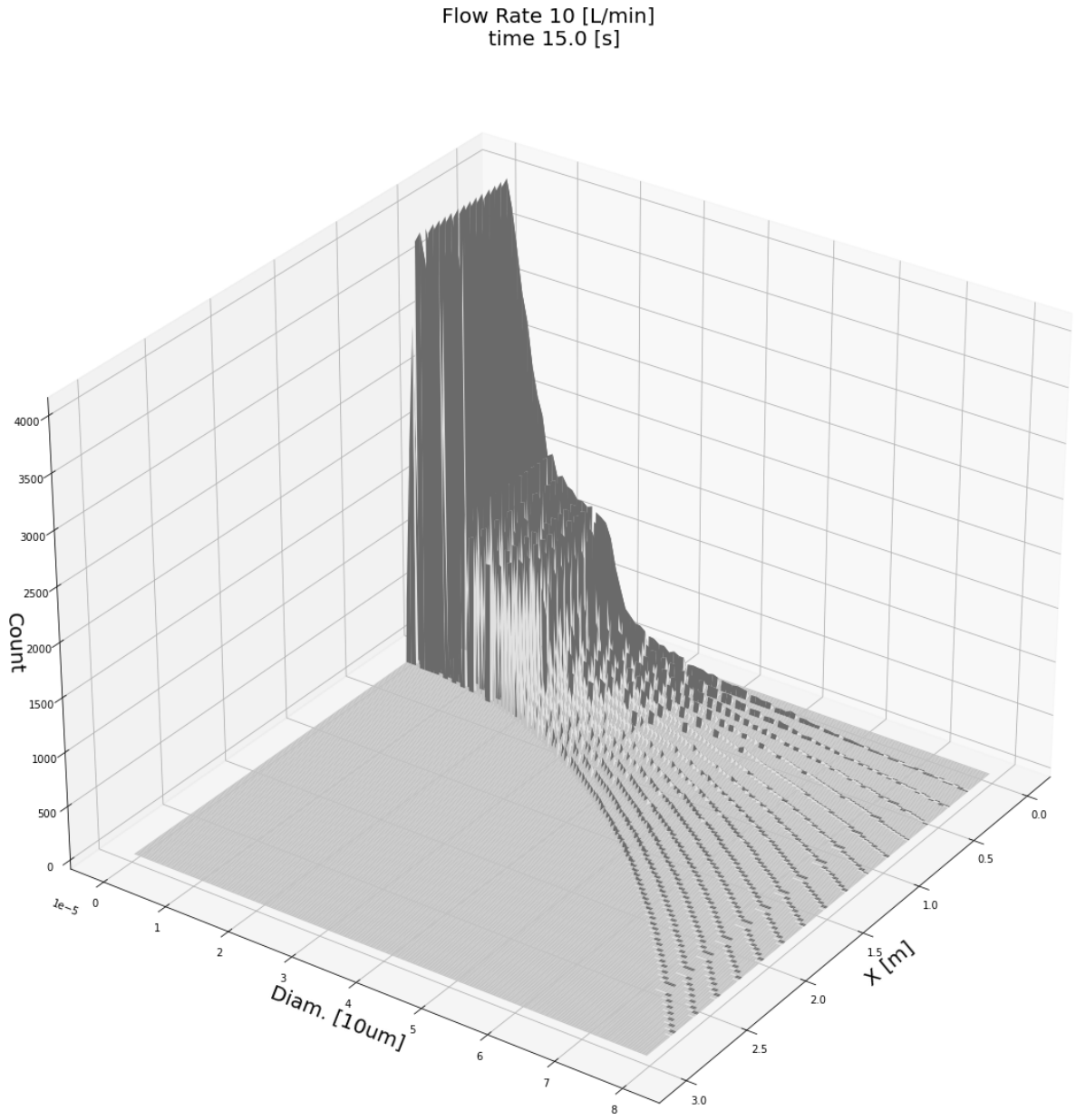

Figure 4.8: Histograms of numerically calculated diameter [10um] and particle count along axis of tube with gas coflow 10 L/min. Time 15s., injection 15 g/min fuel.

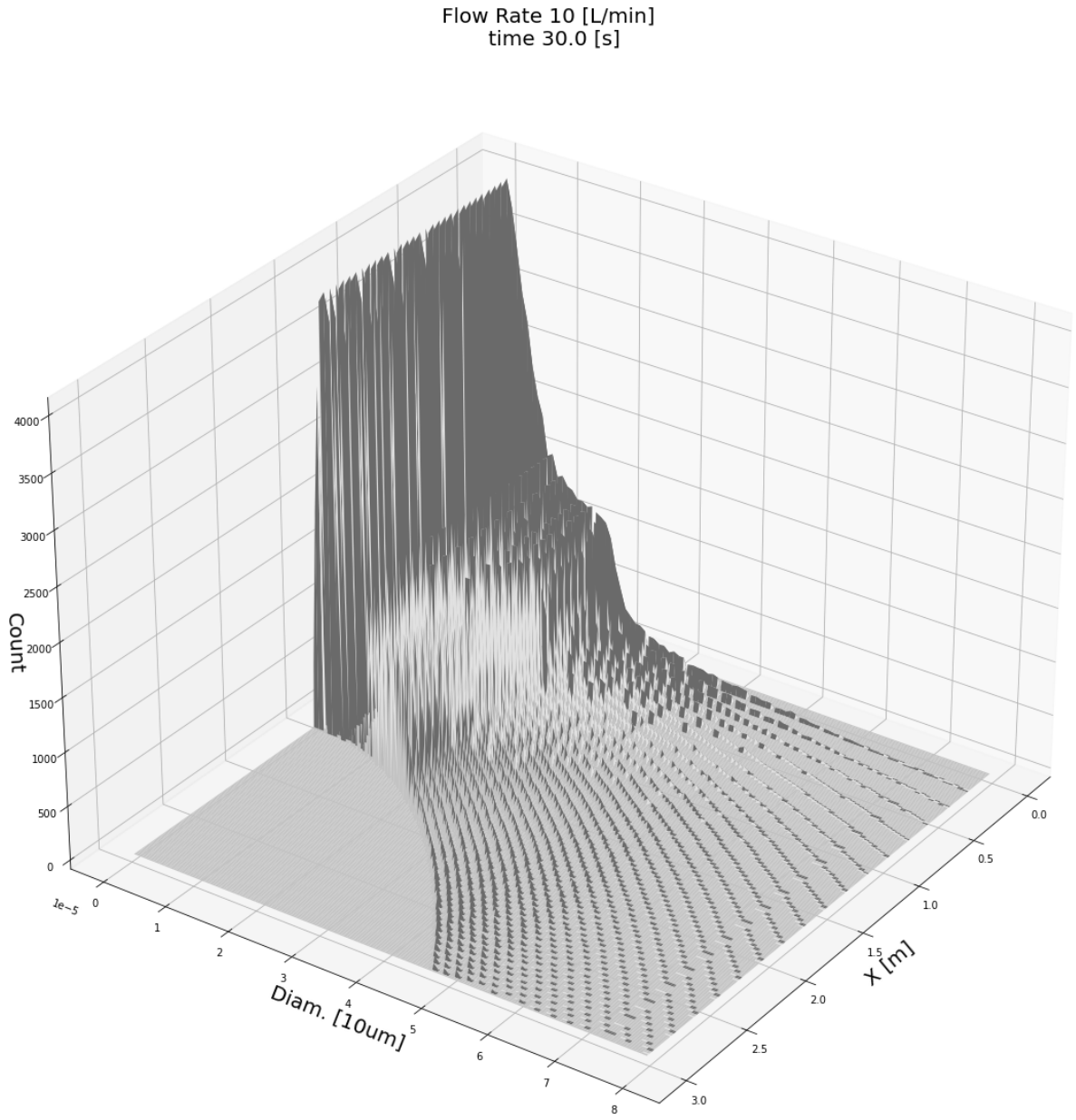

Figure 4.9: Histograms of numerically calculated diameter [10um] and particle count along axis of tube with gas coflow 10 L/min. Time 30s., injection 15 g/min fuel.

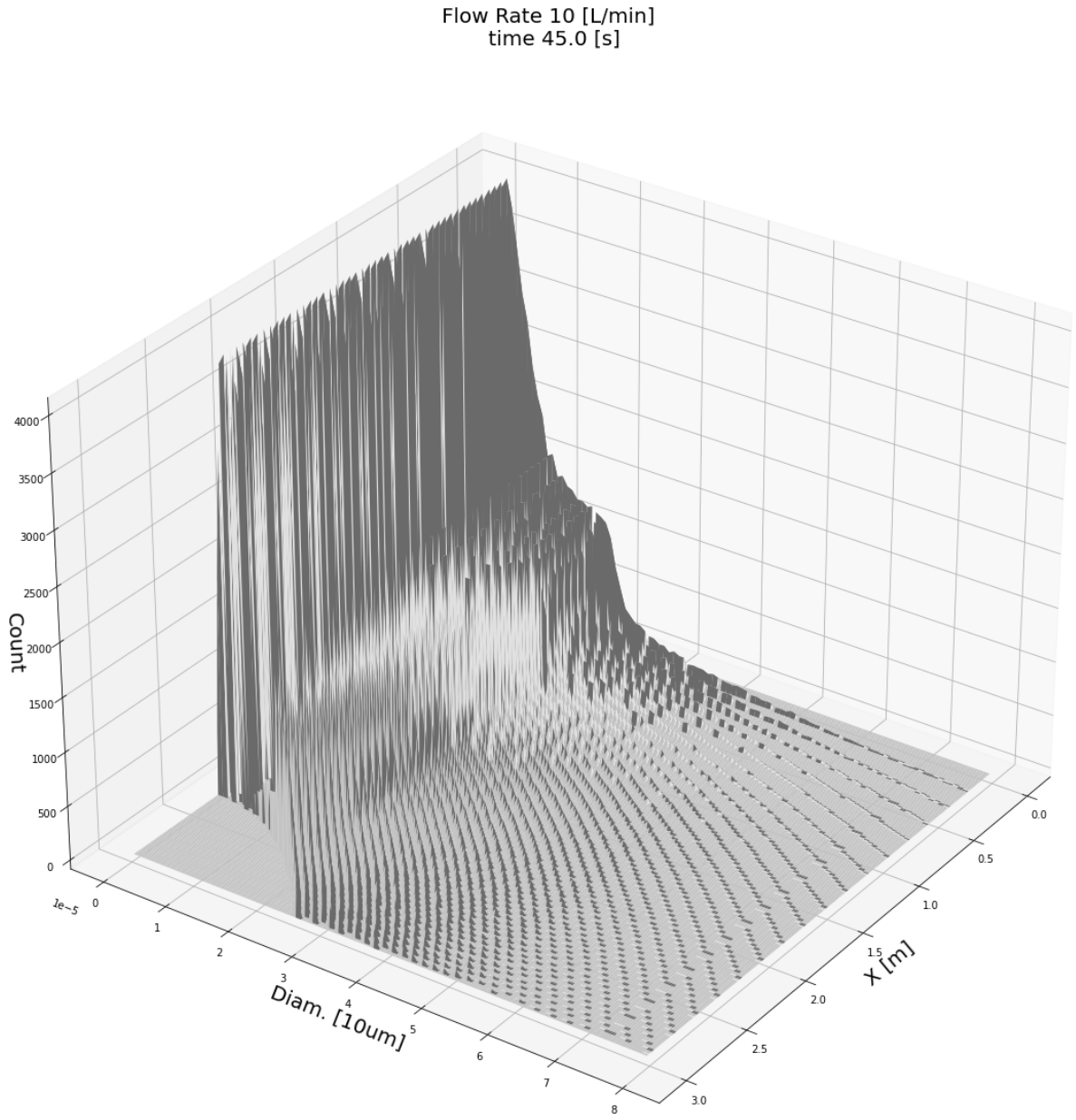

Figure 4.10: Histograms of numerically calculated diameter [10um] and particle count along axis of tube with gas coflow 10 L/min. Time 45s., injection 15 g/min fuel.

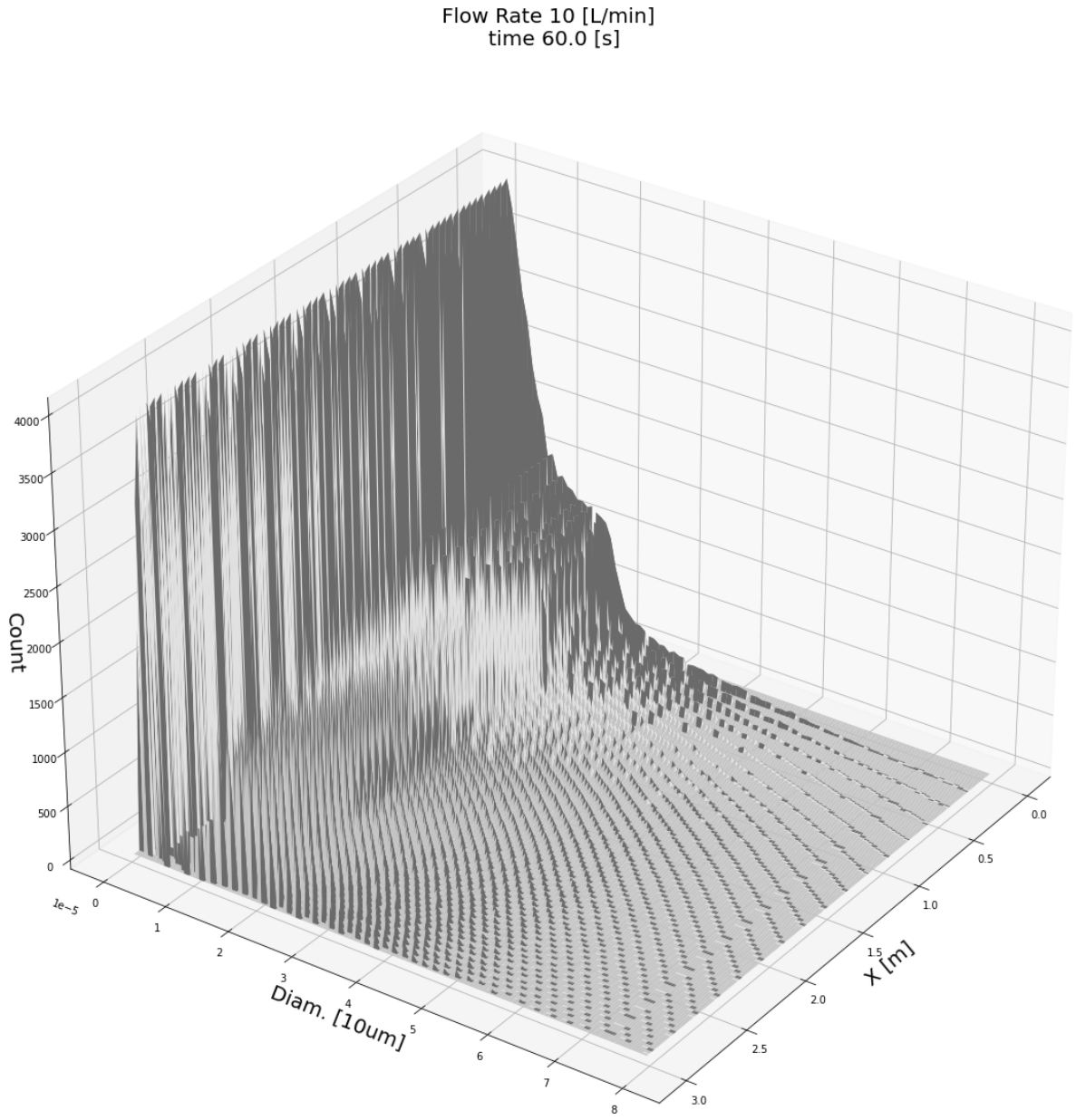

Figure 4.11: Histograms of numerically calculated diameter [10um] and particle count along axis of tube with gas coflow 10 L/min. Time 60s., injection 15 g/min fuel.

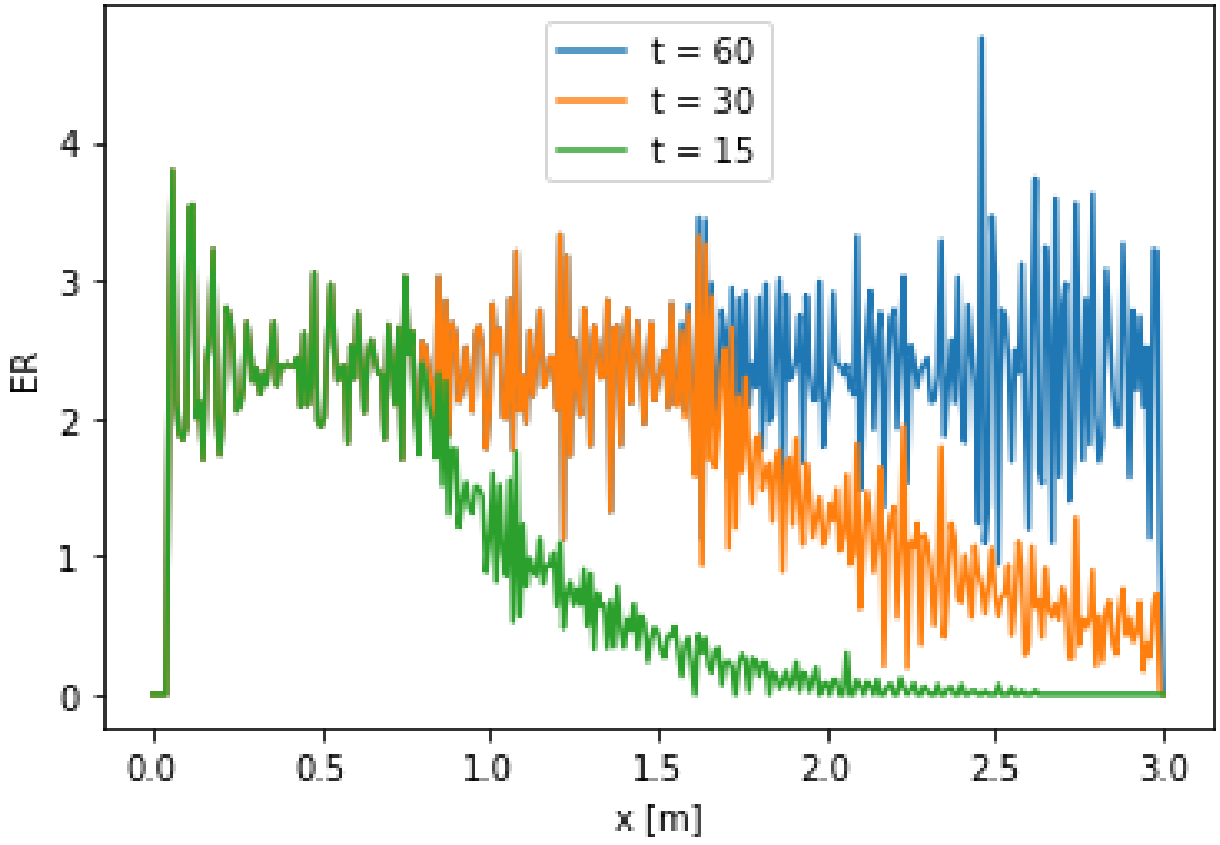

Figure 4.12: . Equivalence ratio for calculated particle distributions along axis of tube with gas injection mass flowrate of 15 g/s, oxygen coflow 10 L/min. Times annotated seconds., injection 15 g/min fuel.

5. SUMMARY AND CONCLUSIONS

5.1 Challenges

As the literature on multiphase detonation tubes is scarce in comparison to shock tubes and other similar facilities, much care was taken in the design process. This involved multiple iterations of various features to ensure both safe and reliable operation, as well as multiple methods of engineering analysis conducted on each major component to rigorously ensure that the facility as designed would meet requirements. Validation experiments with propane and oxygen detonations were seen as a necessity in order to test both the safety and functionality of the facility. These provided both assurance in the facility and familiarity with the systems in a controlled manner. Moving on to the more complex problem of a multiphase detonation revealed many facets to be considered in the experiment, requiring thorough testing and measurement before proceeding with confidence in repeatable experiments.

5.2 Further Study

Going forward work will continue on establishing the initial conditions inside the tube, primarily towards measuring the gradient of droplet size distribution and equivalence ratio in the tube working towards a repeatable experiment with controllable initial conditions. These experiments will provide bulk data on mulitphase detonations, furthering and improving upon similar work in the literature. This campaign will also serve to establish a repeatable experiment working towards imaging of multiphase detonations. The end goal will be to image phenomena occurring at the bulk scales as well as at the particle level. At the bulk scale, laser-illuminated and schlieren imagary will provide data on induction and reaction times and length, vapor production, droplet survival times, and the nature of the cellular structure of the detonation. Similarly at the droplet scale it is desired to observe the simultaneous breakup, vaporization, and reaction phenomena occurring. Data collected will serve to enhance current and future models used to simulate droplet processing by detonation, working towards a proper understanding of the multiphase detonation phenomena

and functional applications in simulating propulsion engine dynamics.

REFERENCES

[1] N. D. DeBarmore, "Characterization of rotating detonation engine exhaust through nozzle guide vanes," Master's thesis, Air Force Institute of Technology, 2013.

[2] A.E.Dahoe, "On deflagrations and detonations," tech. rep., University of Ulster, UK, 2007.

[3] D. Hebert, J.-L. Rullier, J.-M. Chevalier, I. Bertron, E. Lescoute, F. Virot, and H. El-Rabii, "Investigation of mechanisms leading to water drop breakup at mach 4.4 and weber numbers above 105," *SN Applied Sciences*, vol. 2, p. 69, 01 2020.

[4] E. K. Dabora, K. W. Ragland, and J. A. Nicholls, "Drop-size effects in spray detonations," 1969.

[5] P. LU, N. SLAGG, B. FISHBURN, and P. OSTROWSKI, "Relation of chemical and physical processes in two-phase detonations," in *Gasdynamics of Explosions and Reactive Systems* (A. OPPENHEIM, ed.), pp. 815–826, Pergamon, 1980.

[6] J. Papavassiliou, "Measurements of cellular structure in liquid aerosol detonation," Master's thesis, McGill University, 1991.

[7] J. S. E. Schultz, "Detonation diffraction through a mixture gradient," tech. rep., CIT GALCIT, 2000.

[8] J. Lee, "Dynamic parameters of gaseous detonations," *Annual Review of Fluid Mechanics*, vol. 16, pp. 311–336, 11 2003.

[9] O. Peraldi, R. Knystautas, and J. Lee, "Criteria for transition to detonation in tubes," *Symposium (International) on Combustion*, vol. 21, no. 1, pp. 1629–1637, 1988. Twenty-First Symposuim (International on Combustion).

[10] C. Crow, *Multiphase Flows with Droplets and Particles*. CRC Press, 2012.

[11] G. Godsave, "Studies of the combustion of drops in a fuel spray—the burning of single drops of fuel," *Symposium (International) on Combustion*, vol. 4, no. 1, pp. 818–830, 1953. Fourth Symposium (International) on Combustion.

[12] W. W.Ranz, "Evaporation from drops," *Journal of Chemical Engineering Progress*, vol. 48, pp. 141–146, 1958.

[13] B. Abramzon and W. Sirignano, "Droplet vaporization model for spray combustion calculations," *International Journal of Heat and Mass Transfer*, vol. 32, no. 9, pp. 1605–1618, 1989.

[14] Z. Dai and G. Faeth, "Temporal properties of secondary drop breakup in the multimode breakup regime," *International Journal of Multiphase Flow*, vol. 27, no. 2, pp. 217–236, 2001.

[15] K. Kailasanath, "Liquid-fueled detonations in tubes," *Journal of Propulsion and Power*, vol. 22, pp. 1261–1268, 2006.

[16] J. Papavassiliou, A. Makris, R. Knystautas, J. H. Lee, C. K. Westbrook, and W. J. Pitz, "Measurements of cellular structure in spray detonation," in *Dynamic Aspects of Explosion Phenomena* (A. Kuhl, ed.), vol. 154, pp. 148–169, AIAA, 10 1991.

[17]

[18] "Guide on explosion protection for gaseous mixtures in pipe systems," standard, NFPA, Quincy, MA, 2019.

[19] "Asme boiler and pressure vessel code section viii," standard, AMSE, New York, NY, 2013.

[20] *Gasdynamics of Combustion*. Mono Book Corp, Baltimore MD, 1965.

[21] S. B. Dorofeev, V. P. Sidorov, M. Kuznetsov, I. D. Matsukov, and V. I. Alekseev, "Effect of scale on the onset of detonations," *Shock Waves*, vol. 10, pp. 137–149, 2000.

[22] B. Khasainov, H.-N. Presles, D. Desbordes, and P. Demontis, "Detonation diffraction from circular tubes to cones," *Shock Waves*, vol. 14, pp. 187–192, 11 2005.

[23] *PRESSURE WINDOW DESIGN*.

[24] J. E. Shepherd, "Structural response of piping to internal gas detonation," *Journal of Pressure Vessel Technology-transactions of The Asme*, vol. 131, p. 031204, 2009.

[25] E. Schultz and J. E. Shepherd, "Validation of detailed reaction mechanisms for detonation simulation," 2000.

[26] N. Matsunaga, M. Hori, and A. Nagashima, "Gaseous diffusion coefficients of propane and propylene into air, nitrogen and oxygen," *Netsu Bussei*, vol. 21, no. 3, pp. 143–148, 2007.

[27] J. S. J.M.Austin, "Detonations in hydrocarbon fuel blends," tech. rep., Explosion Dynamics Laboratory, Behalf of Air Force and Advanced Projects Research Inc., 2000.

APPENDIX A

ENGINEERING DRAWINGS AND FINITE ELEMENT ANALYSIS

Finite element analysis was performed for all tube components in order to verify design integrity. Each simulation performed with 1200 PSI (Approx 8 MPa) internal pressure loading unless otherwise noted (corresponds to double the estimated CJ pressure of a dodecane - oxygen detonation, estimated DDT condition). Factor of safety greater than or equal to 2 desired for each component unless otherwise noted. Where analysis returned FOS less than desired an engineering decision was made whether such condition was a limitation of the software package or a design concern.

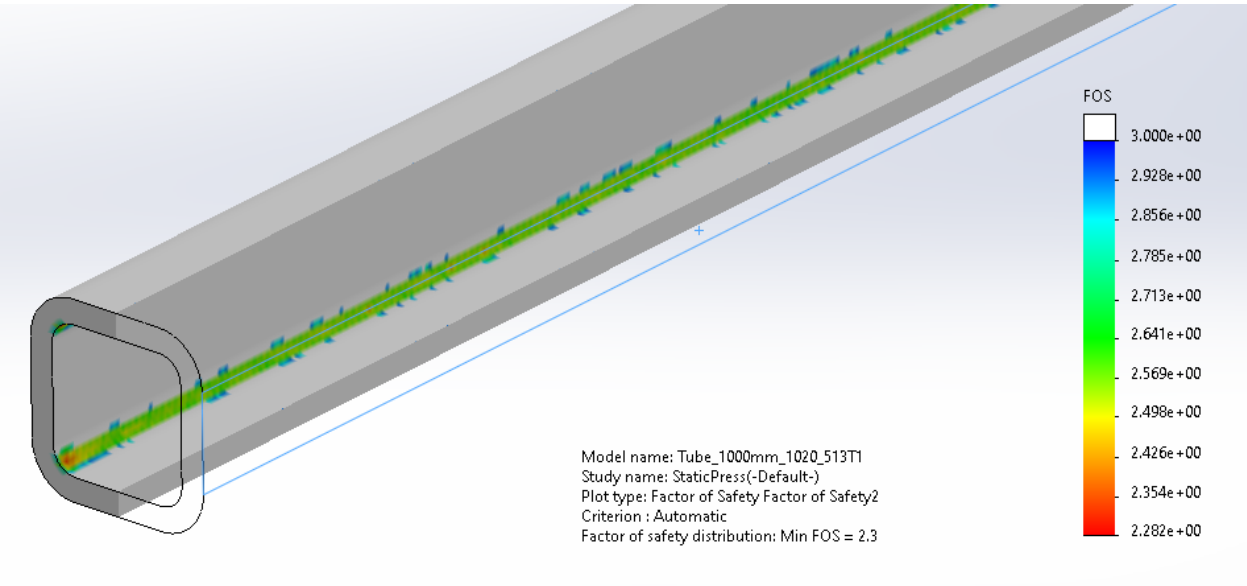

Figure A.1: Drawing of Entire Tube Assembly, Components Annotated

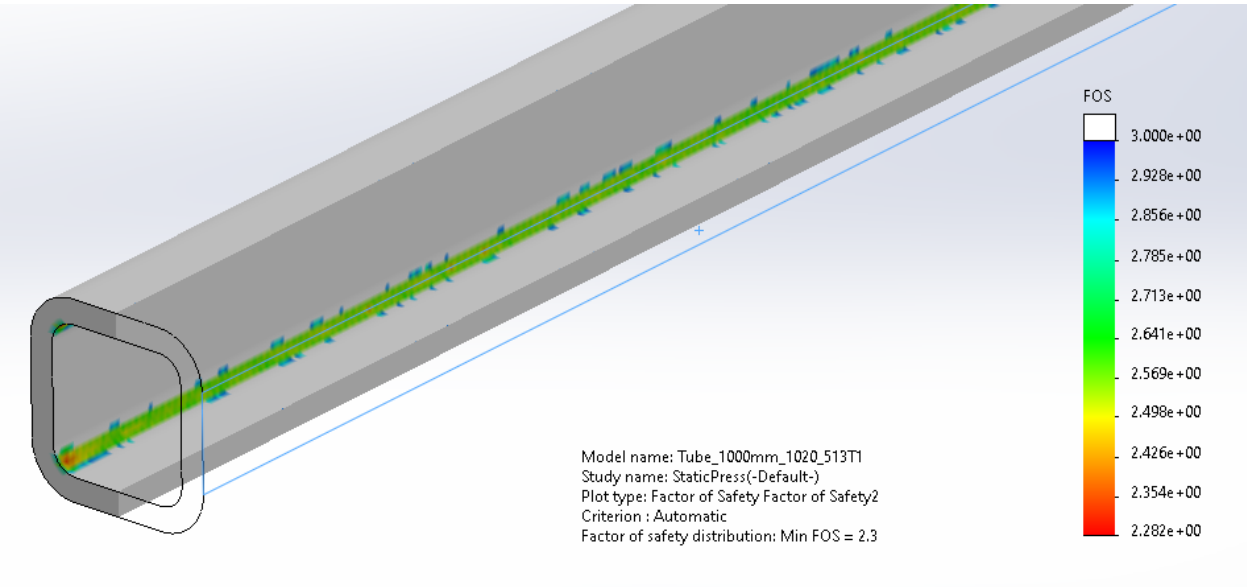

Figure A.2: Finite element analysis of bare 3 inch OD x 0.375 Carbon Steel tube section for internal pressure. Simulation performed to verify calculations of ASME BPVC Section VIII for stresses/FOS.

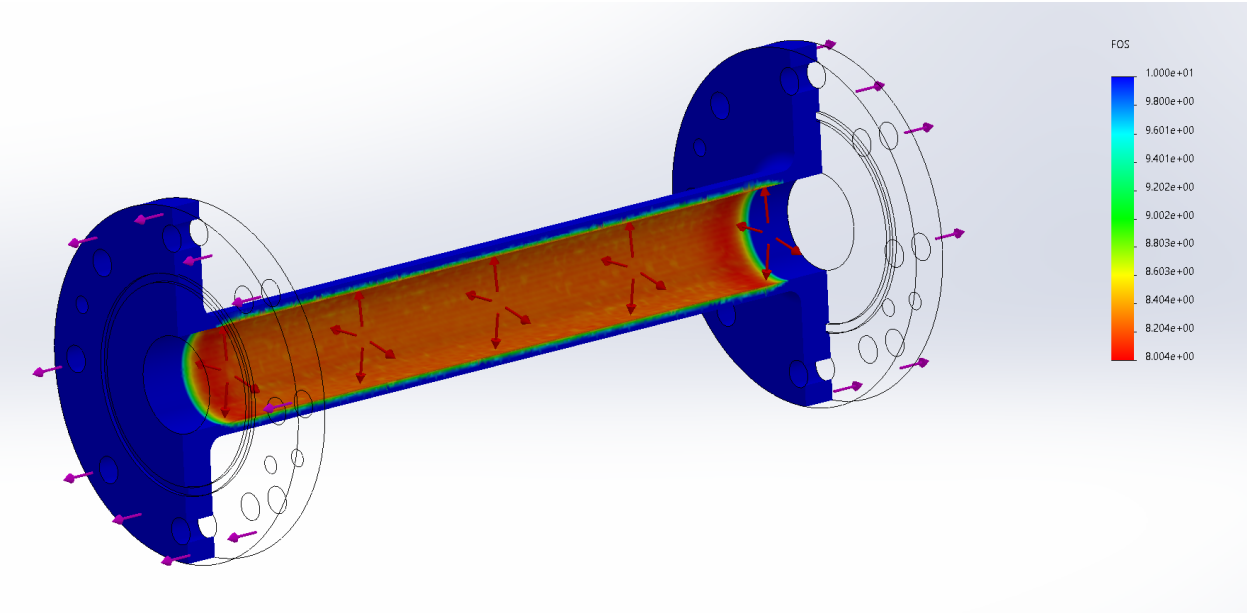

Figure A.3: Finite element analysis of acceleration section for internal pressures.

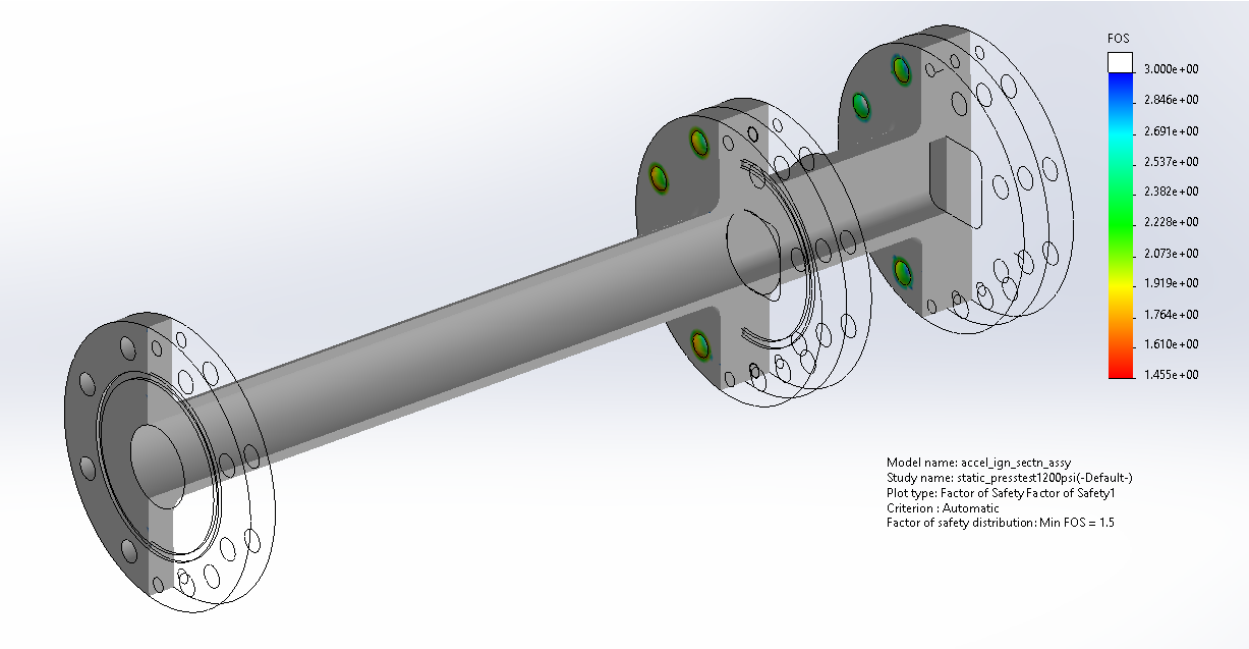

Figure A.4: Finite element analysis of bolted acceleration and ignition section assembly for internal pressures and pressures acting on blank end flange.

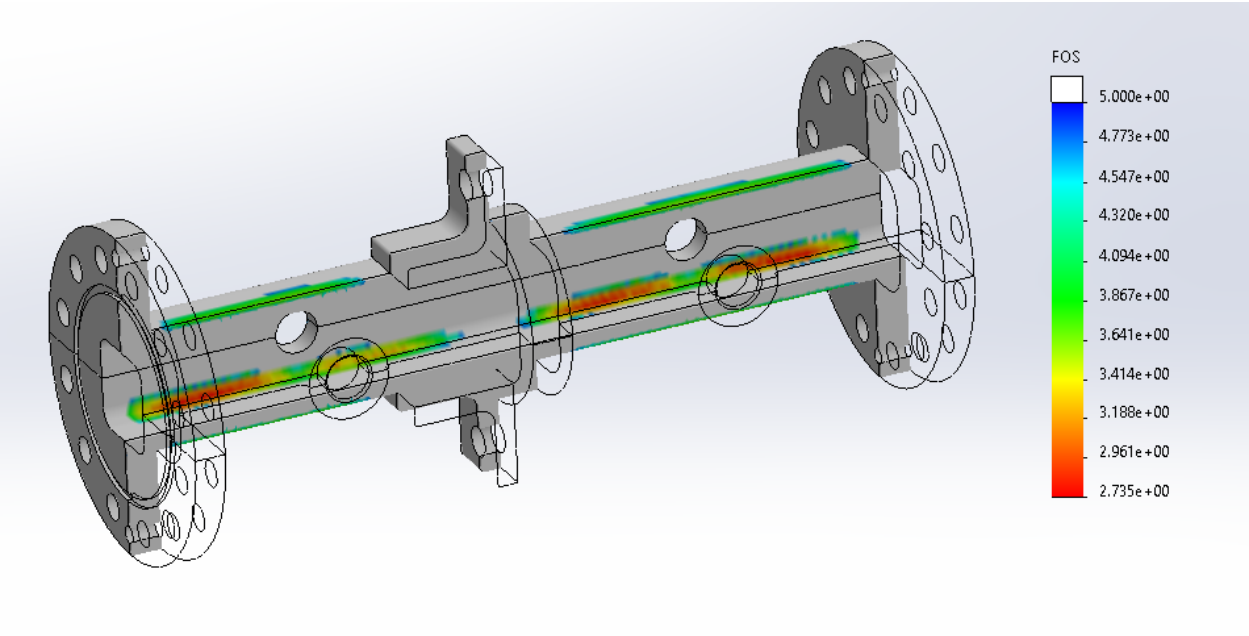

Figure A.5: Finite element analysis of development section for internal pressures.

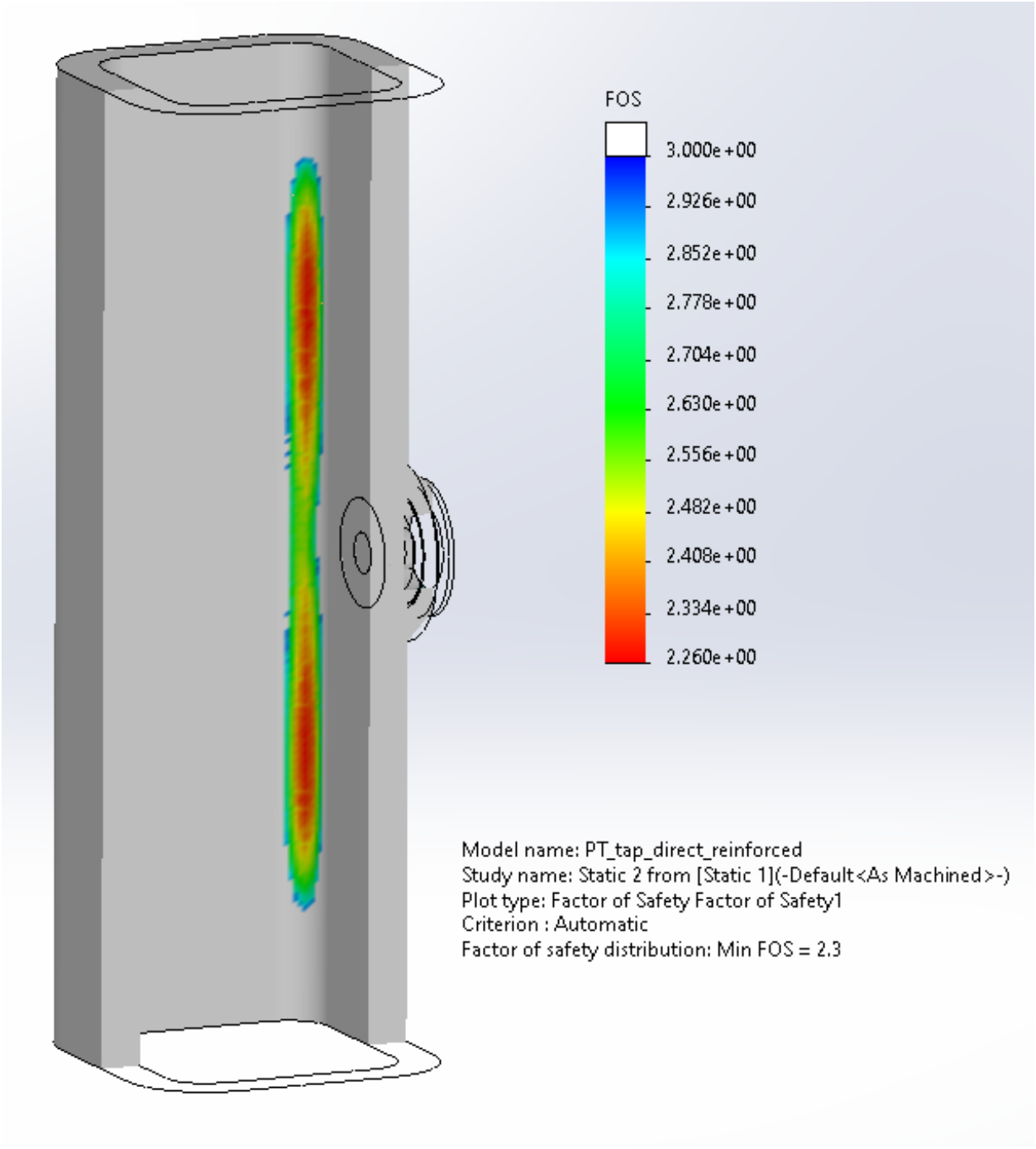

Figure A.6: Finite element analysis of tube section with reinforcement for DPT mounting and DPT for internal pressure. View shows areas of interest (no appreciable degradation in FOS externally).

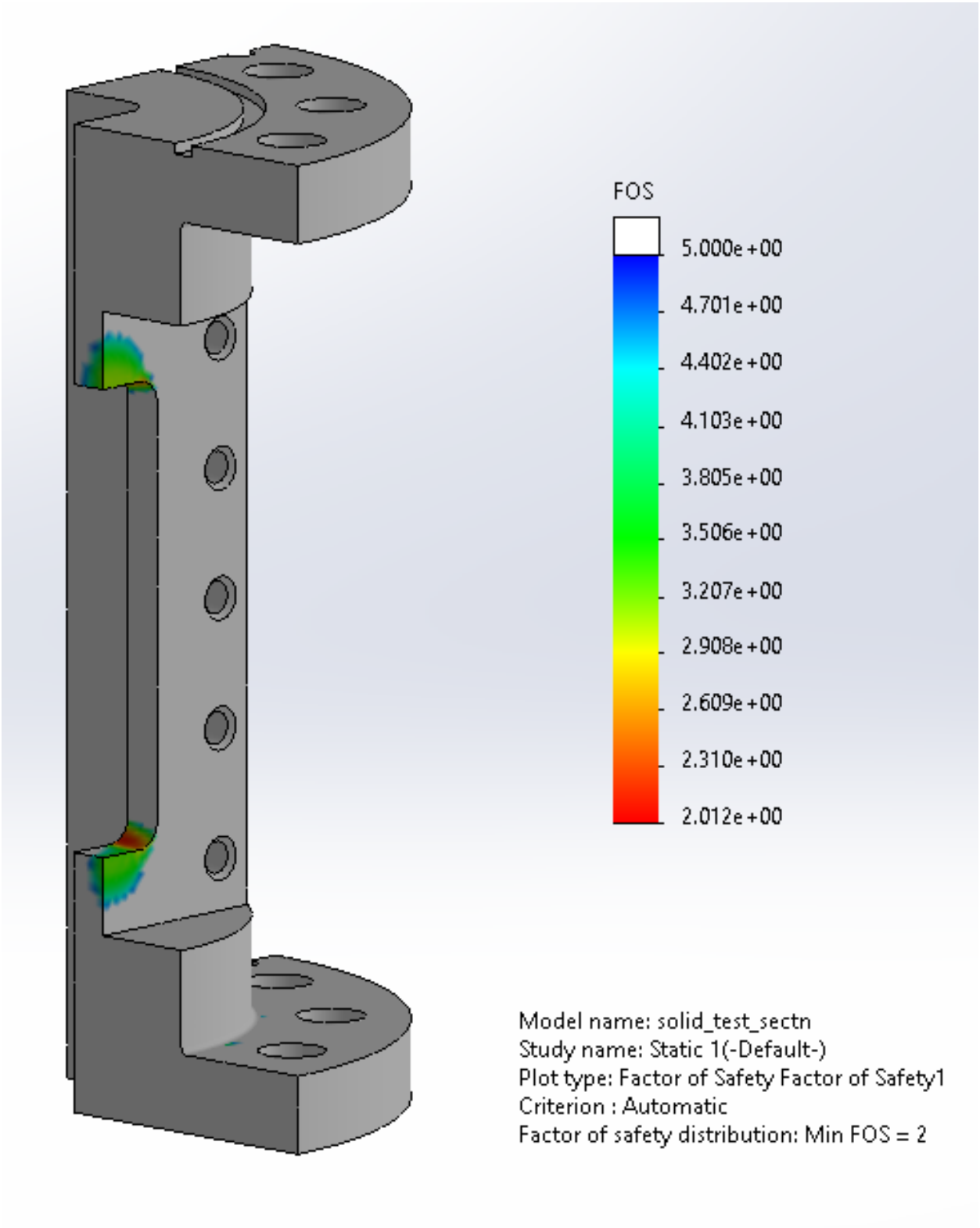

Figure A.7: Finite element analysis of bare test section for internal pressures.

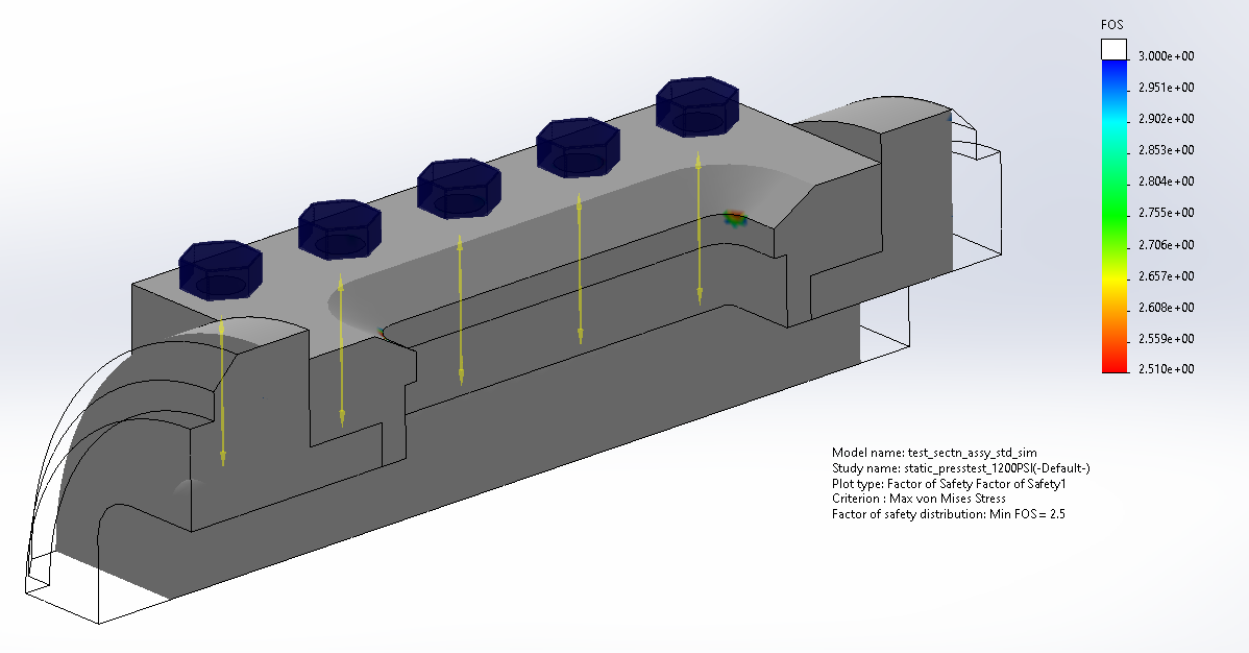

Figure A.8: Finite element analysis of test section with bolted coverplate and borosilicate window (not shown) for internal pressures.

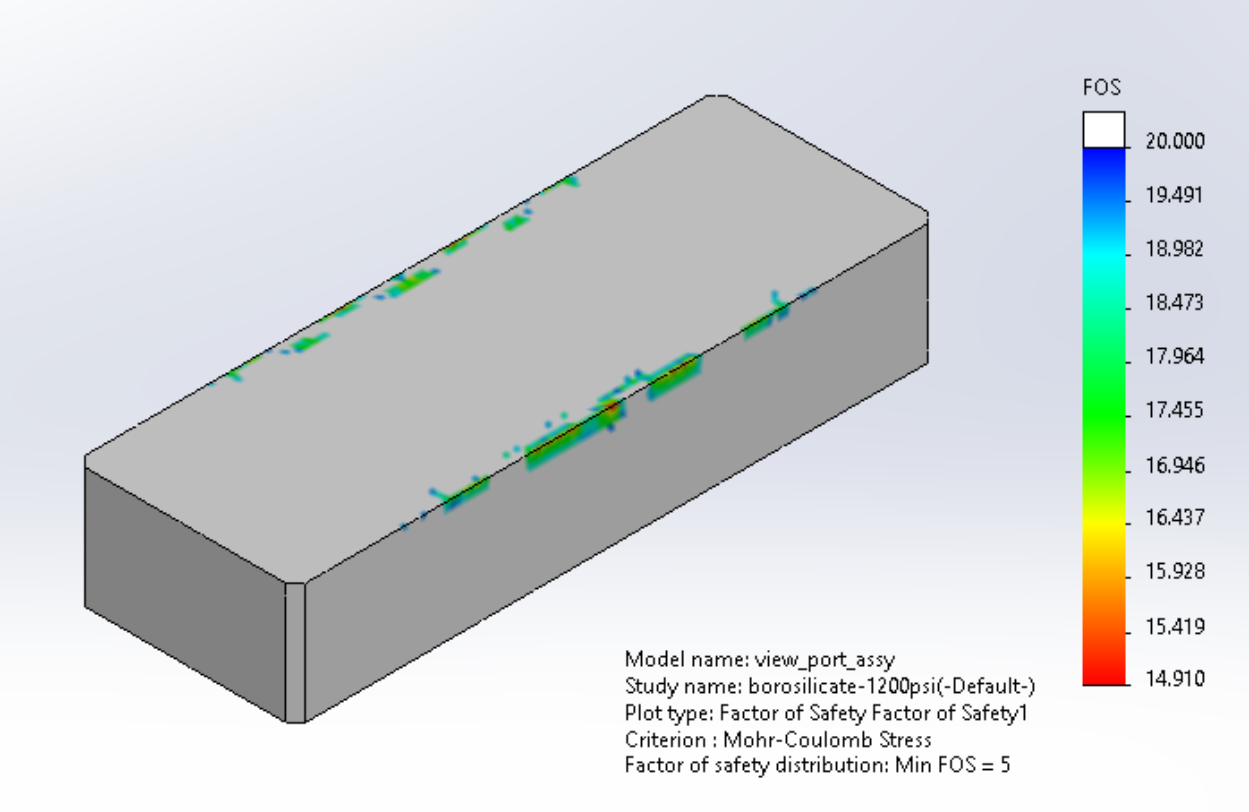

Figure A.9: Finite element analysis of test section coverplate (not shown) and borosilicate window assembly.

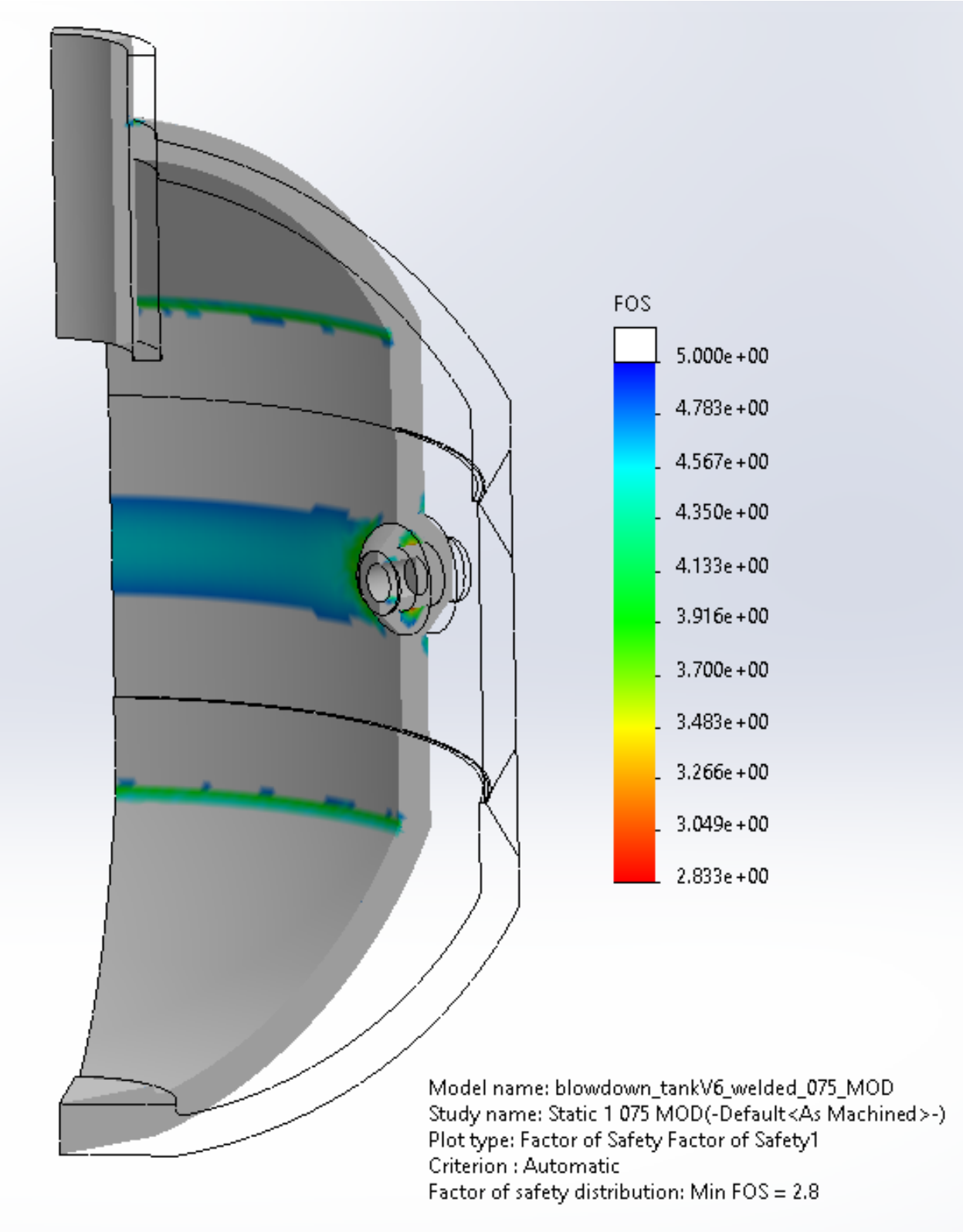

Figure A.10: Finite element analysis of internal pressure on expansion/blowdown tank.

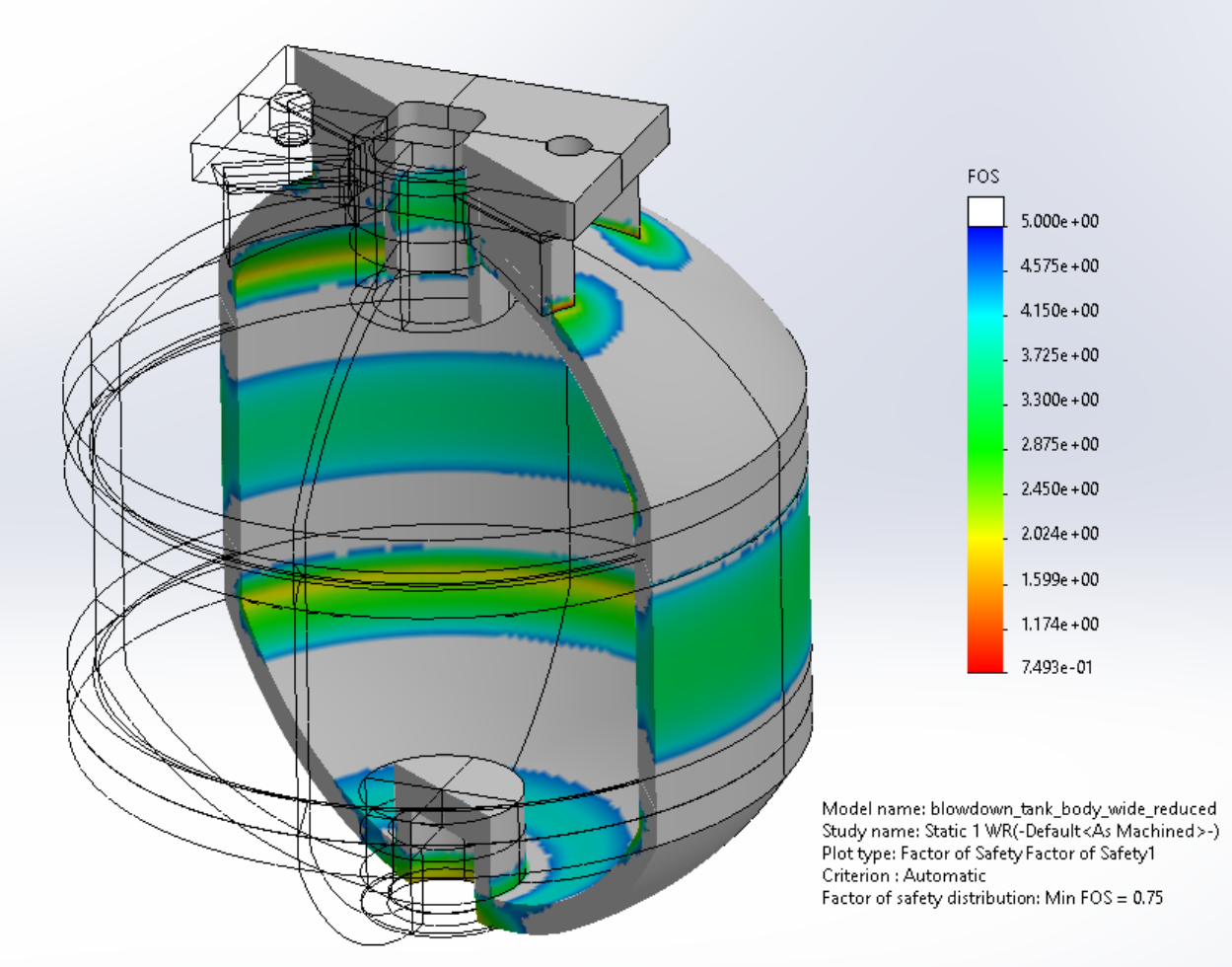

Figure A.11: Finite element analysis of stresses on expansion/blowdown tank and mounting plate. Note low FOS on reinforcement ribs; analysis software was unable to simulate weldments due to curvature.

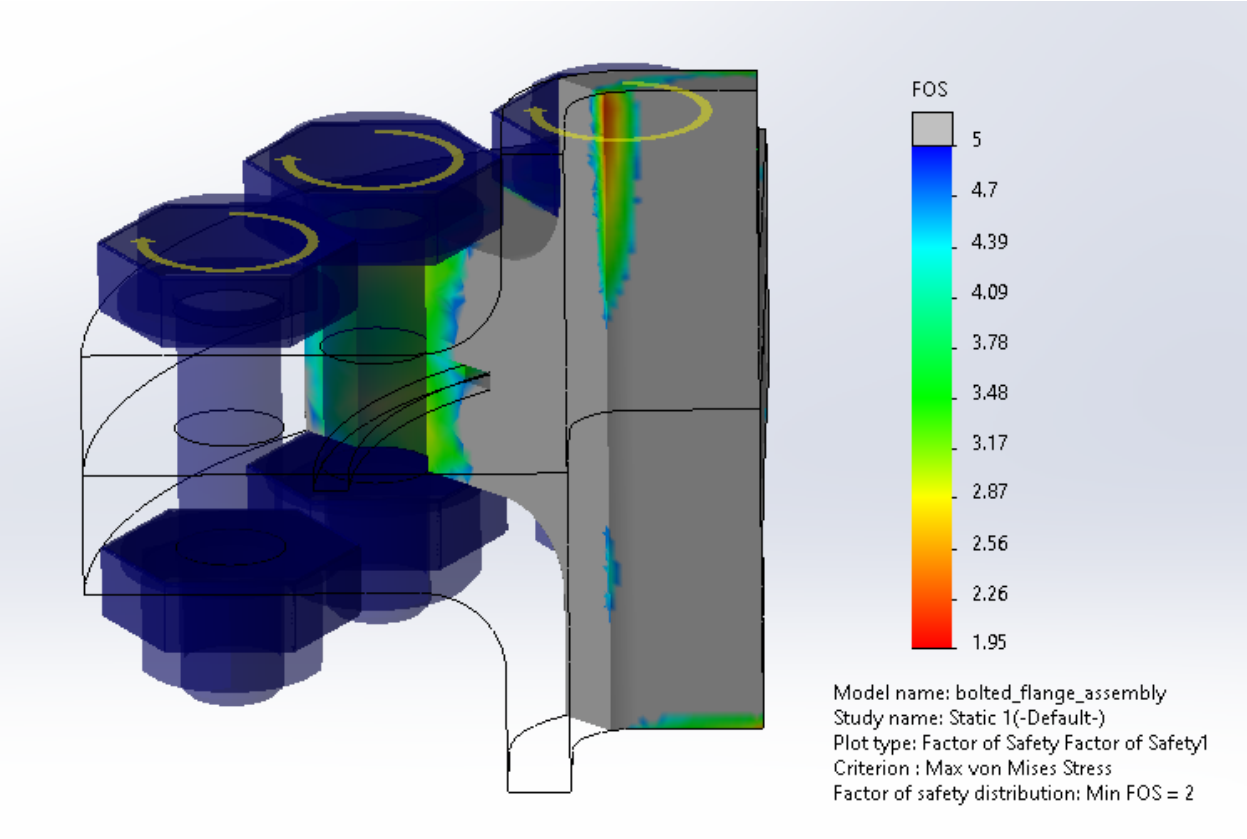

Figure A.12: Finite element analysis of bolted joint common to tube sections for internal pressure. Axial loading applied as internal pressure by cross sectional area of tube in both directions. Acceptable FOS on joints. Approx 4" of tube in either direction added to flange to isolate flange from axial loading; as all tube sections otherwise simulated independently low FOS on tube 'extension' disregarded.

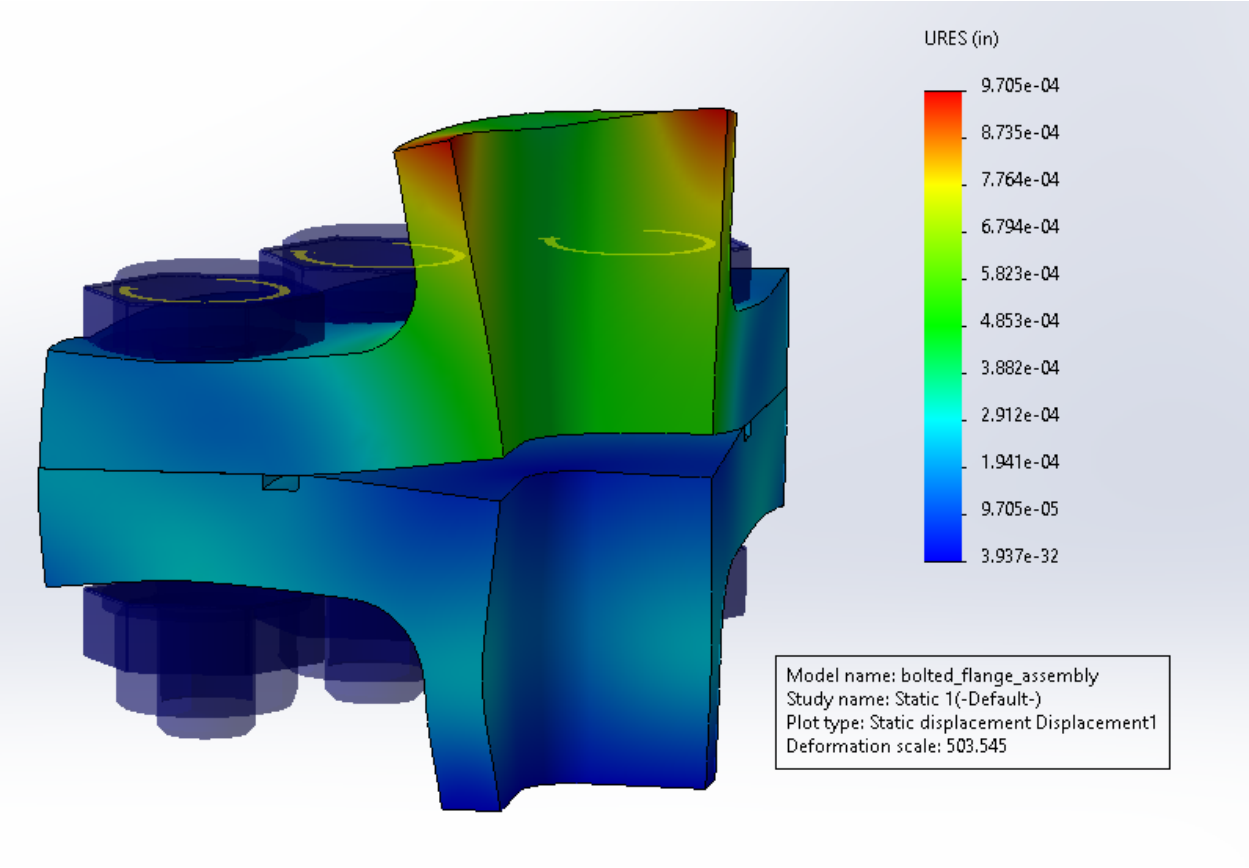

Figure A.13: Finite element analysis of bolted joint common to tube sections for separation. Deformation exaggerated for illustrative purposes.

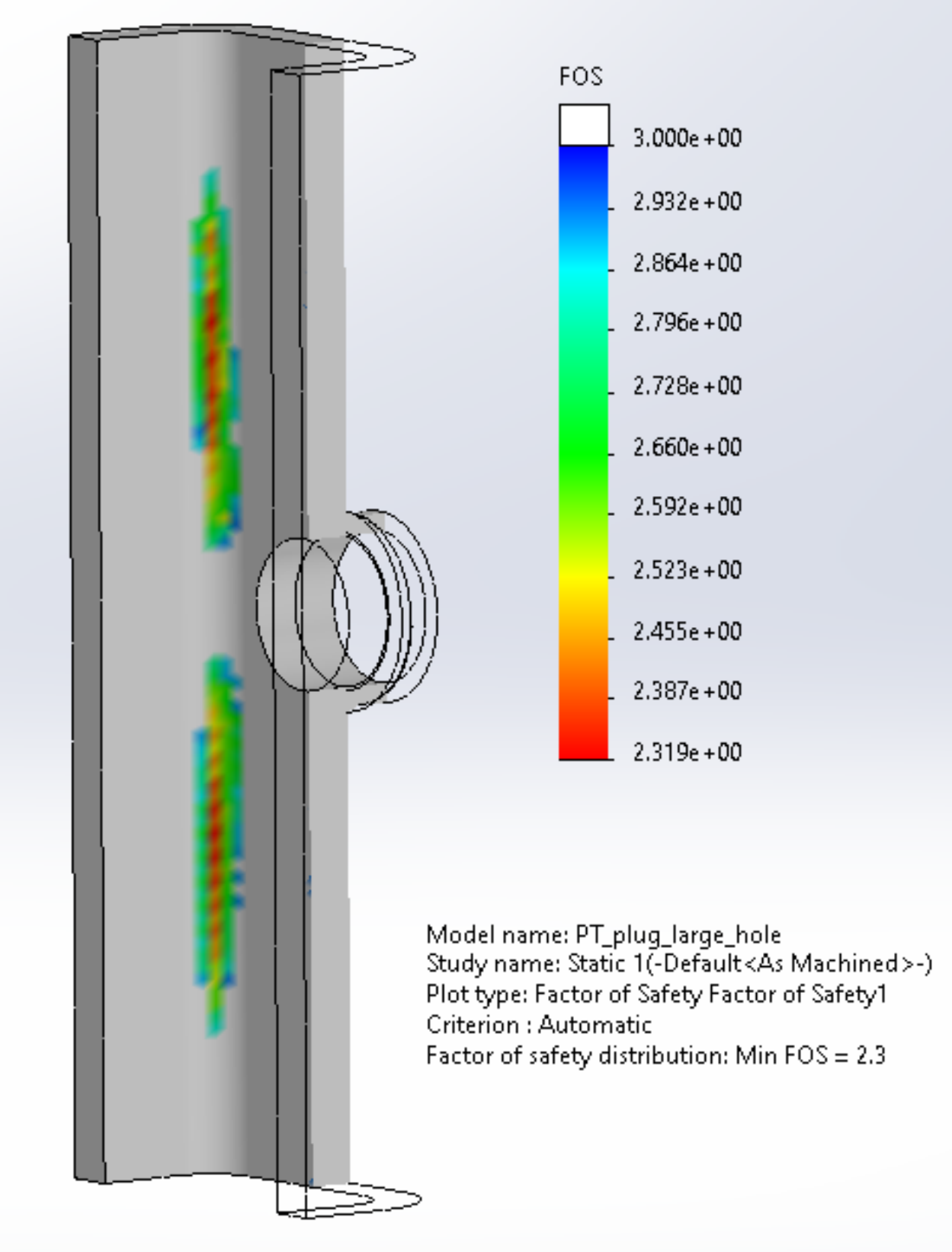

Figure A.14: Finite element analysis of tube section with reinforced and tapped for 1-1/8 x 12 common plug and plug for internal pressure. View shows areas of interest (no appreciable degradation in FOS externally).

APPENDIX B

GASEOUS FUEL EXPERIMENT RESULTS

B.1 Pressure Traces and Measured vs. 1D Predicted values from Shock and Detonation Toolbox

Here are presented dynamic pressure traces from propane-oxygen experiments. Experiments were conducted at nominally 1 atm and ambient temperature of 298K. Results for each run are presented as pressure trace plots with accompanying measured and calculated 1D values from SD Toolbox at the experimental conditions.

Velocities are reported between pressure transducers as dt/dx. Pressures are reported as the spike pressure. In the case of numerous pressure transducers average velocity is reported. Timing from system ignition signal to the first registered pressure signal is also reported.

Experiments are numbered in chronological order. Select experiments are presented for brevity. Several experiments were conducted as tests to determine timing, triggering, etc. and recorded either no data or data of no significance.

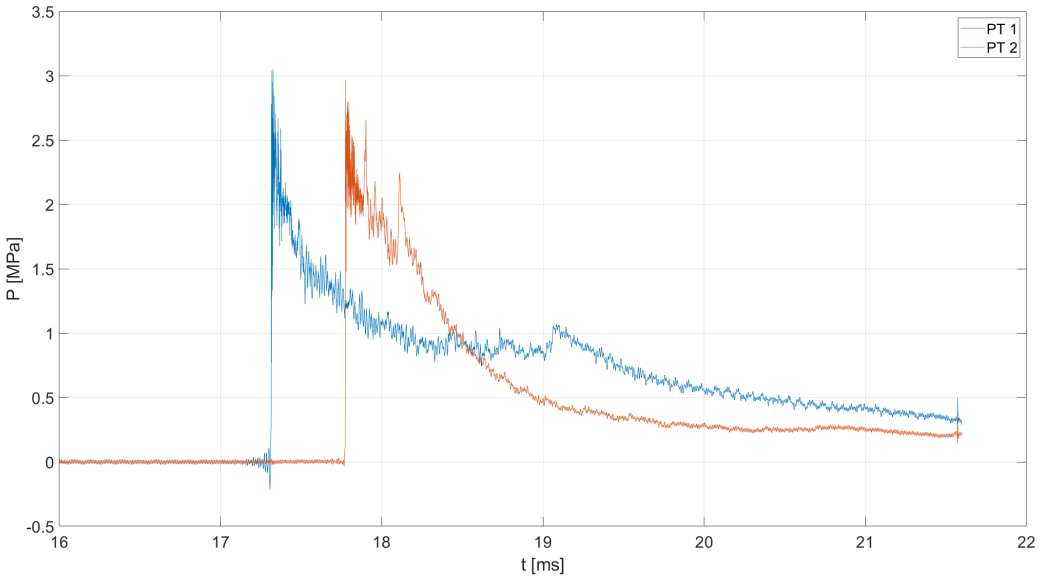

Figure B.1: Pressure traces from propane-oxygen experiment RUN 05, nominal ER 0.62

ER = 0.619	P [MPa]	V [m/s]	V_ign [m/s]
Experiment	3.05	2177	278
SD Toolbox (CJ Cond.)	2.97	2134	

Table B.1: Measured and Calculated CJ velocities and pressures, Propane Oxygen Experiment RUN 05

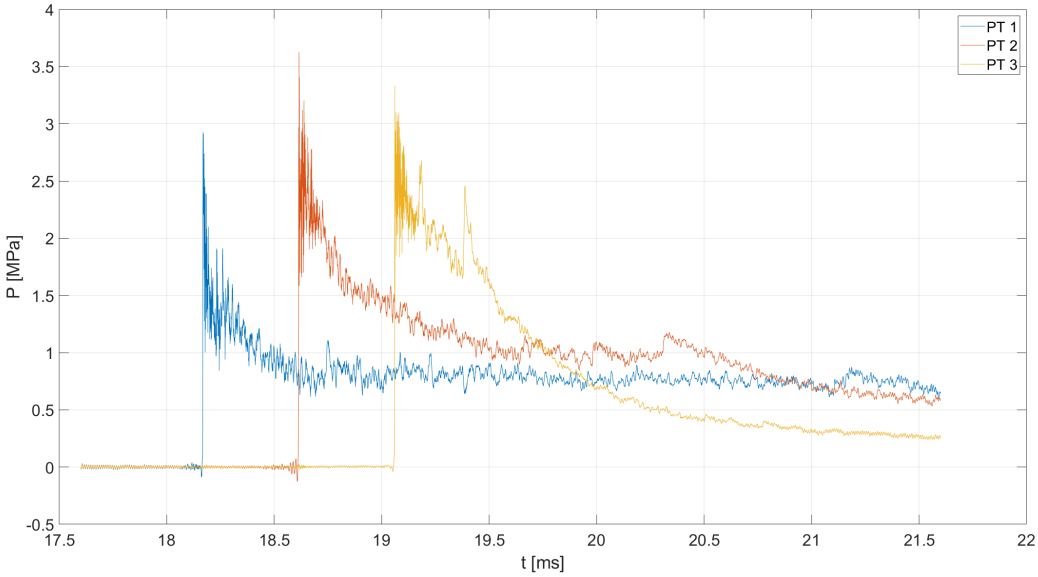

Figure B.2: Pressure traces from propane-oxygen experiment RUN 06, nominal ER 0.75

ER=0.746	P [MPa]	V_12 [m/s]	V_23 [m/s]	V_ign [m/s]
Experiment	3.35	2244	2236	404.5
SD Toolbox (CJ Cond.)	3.25	2218.4		

Table B.2: Measured and Calculated CJ velocities and pressures, Propane Oxygen Experiment RUN 06

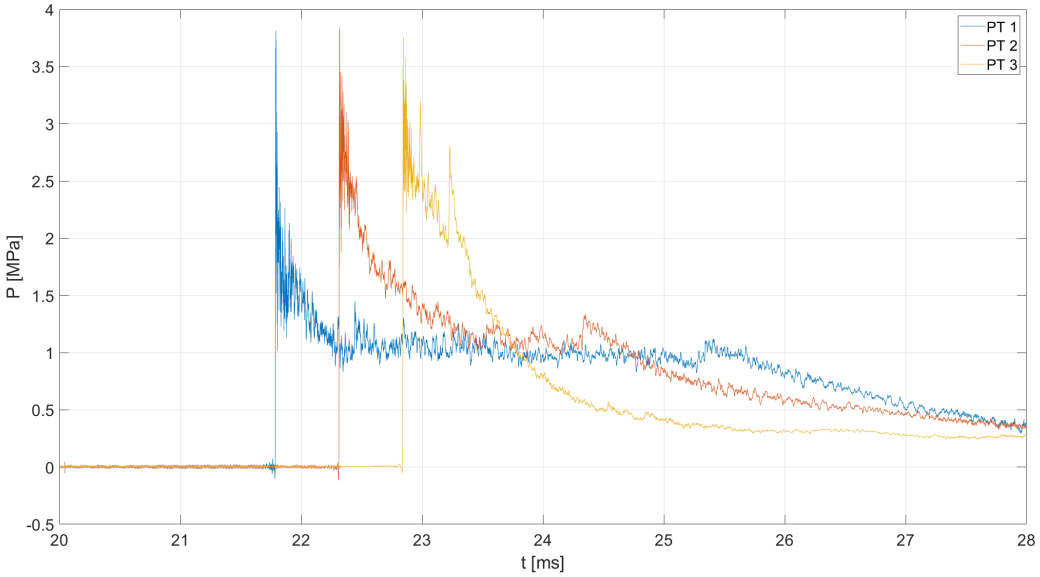

Figure B.3: Pressure traces from propane-oxygen experiment RUN 07, nominal ER 1.041

ER=01.041	P [MPa]	V_12 [m/s]	V_23 [m/s]	V_ign [m/s]
Experiment	3.757-.844	2376	2367	483.22
SD Toolbox (CJ Cond.)	3.759	2377.5		

Table B.3: Measured and Calculated CJ velocities and pressures, Propane Oxygen Experiment RUN 07

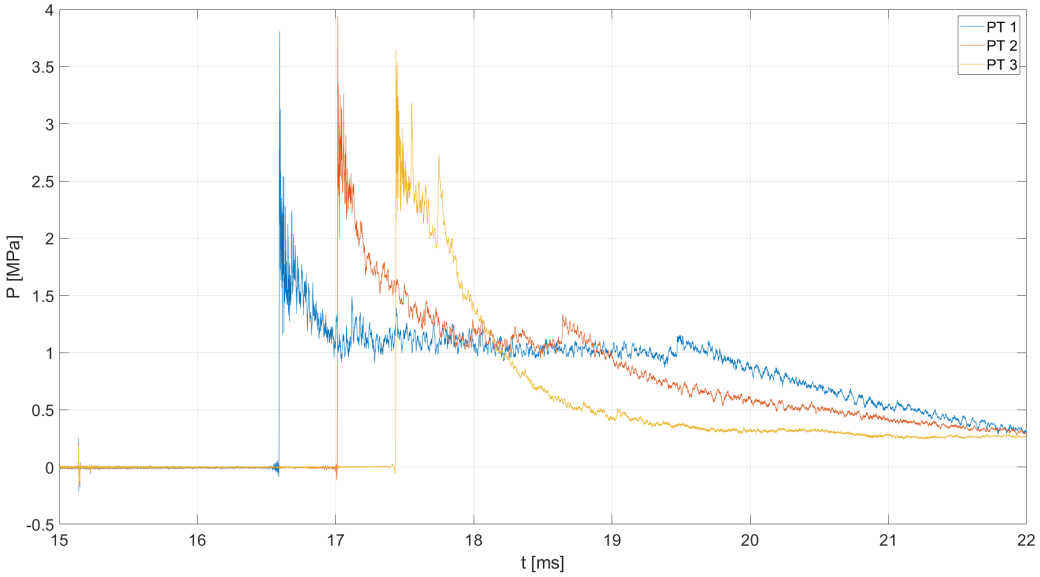

Figure B.4: Pressure traces from propane-oxygen experiment RUN 10, nominal ER 1.026

ER=01.041	P [MPa]	V_12 [m/s]	V_23 [m/s]	V_ign [m/s]
Experiment	3.757-.844	2376	2367	483.22
SD Toolbox (CJ Cond.)	3.759	2377.5		

Table B.4: Measured and Calculated CJ velocities and pressures, Propane Oxygen Experiment RUN 10

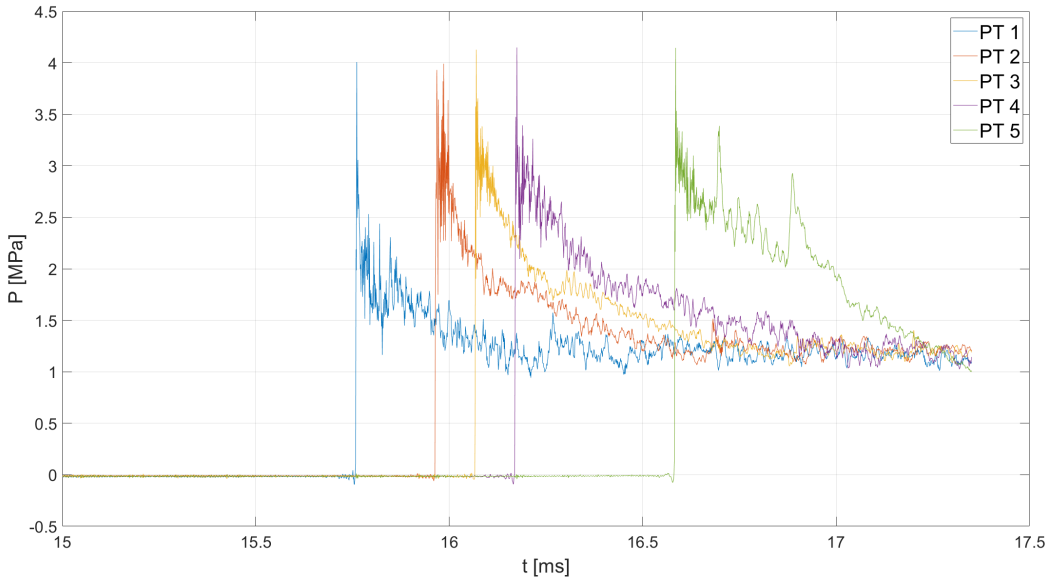

Figure B.5: Pressure traces from propane-oxygen experiment RUN 13, nominal ER 1.1

ER=01.112	P [MPa]	V_CJ [m/s]	V_ign [m/s]
Experiment	3.93-4.148	2427-2433	517
SD Toolbox (CJ Cond.)	3.83	2409	

Table B.5: Measured and Calculated CJ velocities and pressures, Propane Oxygen Experiment RUN 13

APPENDIX C

LIQUID FUEL EXPERIMENTAL DATA

Included in this section are representative datasets of PDPA measured particle size distribution and nozzle mass flow rates.

C.1 Droplet Size Distribution

C.1.1 ex-situ Measurements

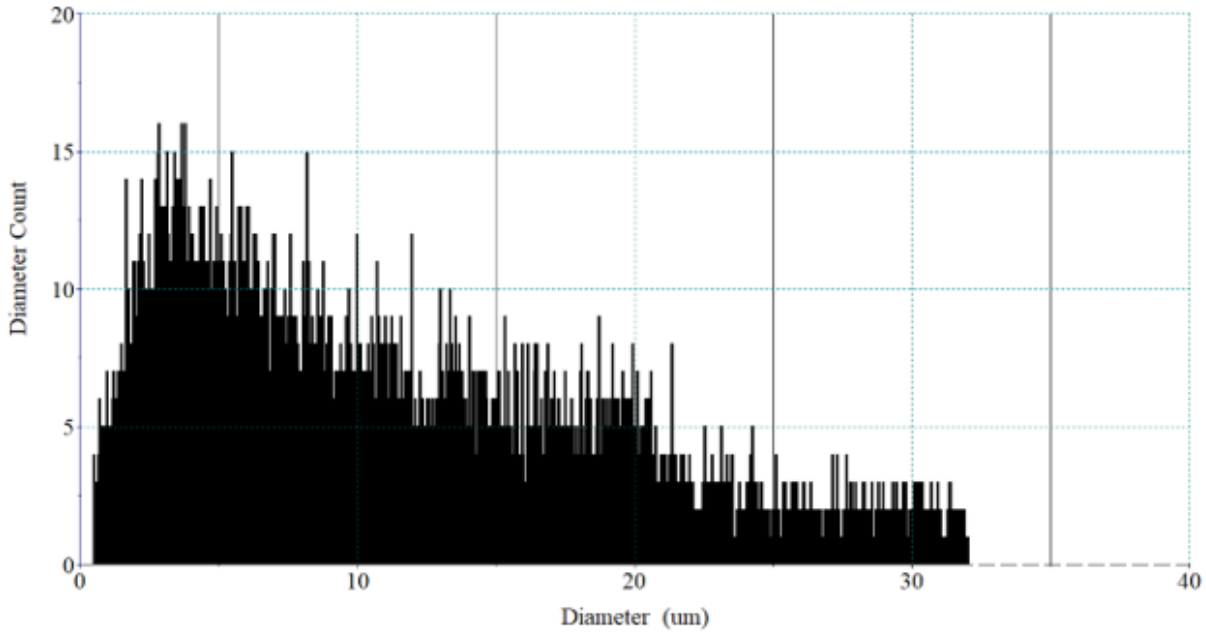

Figure C.1: Particle size histogram from 0.1 mm nozzle at 40 PSI supply pressure, measured 100mm from nozzle exit on centerline. Diameters in [um].

ER = 0.619	P [MPa]	V [m/s]	V_ign [m/s]
Experiment	3.05	2177	278
SD Toolbox (CJ Cond.)	2.97	2134	

Table C.1: Ex situ droplet size distribution data for 0.1 mm nozzle at 40 psi supply pressure

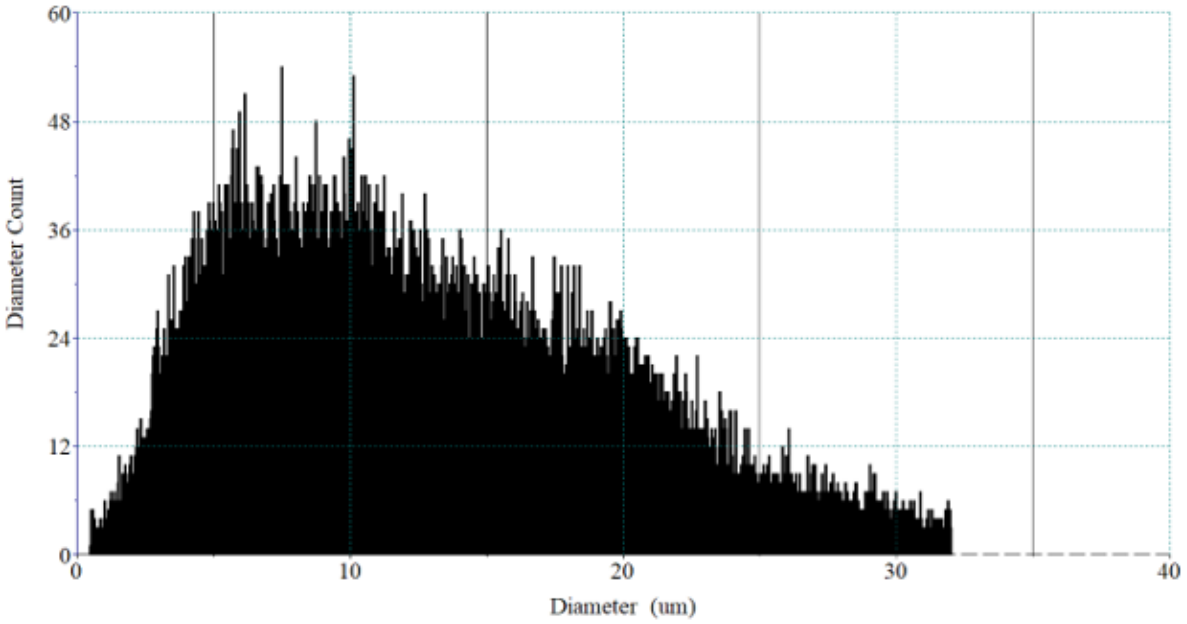

Figure C.2: Particle size histogram from 0.1 mm nozzle at 80 PSI supply pressure, measured 100mm from nozzle exit on centerline. Diameters in [um].

0.1 mm Nozzle					
80 PSI					
Run	D10 (um)	D20 (um)	D30 (um)	D32 (um)	D43 (um)
1	13.29239	15.40759	17.45402	22.39839	27.03171
2	13.52391	16.10214	18.56272	24.66935	30.2817
3	12.76355	15.30456	17.64131	23.43966	28.2435
Avg	13.19	15.6	17.89	23.5	28.52

Table C.2: Ex situ droplet size distribution data for 0.1 mm nozzle at 80 psi supply pressure

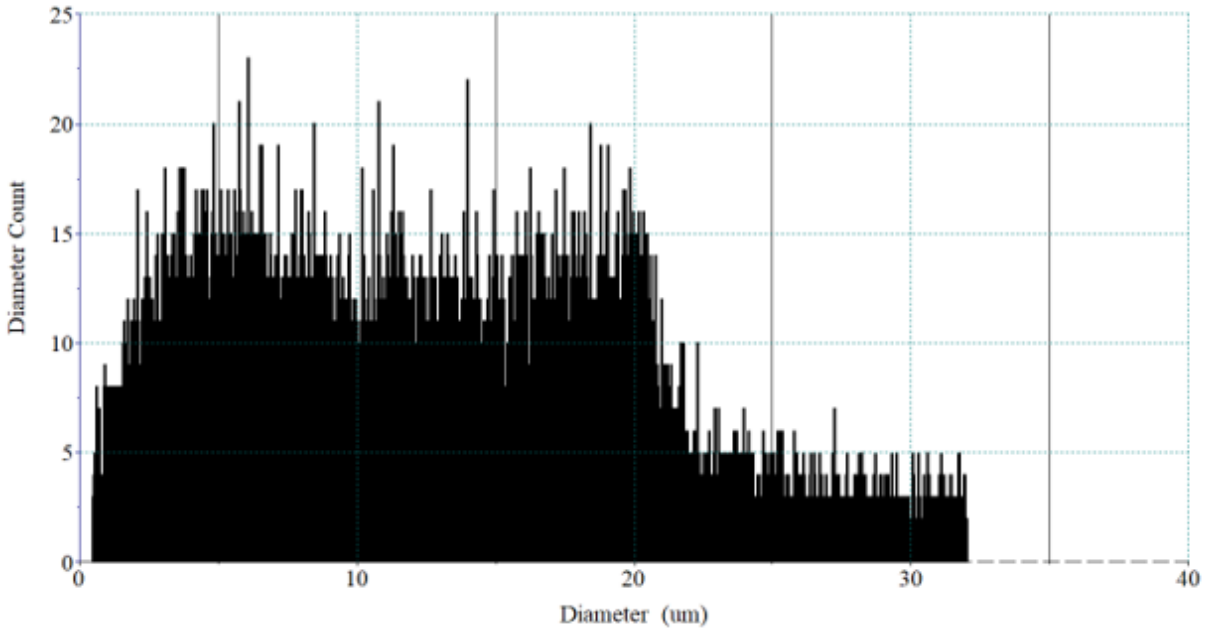

Figure C.3: Particle size histogram from 0.3 mm nozzle at 40 PSI supply pressure, measured 100mm from nozzle exit on centerline. Diameters in [um].

0.1 mm Nozzle					
40 PSI					
Run	D10 (um)	D20 (um)	D30 (um)	D32 (um)	D43 (um)
1	16.08695	20.84003	25.89065	39.96061	52.32001
2	14.69058	20.13315	26.16414	44.18713	58.20771
3	11.96372	15.28675	18.91275	28.94899	40.48391
Avg	14.25	18.75	23.66	37.7	50.34

Table C.3: Ex situ droplet size distribution data for 0.3 mm nozzle at 40 psi supply pressure.

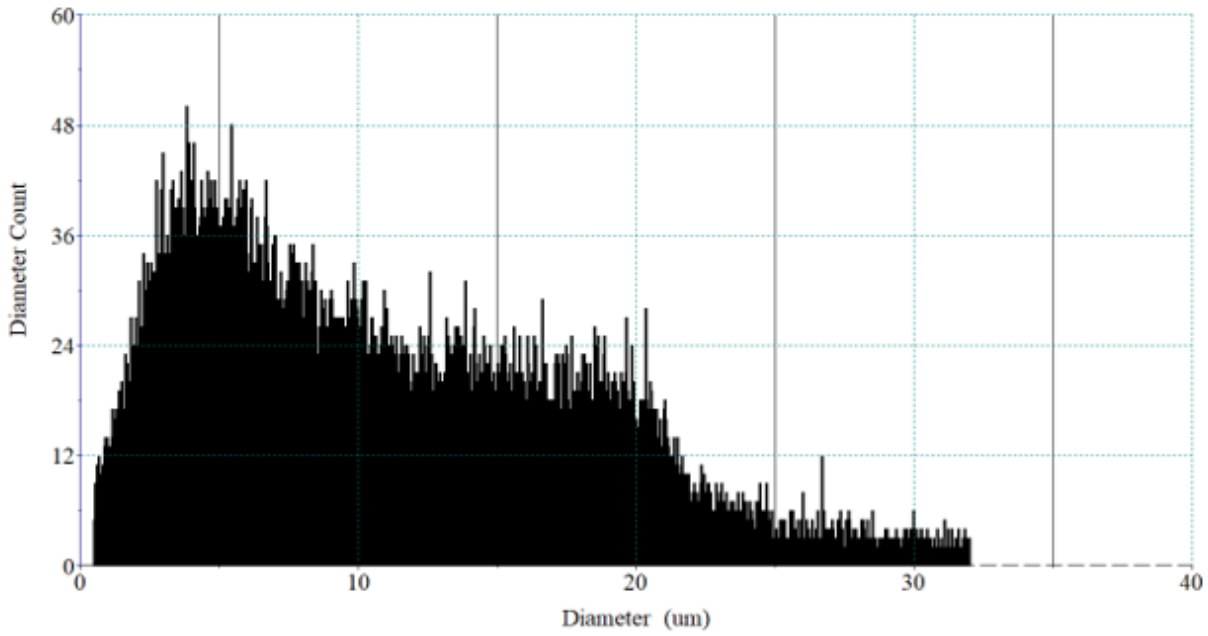

Figure C.4: Particle size histogram from 0.3 mm nozzle at 80 PSI supply pressure, measured 100mm from nozzle exit on centerline. Diameters in [um].

C.1.2 in-situ Measurements

Note: Particle data collection without co-flow was too sparse to create a meaningful dataset.

0.1 mm Nozzle					
80 PSI					
Run	D10 (um)	D20 (um)	D30 (um)	D32 (um)	D43 (um)
1	15.65579	17.78423	20.03418	25.42404	31.49548
2	11.31648	13.77595	16.20767	22.43462	29.05346
3	11.68788	14.60036	17.46962	25.01056	31.95903
Avg	12.89	15.39	17.9	24.29	30.84

Table C.4: Ex situ droplet size distribution data for 0.3 mm nozzle at 80 psi supply pressure.

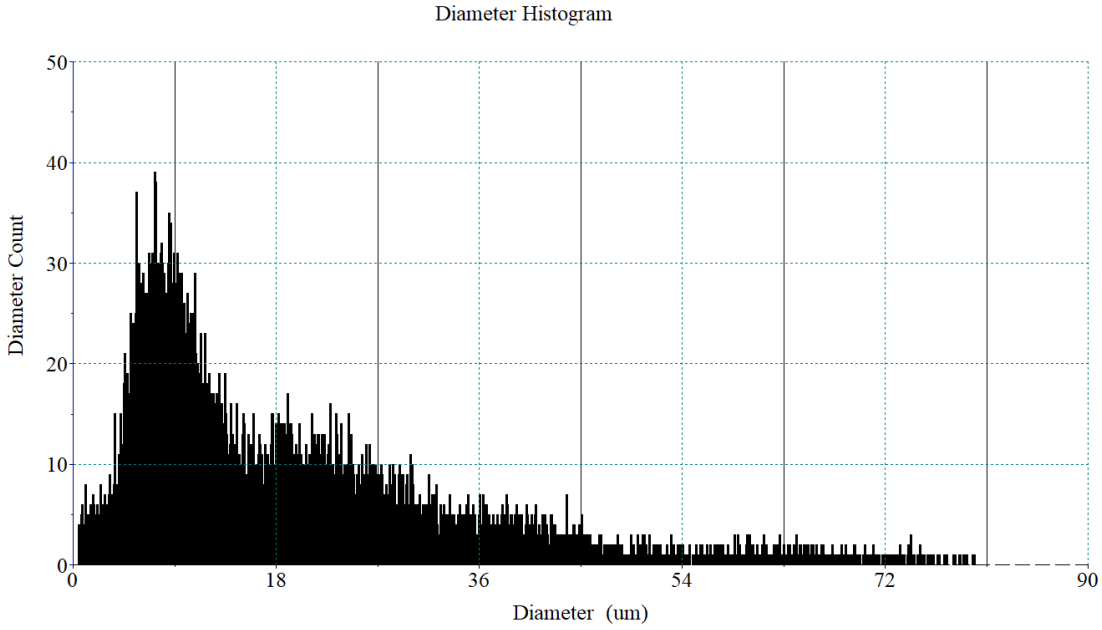

Figure C.5: Particle size histogram from 0.1 mm nozzle at 80 PSI supply pressure, measured in-situ in test section approx. 2.5 meters from injection. Measurement time 45-120s. Qualitatively light co-flow of dry nitrogen. Diameters in [um].

C.2 Initial Experimental Results

Initial experiments injecting particles into a quiescent oxygen atmosphere were conducted, resulting in deflagrations and DDT-like events.

D10 (um)	D20	D30	D32	D43
17.81	22.93	28.45	43.81	58.14

Table C.5: In situ droplet size distribution data for 0.1 mm nozzle at 80 psi supply pressure.

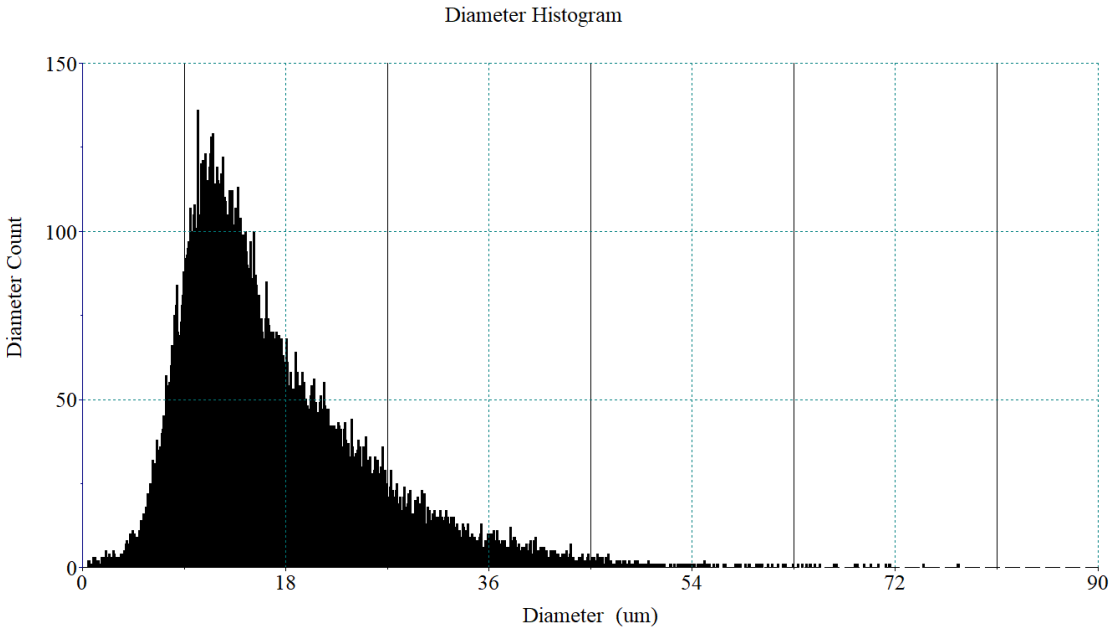

Figure C.6: Particle size histogram from 0.1 mm nozzle at 80 PSI supply pressure, measured in-situ in test section approx. 2.5 meters from injection. Measurement time 45-120s. Qualitatively light co-flow of dry nitrogen. Diameters in [um].

D10 (um)	D20	D30	D32	D43
16.38	18.08	19.93	24.20	29.07

Table C.6: In situ droplet size distribution data for 0.1 mm nozzle at 80 psi supply pressure.

	PT4	PT 5	dt (ms)	dx/dt (m/s)
Rise-Rise	72.28	73.14	0.86	1163
Peak-Peak	72.38	73.53	1.15	869

Table C.7: Estimates of wave velocity at pressure transducers PT4 and PT5, measured from initial rise times and peak-to-peak of pressure spikes for DDT like event.

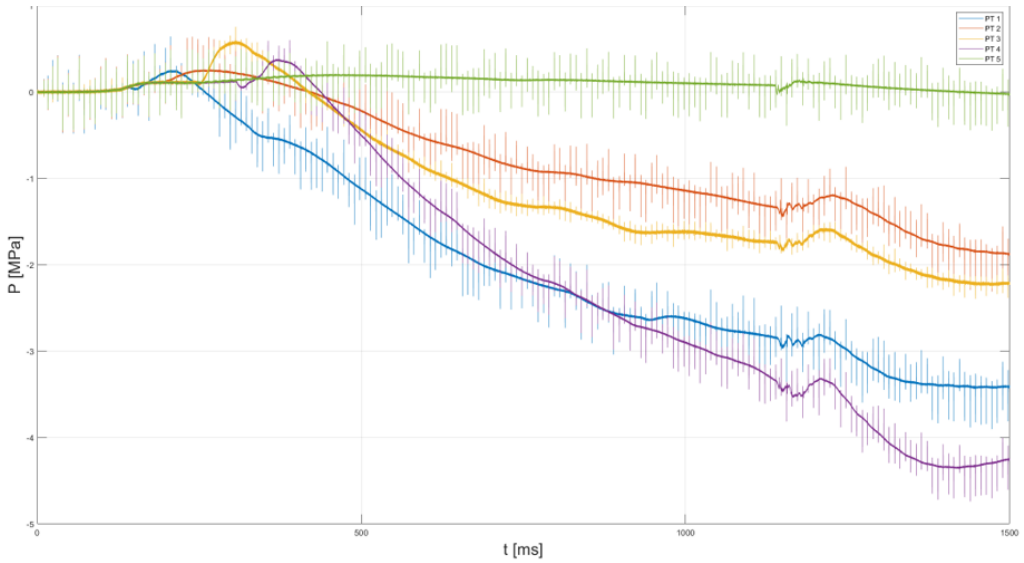

Figure C.7: Pressure profiles of observed deflagration.

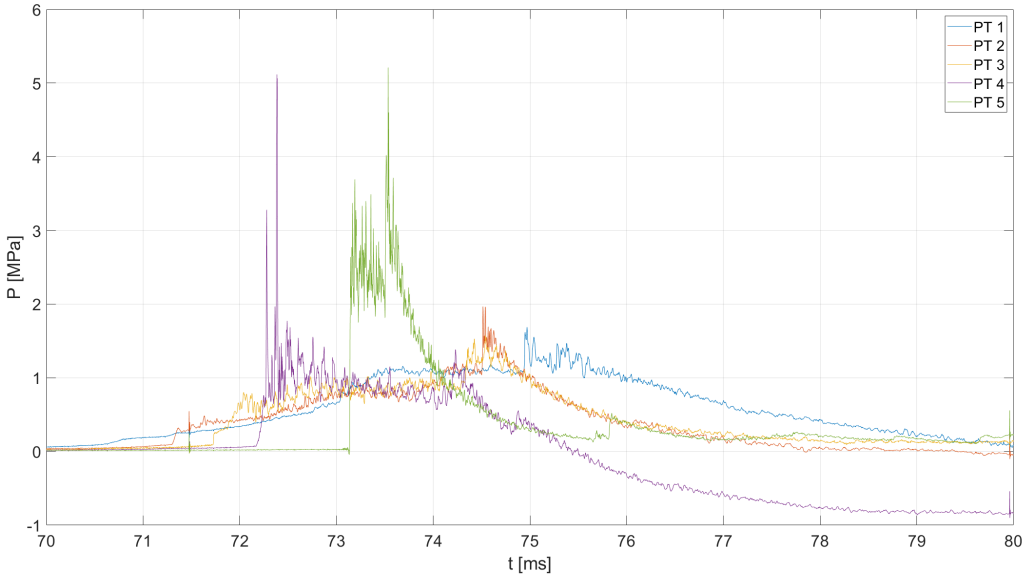

Figure C.8: Pressure profiles of observed DDT-like event.